Laminar-flow Liquid-to-air Heat Exchangers - Energy-efficient Display Cabinet Applications

Haglund Stignor, Caroline

2009

Citation for published version (APA):
Haglund Stignor, C. (2009). *Laminar-flow Liquid-to-air Heat Exchangers - Energy-efficient Display Cabinet Applications*. [Doctoral Thesis (compilation), Faculty of Engineering, LTH]. Faculty of Engineering, Department of Energy Sciences, Division of Heat Transfer.

Total number of authors:
1

Laminar-flow Liquid-to-air Heat Exchangers
– Energy-efficient Display Cabinet Applications

Caroline Haglund Stignor

Abstract

Provisions are stored and displayed in supermarkets and grocery stores, at a temperature lower than the ambient, in display cabinets, which are responsible for a significant amount of the energy use in this sector. During the 1990s, major changes in the regulations governing the use of synthetic refrigerants took place in Sweden. This resulted in many refrigeration systems being converted to systems with indirect cooling by means of a liquid secondary refrigerant. The cooling coil is an important component in a display cabinet and traditionally, different kinds of tube-coils, with aluminium fins on expanded circular copper tubes, have been used. Many secondary heat transfer media have relatively high viscosities at low temperatures, and so the flow regime is often laminar, which may lead to poor heat transfer. However, it is possible to achieve high heat transfer coefficients even for laminar flows if an appropriate design of the heat exchanger is applied. Flat-tube heat exchangers have been used for a long time in automotive applications, where compactness is important. The display cabinet application involves low air velocities in combination with condensation of water vapour, and sometimes even frosting, and is therefore different from other applications where flat-tube heat exchangers have been used earlier.

The objective of this research work has been to find a suitable, more energy-efficient, heat exchanger design for indirectly cooled display cabinets. An efficiency that would mean that temperature differences would be so small that frosting could be avoided was aimed for. This research work has sandwiched experimental investigations with theoretical modelling and parameter studies. Initially, the heat transfer and pressure drop performance of conventional cooling coils operating with liquid secondary refrigerants was studied in full-scale experiments. Thereafter, the liquid-side (or tube-side) heat transfer was studied experimentally in small-scale experiments on three single multiport extruded flat tubes with different cross-sections. In both studies, the best agreement was found with predictions using the Gnielinski correlation for thermally developing laminar flows with the constant temperature boundary condition. After this, two different heat exchangers having flat tubes and plain fins on the air side were evaluated experimentally - one with continuous plate fins and one with serpentine fins. The results show that, for conditions similar to those of display cabinets, the heat transfer and pressure drop performance is affected to little or no extent by the occurrence of condensate water. Models for different types of flat-tube heat exchangers were thereafter created using the results from the experimental studies.

In order to find appropriate optimising criteria for the display cabinet heat exchangers, the energy efficiency of a complete cooling system of an imagined supermarket has been studied. Finally, different designs of flat-tube heat

exchangers with plain fins have been evaluated theoretically in a parameter study. The results show that considerable savings in the required electric drive power can be obtained in comparison with the traditional cooling coil. The savings can be up to 15 %. In addition, the flat-tube heat exchangers could operate with a minimum temperature difference of around 1 K. This makes frost-free operation possible for many display cabinet applications and thereby the savings potential even larger.

Populärvetenskaplig sammanfattning

Resultaten som presenteras i denna doktorsavhandling visar att det går att spara stora mängder energi genom att använda samma typ av värmeväxlare, som normalt används i bilar och lastbilar, i livsmedelsbutikernas kyldiskar.

För att hålla maten kall när den ligger ute i butiken cirkuleras en kyld luftström runt i kyldiskarna. Denna kyls i en så kallad värmeväxlare som ofta finns i botten på kyldiskarna under den nedersta hyllan. Bakgrunden till forskningsprojektet är att det i Sverige under 90-talet infördes en anvisning som inte tillät att luften i kyldiskarna kyldes direkt med hjälp av konstgjorda köldmedier. Anvisningen gällde vid nybyggen av butikernas kylsystem. Istället skulle en vätska kylas i kylmaskinerna och denna vätska, den så kallade köldbäraren, skulle sedan pumpas ut till kyldiskarna. Dessa system kallas indirekta kylsystem. Anledningen var att de konstgjorda köldmedierna bidrar till växthuseffekten om de släpps ut i luften. Genom att använda indirekta system behöver systemen inte fyllas med lika mycket köldmedium och det blir då lättare att hålla läckagen låga.

Köldbärarvätskorna är ofta ganska trögflytande vid låga temperaturer vilket gör att värme inte överförs så bra från luften till vätskan när luften kyls. Detta leder i sin tur till att det måste vara stora temperaturskillnader mellan luft och vätska när luften ska kylas. Ju större temperaturskillnad, desto mer elenergi måste användas. De värmeväxlare, så kallade kylbatterier, som normalt finns i kyldiskar har runda rör och var från början konstruerade för att ett köldmedium skulle koka vid låg temperatur inne i rören. När luften istället ska kylas med en trögflytande köldbärarvätska skulle kylbatterierna behöva byggas på ett annat sätt för att vara mer energieffektiva.

I bilar och lastbilar används ofta värmeväxlare med platta tuber istället för runda rör, eftersom värmeväxlarna då kan göras mindre och lättare. I detta forskningsprojekt har vi undersökt hur en värmeväxlare med platta tuber ska se ut för att fungera optimalt i en kyldisk. I bilar är luften torr och dess hastighet genom värmeväxlaren hög. I en kyldisk är hastigheten låg och dessutom bildas kondens av vattenånga när luften kyls. Dessa annorlunda förutsättningar gör att värmeväxlarna behöver se lite annorlunda ut, t.ex. vara glesare, för att fungera bra. För att komma fram till förslag på hur värmeväxlare med platta tuber bör se ut när de ska användas i kyldiskar har experiment varvats med beräkningar i många omgångar.

Resultaten visar att åtminstone 15 % elenergi kan sparas med hjälp av dessa "nya" värmeväxlare och det kan bli stora mängder eftersom 5 meter kyldisk i en

affär använder ungefär lika mycket energi per år som en eluppvärmd villa. Dessa "nya" värmeväxlare kan eventuellt bli dyrare att producera. Hur mycket dyrare är svårt att säga eftersom det till stor del beror på tillverkningsvolym.

Den anvisning som inte tillät direkt kylning med ett konstgjort köldmedium som infördes i Sverige på 90-talet har nu tagits bort och ersatts med EU-lagstiftning. Enligt denna finns det inte längre någon motsvarande anvisning, men ju mer konstgjort köldmedium som en kylanläggning fylls med, desto oftare måste man kontrollera att den inte läcker. Svenska butiker har många positiva erfarenheter av de indirekta kylsystemen – de är något dyrare att bygga, men billigare att sköta och de underlättar en jämn temperaturhållning av matvarorna. Dessutom har intresset för indirekta kylsystem ökat i resten av världen, eftersom de är miljövänliga alternativ till system med konstgjorda köldmedium. Därför är sannolikheten stor att de indirekta kylsystemen kommer att fortsätta att användas i stor utsträckning och att användningen till och med kommer att öka i framtiden.

Detta forskningsprojekt utfördes på SP Sveriges Tekniska Forskningsinstitut, i samarbete med Lunds Tekniska Högskola, LTH, där avhandlingen publiceras. Chalmers Tekniska Högskola och ett antal företag som arbetar med livsmedelskyla eller värmeväxlare har också deltagit och bidragit till projektet. Projektet har huvudsakligen finansierats av Energimyndigheten, Svensk Fjärrvärme, SP och LTH.

Acknowledgements

List of Publications

This thesis is based on the following papers, which will be referred to by their roman numerals in the text.

I. Haglund Stignor, C., Sundén, B., and Fahlén, P., 2007, Liquid Side Heat Transfer and Pressure Drop in Finned-Tube Cooling-Coils Operated with Secondary Refrigerants, *International Journal of Refrigeration*, Vol. 30, pp. 1278-1289.

II. Haglund Stignor, C., Sundén, B., and Fahlén, P., 2009. An Experimental Study of Liquid Phase Heat Transfer in Multiport Minichannel Tubes, *Accepted for publication in Heat Transfer Engineering*, Vol. 30, No. 12 or 13.

III. Haglund Stignor, C., Sunden, B., Fahlén, P, 2007. Design of different types of secondary loop cooling systems in supermarkets - comparison of energy use and costs. In: *Proceedings of International Congress of Refrigeration*, Beijing, China, ICR07-B01-387.

IV. Haglund Stignor, C., Sunden, B., Fahlén, P., Stensson, S, 2010. Heat transfer and pressure drop under dry and humid conditions in flat-tube heat exchangers with plain fins. *Accepted for publication in Heat Transfer Engineering*, Vol. 31, No. 3 or 4.

V. Caroline Haglund Stignor, Bengt Sundén, and Per Fahlén, Energy Efficient Flat-Tube Heat Exchangers for Indirectly Cooled Display Cabinets, *Accepted for publication in International Journal of Refrigeration, 2009.*

Publications not included in the thesis

Haglund, C. and Fahlén, P., 2001, Jämförelse av metoder för att förbättra värmeöverföring och tryckfall i köldbärarkylda kylbatterier med laminära vätskeflöden (In Swedish, English title: A comparison of methods for improvement of heat transfer and pressure drop in cooling coils cooled by a liquid in the laminar flow regime), In: *Proceedings of the Nordic Conference "16. Nordiske kølemøde, 9. Nordiske varmepumpedage"*, Copenhagen, Denmark, pp. 263-272.

Haglund, C., Fahlén, P., Sundén, B. and Eriksson, D., 2002, Improvement of conventional indirect cooling-coils for display cabinets – theory and experiments, In: *Proceedings of the International Conference "New Technologies in Commercial Refrigeration, IIR/IIF Commission D1/B1"*, Urbana, USA, pp. 120-129.

Haglund, C., Fahlén, P., Sundén, B., and Eriksson, D., 2002, Enhancement of the performance of indirect cooling-coils for display cabinets, In: *Proceedings of the International Conference "Zero Leakage - Minimum Charge, IIR/IIF"*, Stockholm, Sweden, pp. 263-270.

Haglund Stignor, C., 2002, Liquid Side Heat Transfer and Pressure Drop in Finned-Tube Cooling-Coils, *Thesis for the degree of Licentiate of Engineering, Lund Institute of Technology*, Sweden, 97 p.

Haglund Stignor, C., Fahlén, P., Sunden, B. and Eriksson, D, 2003, Optimal Operation of Cooling-Coils in Secondary Loop Refrigeration Systems, In: *Proceedings of International Congress of Refrigeration,* Washington D. C., USA, pp. ICR0275

Haglund Stignor, C., Fahlén, P., Sundén, B., Eriksson, D., 2005, Flat-tube heat exchangers for indirectly cooled display cabinets - theory and experiments. In: *Proceedings of IIR International Commercial Refrigeration Conference*, Vicenza, Italy, pp. 47-54.

Haglund Stignor, C., 2005, *Indirectly Cooled Flat-Tube Heat Exchangers for Display Cabinet and Air-Conditioning Applications - A Literature Survey,* SP Work report 2005:22, SP Technical Research Institute of Sweden.

Fahlén, P, Markusson, C., Haglund Stignor, C., 2007. Capacity Control of Liquid-Cooled Air-Coolers. In: *Proceedings of International Congress of Refrigeration*, Beijing, China, ICR07-E1-423.

Haglund Stignor, C., 2007, *Design of different types of indirect cooling systems in supermarkets - comparison of energy use and costs,* SP Work report 2007:07, SP Technical Research Institute of Sweden.

Nomenclature

A	area (m^2)
A_c	minimum free-flow area (m^2)
C_1	heat capacity flow rate on side No. 1 (W·K^{-1})
C_2	heat capacity flow rate on side No. 2 (W·K^{-1})
C_1	heat capacity flow rate on side No. 1 (W·K^{-1})
C_2	heat capacity flow rate on side No. 2 (W·K^{-1})
C_c	heat capacity flow rate on the cold side (W·K^{-1})
C_h	heat capacity flow rate on the hot side (W·K^{-1})
C_r	heat capacity flow rate ratio, $C_r \le 1$ by definition (-)
C_{min}	heat capacity flow rate on the minimum side (W·K^{-1})
C_{max}	heat capacity flow rate on the maximum side (W·K^{-1})
c_p	specific heat capacity (J·kg^{-1}·K^{-1})
D	outer diameter (m)
d	inner diameter (m)
d_h	hydraulic diameter $d_h = 4 \cdot A_c/P$, P = perimeter (m)
De	depth
EB	energy balance (-)
F	correction factor (-)
F_d	fin depth (m)
F_l	fin length (m)
F_p	fin pitch (m)
f	Fanning friction factor, $f = \Delta p \cdot d \big/ \left(2 \cdot \rho \cdot L_{tube} \cdot u^2 \right)$ (-)
f_{app}	apparent Fanning friction factor, developing flows (-)
G_c	mass flux in the minimum free flow area (kg·s^{-1}·m^{-2})
H	height (m)
k	coverage factor (-)
K_c	contraction loss coefficient at heat exchanger inlet (-)
K_e	expansion loss coefficient at heat exchanger outlet (-)
L	characteristic length, e.g. in the definition of Reynolds number (m)
L_p	louver pitch (m)
L_{tube}	tube length between U-bends (m)
l	fin length for heat conduction from primary surface to fin tip or midpoint between tubes (m)
l_1	length of shortest duct side (m)
l_2	length of longest duct side (m)
l_{tube}	heated tube length (m)
l_x	length of cell in stepwise calculations (m)

m	fin parameter (-)
$\dot{m}$	mass flow rate (kg·s^{-1})
N	number of tubes, fins or passes (-)
N_{pc}	number of parallel circuits (-)
n	number of heat exchangers (-)
n_l	number of tubes in longitudinal direction, cooling coil (-)
n_t	number of tubes in transversal direction, cooling coil (-)
NTU	number of transfer units (-)
Nu	Nusselt number, $Nu = \dfrac{\alpha \cdot d_h}{\lambda}$ (-)
P	perimeter (m or mm)
P_1	temperature effectiveness related to side No. 1 (-)
$P_{1,p}$	temperature effectiveness per heat exchanger/pass (-)
P_d	wave height (m)
p	pressure (Pa)
p_f	fin pitch, cooling coil (m or mm)
p_l	longitudinal tube pitch, cooling coil (m)
p_t	transveral tube pitch, cooling coil (m)
Pr	Prandtl number, $\mathrm{Pr} = \dfrac{c_p \cdot \mu}{\lambda}$ (-)
$\dot{Q}$	cooling capacity or heat flow rate (W)
R	heat transfer resistance (K·W^{-1})
R_1	heat capacity flow rate ratio, $R_1 = \dfrac{C_1}{C_2}$ (-)
r_h	hydraulic radius $r_h = A_c/P$, P = perimeter (m)
Re	Reynolds number, $\mathrm{Re} = \dfrac{\rho \cdot u \cdot L}{\mu}$, $L = d_h$ or L_p (-)
T_d	tube depth (m)
T_h	tube height (m)
T_p	tube pitch (m)
T_w	tube width (m)
t	temperature (°C)
t	temperature difference (K)
U	expanded (total) uncertainty of measurements (Appendix A)
U	overall heat transfer coefficient, (W·m^{-2}·K^{-1})
u	uncertainty of measurements (Appendix A)
u	velocity (m·s^{-1})
$\dot{V}$	volume flow (m^3·s^{-1})
W	width (m)
$\dot{W}_e$	electric power (W)
X	factor, ratio (-)
X_f	half wave length (m or mm)

x	axial location (-)
x^*	dimensionless length, thermally developing flows, d_h characteristic length (-)
x^+	dimensionless length, hydrodynamically developing flows, d_h characteristic length (-)
z^*	dimensionless length, thermally developing flows, (A_c characterstic length (-)

Greek letters

	heat transfer coefficient (W·m^{-2}·K^{-1})
Δ	difference
	thickness (m)
ε	heat exchanger effectiveness (-)
φ	relative humidity (%)
	thermal conductivity (W·m^{-1}·K^{-1})
γ	aspect ratio of duct (-)
	dynamic viscosity (Pa·s)
	density (kg·m^{-3})
σ	ratio of free flow area to frontal area (-)
η	efficiency (-)
η_0	expanded area efficiency (-)
φ	relative humidity (vapour pressure) (-)

Subscripts

a	air
am	arithmetic mean
b	liquid secondary refrigerant (brine)
c	cold side
calc	calculated
dp	dew point
duct	duct
f	fouling
fd	fully developed
fin	fin
H	uniform heat flux boundary condition
h	hot side
heater	heater
i	inner
i	integer, cell number in stepwise calculations (Appendix B)
iso	isothermal
in	in to heat exchanger, at inlet conditions
L$_p$	based on louver pitch

l	longitudinal (direction of air flow)
lam	laminar
lm	logarithmic mean
m	mean
max	maximal
o	outer
out	out from heat exchanger
p	per pass / heat exchanger
pc	parallel circuits
s	sensible
sd	simultaneously developing
T	uniform temperature boundary condition
t	transversal (direction of air flow)
theo	theoretical
tot	total
tube	tube
turb	turbulent
$\dot{V}$	at temperature in volume flow measuring point ($m^3 \cdot s^{-1}$)
W	water, at mean temperature of water
w	wall, at wall temperature
w	by weight (if preceded by %)
x	at a distance x from inlet
0	without considering fin efficiency
1	part of heat exchanger with tubes
2	part of heat exchanger without tubes

Contents

1   Introduction

A background to put the significance of the present study into context is given below, followed by the objectives of the study and the methodology used in the research work. This is followed by a literature survey, and finally the selection of the studied parameter range is motivated.

1.1   Background

Refrigeration of merchandise in supermarkets is responsible for a significant amount of the energy use in this sector. Open vertical display cabinets are commonly used and despite their frequent occurrence, they have a large energy requirement.

The merchandise in the display cabinet has to be kept at a temperature that is lower than the ambient, while at the same time allowing customers easy access to reach it. For example, according to earlier regulations issued by The Swedish National Food Administration (Livsmedelsverket, 1996), fresh meat should be kept at 0 - 4 °C, and dairy products at 0 - 8 °C . These regulations are no longer valid, since the appropriate storage temperature is now stated by the food manufacturer and the merchandiser is responsible for fulfilling this temperature requirement (European Regulation (EC) no. 852/2004). Nevertheless, the figures above give a conception of what temperature range that should be reached in a refrigerated display cabinet.

The lower temperature of the provisions is obtained by cooling air in a cooling coil and then distributing the air partly in a cold air curtain in front of the merchandise, and partly through the back of the cabinet and above the merchandise. The air is then returned via a fan back to the cooling coil. The arrows in Figure 1.1 show how the air is circulated in the display cabinet. The cold air curtain is supposed to work as a cold barrier between the warm ambience outside the cabinet and the cold space within the cabinet. However, due to infiltration, i.e. mixing with the warm outside air, radiation through the cabinet opening, heat conduction through the cabinet walls and internal lighting etc., the circulating air is heated and has to be cooled to its original temperature by the cooling coil. The cooling is achieved by electrically driven chillers. A typical key figure for the energy requirement of modern display

cabinets is 4000-8000 kWh electricity per meter length of cabinet and year. In connection with a technology procurement project that was held in Sweden in 1997, the total installed length of display cabinets in Sweden was approximated to 100 km. This resulted in a total energy use for display cabinets in Sweden that amounted to 0.4 - 0.8 TWh electricity per year, according to Axell and Fahlén (1998).

The 1990s saw major changes regarding regulations for the use of synthetic refrigerants in Sweden. A new national proclamation for the use of synthetic refrigerants in Sweden, "The refrigerant order" (Naturvårdsverket, 1988), was issued by the National Environmental Protection Agency in 1989. As a result, the Swedish Refrigeration Foundation included instructions in the "Swedish Refrigeration Code" (Kylbranschens Samarbetsstiftelse, 1994) not to build new direct-expansion systems for medium-temperature display cabinets in supermarkets that contained more than 50 kg of refrigerant. At the same time, the phase-out of CFC refrigerants started with a ban on new installations in 1995, a ban on refilling in 1998, and prohibition of their use in 2000 (Naturvårdsverket, 1997). This resulted in many refrigeration systems being converted to systems with indirect cooling by means of a liquid secondary refrigerant. For many years, almost all new systems, with the exception of those containing only small quantities of refrigerant, as used in smaller grocer's shops, were built as indirect systems.

Figure 1.1.   A display cabinet cooled by an indirect cooling system by means of a secondary refrigerant. The cooling coil is placed at the bottom of the display cabinet.

Indirect cooling means that, instead of circulating the primary refrigerant through the cooling coils of the display cabinets, and hence using the cooling coils as evaporators, a secondary refrigerant (a heat transfer medium) is cooled

by heat exchange with a primary refrigerant in a chiller (normally in a plate heat exchanger). Then the secondary refrigerant is circulated to the cooling coils placed in the display cabinets. In Figure 1.1 is a schematic diagram of an indirect refrigeration system. In reality, one chiller serves several display cabinets, and not just one as shown in the diagrams. Application of indirect cooling for the display cabinets in supermarkets enables minimisation of the refrigerant charges and thus also the leakage of refrigerant. In addition, there are other advantages associated with indirect cooling, such as a more homogeneous cooling of the merchandise. However, one disadvantage of indirect cooling is that an extra temperature difference is introduced by the liquid cooler, which in turn theoretically leads to the chiller having to work with a lower evaporation temperature than in the case of direct evaporation. In addition, additional pumping power is necessary for distributing a liquid secondary refrigerant out to the display cabinets.

Lately, this system solution has received more attention and is becoming more and more common in other parts of the world as well (see e.g. Kazachki, 2006 and Minea, 2007). Indirect refrigeration systems can have some significant potential advantages over direct refrigerant systems, such as the use of compact refrigeration units with a small primary refrigerant charge (Ure, 2003a, 2003b) and more evenly distributed and lighter frost formation (Lindborg, 2004). Even though, from a theoretical point of view, an indirect (or secondary loop) cooling system ought to be less energy-efficient than a direct-expansion system, there are studies showing the opposite (Horton and Groll, 2003, Lindborg, 2004). (For more information, see Section 1.4.4.)

During the course of this research project, direct-expansion systems operated with carbon dioxide, which is an environmentally friendly natural refrigerant, have begun to make their appearance as an alternative to indirect cooling systems. Such systems involve high working pressures, and often transcritical operation during some parts of the year. The energy efficiency of such systems is not totally outlined yet. Today harmonised new F-gas regulations (SFS 2007:846 and EC Regulation no. 842/2006) at a European level do not prohibit or dissuade designers from the use of direct-expansion systems with an F-gas (synthetic refrigerants) in the medium-temperature zone of supermarkets. However, they do stipulate leakage control and frequent inspections (at time intervals dependent upon the amount of synthetic refrigerant in the system). Whether or not this development leads to a shift back to direct-expansion systems remains to be seen. Since there are many advantages with indirect systems, such as lower maintenance costs and less frost formation, and because they have proved to be at least equally or more energy-efficient than direct evaporation systems in many cases, it is likely that

many merchandisers will prefer to stay with indirect cooling systems (especially if more energy-efficient heat exchangers / cooling coils are available). However, the results from the experimental work performed for paper IV are also applicable to heat exchangers operated as evaporators, since the air side was the focus of the investigation in that study.

The cooling coil is one of the key components in a display cabinet and traditionally, different kind of tube coils, with aluminium fins on expanded copper tubes, have been used. An example of such a coil is shown in Figure 1.2. The cooling coil is either placed in the bottom of the display cabinet, as in Figure 1.1 or in the back of the display cabinet. The tube-coil heat exchanger was originally designed for evaporation of a refrigerant. When evaporation takes place in the tubes, the heat transfer coefficient on the tube side is very high. Then the tube-side heat transfer resistance constitutes a contribution to the total heat transfer resistance of the heat exchanger, which is almost negligible, since the air-side resistance is of such a high magnitude. Using a liquid secondary refrigerant as the heat transfer medium, heat transfer coefficient on the tube side will be much lower compared to the case of evaporation of a refrigerant, especially in the laminar flow regime. A lower heat transfer coefficient must be compensated by a greater temperature difference in the cooling coil, i.e. a lower supply temperature of the secondary refrigerant to the cooling coil. This in turn leads to the need for a lower evaporation temperature for the chiller and hence to a higher electric energy requirement. Although the heat transfer and pressure drop performance on the air side of finned tube coils has been thoroughly analysed by many researchers, see e.g. the article by Wang (2000), there are not many investigations concerning the liquid-side heat transfer and pressure drop performance of a cooling coil operated in the laminar flow regime in the open literature. Therefore, it was appropriate to investigate the heat transfer and pressure drop characteristics on the liquid side in this kind of heat exchanger for the purpose of finding ways for improvement.
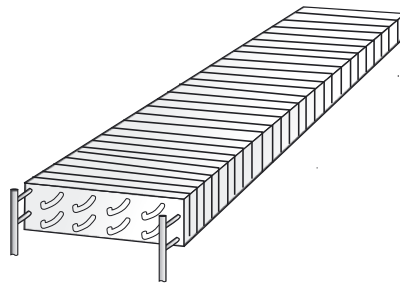
Figure 1.2.   A traditional cooling coil consisting of aluminium fins on expanded copper tubes.

Due to the fact that many secondary heat transfer media have relatively high viscosities at low temperatures, the flow regime is often laminar. This may lead to poor heat transfer, especially in tubes having circular cross-section. However, even though good heat transfer is often associated with a turbulent flow regime or a change of phase, such as evaporation or condensation, it is possible to achieve high heat transfer coefficients even for laminar flows if an appropriate design of the heat exchanger is applied. In addition, a single-phase laminar flow regime offers a better ratio between heat transfer and pressure drop than does the turbulent flow regime (Fahlén, 2000, Haglund *et al.*, 2001). Therefore, for the purpose of optimisation, a cooling coil for secondary heat transfer media could be designed in a totally different manner compared to the traditional tube coil with aluminium fins on expanded copper tubes.

Flat-tube heat exchangers, predominately with multiport minichannels on the liquid side and louvered fins on the air side, have been used for a long time in automotive applications, where compactness is important. Typical applications are radiators, intercoolers and condensers in the air-conditioning equipment. Haglund Stignor (2002) and Haglund Stignor *et al.* (2003) showed that good energy efficiency could be obtained in a display cabinet application even in the laminar flow regime if the geometry of the cooling coil is adapted to this flow regime e.g. with smaller hydraulic diameters on the liquid side. Therefore the display cabinet application could be a possible field where heat exchangers consisting of multiport extruded tubes, with several parallel minichannels, could be used. However, in order to select suitable cross-sectional geometry of the tubes and for predicting the heat transfer performance of the heat exchanger, it is of significant importance for engineers to know how to predict the tube-side heat transfer performance.

When it comes to the air side, the flat-tube configuration has some advantages over the round-tube configuration, according to Webb (1994). For example, it has better fin efficiency, and the wake region behind the flat tube does not reduce the heat transfer on the downstream fin region, as much as the can occur in round-tube heat exchangers. A limited range of operating conditions had been studied earlier, probably due to the fact that flat-tube heat exchangers have mostly been used in automotive applications. However, in recent years the studied operating ranges have been widened also to include HVAC&R (Heating, Ventilation, Air-Conditioning and Refrigeration) applications. This brings in operating conditions involving wet and frosted surfaces on the air side. The display cabinet application is different from many other heat exchanger and HVAC&R applications, since it involves low air velocities (down to 0.3 m/s) in combination with condensation of water vapour and sometimes even frosting. However, an energy-efficient indirectly cooled

cooling coil in a medium-temperature display cabinet should be able to operate without frosting. The question is, how to design the liquid and air side of the cooling coil / heat exchanger to achieve the best performance and avoid frosting?

1.2   Objectives

The objective of this research work has been to find a suitable heat exchanger design for indirectly cooled display cabinets that was considerably more energy-efficient than a traditional cooling coil with circular tubes. An efficiency that would mean that temperature differences would be so small that frosting could be avoided was aimed for. To be able to reach this goal, one purpose of the research work was to start with obtaining better knowledge of the liquid- (or tube-) side heat transfer of both traditional cooling coils and flat-tube heat exchangers when operated with liquid secondary heat transfer media. Secondly, since the flat-tube heat exchanger design seemed to be an attractive alternative to the traditional cooling coil, another purpose was to outline the heat transfer performance on the air side of such heat exchangers under dehumidifying conditions and lower air velocities than encountered in their normal operating range.

1.3   Methodology

This research work has sandwiched experimental investigations with theoretical modelling and parameter studies. Literature studies and reviews have of course been performed continuously during the research work. To start with, heat transfer and pressure drop performance of conventional cooling coils with circular tubes containing liquid secondary refrigerants were studied in full-scale experiments. The results were then used to propose more energy-efficient designs of conventional cooling coils, which are presented in the "Thesis for the degree of Licentiate of Engineering" (Haglund Stignor, 2002). The experimental results were then analysed further and are presented in Paper I.

The flat-tube heat exchanger seemed to be an interesting alternative to the traditional cooling coil for indirectly cooled display cabinets. The liquid-side (or tube-) side heat transfer was therefore studied experimentally in small-scale experiments on three single multiport extruded flat tubes with different cross-section. The results are presented in Paper II.

An outcome from the research work was that the optimising criteria for an indirectly cooled display cabinet, applied in the parameter studies presented in the "Thesis for the degree of Licentiate of Engineering" (Haglund Stignor, 2002) needed to be developed further, and so the energy efficiency of a complete cooling system, including chillers, pumps, tubing and valves, of an imagined case supermarket, was studied. Various case systems with different cooling coils / heat exchangers in the display cabinets and operated with different liquid secondary refrigerants, were compared theoretically. The results are presented in Paper III.

The study presented in Paper III showed promising results for a flat-tube heat exchanger consisting of multiport extruded flat tubes. The liquid-side heat transfer had been investigated experimentally in Paper II, but the air-side performance needed to be verified for a display cabinet condition (low air velocities in combination with condensation of water vapour). This was done in an experimental study, presented in Paper IV. In addition, this study investigated another alternative flat-tube heat exchanger design (not having multiport tubes). The studied heat exchangers were scaled down in terms of tube length and, to some extent, the depth of the heat exchangers, but the rest of the design parameters were to scale.

The model for the flat-tube heat exchanger described in Paper III was then adjusted somewhat in accordance with the results presented in Paper IV. A model was also created for the other flat-tube heat exchanger type investigated in that study. The performances of different designs of these two flat-tube heat exchanger types were then outlined and compared in a parameter study, which is presented in Paper V. Comparisons were also made with a traditional cooling coil. For this study, new optimising criteria were established and applied by consulting the results presented in Paper III. (Compared to the original optimising criteria, applied in the licentiate work, these criteria included pressure drop from the rest of the cooling system. In addition, the prediction of performances of the pumps and the compressors was also modified.)

1.4   Literature Review

1.4.1   Liquid-side Performance of Conventional Cooling Coils

Mao et al. (1998) and Hrnjak (2000) investigated heat transfer in a display cabinet cooling coil with secondary refrigerants. They reported unexpectedly

high heat transfer coefficients on the secondary refrigerant side at low Reynolds numbers. This is explained by the occurrence of thermally developing regions after the U-bends. Hong and Hrnjak (1999) investigated the U-bend effect further, and correlations for different fluids were developed (i.e. curve fits from experiments with a coaxial heat exchanger). The researchers concluded that the thermal development and heat transfer following a U-bend is very similar to that after the inlet of the tube. Later, the enhancement of internal convection heat transfer following a heat exchanger U-bend was studied further by Clarke and Finn (2008), who performed a numerical investigation by using computational fluid dynamics (CFD). They quoted Moshfeghian (1978) who found that surface temperatures following the U-bend vary circumferentially, which makes conditions different from the original inlet of the tube. The studies by Clarke and Finn (2008) were performed at a constant heat flux of magnitudes higher than that which normally occurs in a display cabinet application. They found that secondary flows in the U-bend partially invert the temperature profile. This leads to a heat transfer enhancement which exceeds that typical of pipe entry conditions. Apart from these studies, there are limited experimental data regarding heat transfer and pressure drop characteristics for cooling coils cooled by secondary refrigerants available in the literature.

Several papers presented during the last years deal with selection of liquid secondary refrigerant for secondary loop refrigeration systems, and they point out that for some liquids the flow regime could be laminar in the cooling coils, see e.g. Melinder (2005) and Ure (2003a). There are several different heat transfer correlations for laminar-flow forced convection in ducts presented in the literature, e.g. by Sieder and Tate (1936), Hausen (1943), Shah and London (1978), Gnielinski (1989, 1995) and Hong and Hrnjak (1999). Two models for laminar flow, developing temperature profile and fully developed velocity profile in circular tubes given by Gnielinski are presented in VDI (1997). One of them was valid for the constant-temperature boundary condition (Gnielinski, 1989), and one for the constant-heat flux boundary condition (Gnielinski, 1995). Predictions by the Hausen correlation (Hausen, 1943) are very similar to those of the Gnielinski, T correlation (0.5 % lower at $x^* = 0.03$ and 1.7 % higher at $x^* = 0.001$). However, this correlation is reproduced somewhat differently in different sources.

1.4.2   Liquid-side Performance of Minichannel Tubes

In the literature, there seems to be only a limited number of studies of single-phase heat transfer in multiport minichannels having a hydraulic diameter > 1 mm, especially for liquids with high viscosity. Examples of such

studies are those by Agostini *et al.*, (2002, 2004, 2006), Garimella *et al.* (2001) and Fernando *et al.* (2008). However, several studies have been performed on single-phase heat transfer in micro- and minichannels, having a hydraulic diameter ≤ 1 mm (Morini, 2004) , e.g. by Morini (2006), Morini and Spiga (2007), Maråk (2007), Lelea *et al.* (2004), Lei *et al.* (2006), Grohmann (2005) and by Caney *et al.* (2007). Several studies on two-phase condensing and boiling heat transfer for different refrigerants in multiport minichannels have also been found in the literature (see e.g. Cavallini *et al.*, 2005, Shin and Kim, 2005, Madrid *et al.*, 2007, Kuznetsov and Shamirzaev, 2007). Kandlikar *et al.* (2006) summarize the latest work on single-phase laminar-flow heat transfer in micro- and minichannels, and state that analytical solutions for macrotubes should be followed for smaller dimensions as well. They explain that the large scatter reported in the literature by many researchers might be due to difficulties in making accurate local heat flux and temperature measurements. They also point out that entrance and roughness effects can be significant for laminar-flow heat transfer. Morini (2006) investigated scaling effects, such as viscous dissipation, entrance effects and conjugate effects, for liquid flow in microchannels, and Morini and Spiga (2007) further studied the role of viscous dissipation in heated microchannels. Morini (2006) reported that scaling effects could have a significant influence on the heat transfer in certain Nusselt and Reynolds number ranges. Grohmann (2005) and Maråk (2007) both reported higher heat transfer coefficients for laminar flows than found in conventional correlations, especially in the entrance region. Both authors explain this by the increased relative surface roughness. This leads to a larger wetted surface, and in addition the roughness breaks up the boundary layers (Maråk, 2007). Moreover, Brackbill and Kandlikar (2007) reported that the roughness elements cause an early transition to turbulent flow in microchannels.

Shah and London (1978), quoted Wilbulswas (1966) and presented tabulated Nusselt numbers for thermally developing flows in rectangular channels with different aspect ratios. These data were based on numerical studies where the effects of transverse velocities in both the momentum and energy equations were ignored. Garimella *et al.* (2001) studied the effect of simultaneously developing flow on heat transfer in rectangular tubes, since most of the studies in the literature on hydrodynamically, thermally or simultaneously developing flow have been performed only on circular geometries. They measured heat transfer coefficients in the Reynolds number range $118 < Re < 10\ 671$, the Prandtl number range $6.48 < Pr < 16.20$ and the bulk-to-wall property variation range $0.243 < \mu_b/\mu_w < 0.630$. As indicated by the latter range, the measurement data were collected when cooling down the liquid inside the tube by a colder medium outside the tubes, which means that the viscosity of

the liquid at bulk temperature is lower than the viscosity at wall temperature. Heat transfer correlations valid within these ranges were developed from the measurement data. Another correlation for multiport rectangular tubes was presented in a paper by Kim and Bullard (2002). This correlation was valid for multiport tubes with adiabatic partition walls for $150 \leq Re_b \leq 500$ (In this paper, the authors refer to private communication regarding these equations). Muzychka and Yovanovich (2004) developed a model for predicting Nusselt number in the combined entrance region of non-circular ducts and channels. This model predicts both local and average Nusselt numbers and is valid for both isothermal and isoflux boundary conditions. The authors used a novel characteristic length scale, the square root of the cross-sectional area, and found that the effect of duct shape on Nusselt number was minimised. Comparisons were made with several existing models for the circular-tube and parallel-plate channel, and with numerical data for several non-circular ducts (square, equilateral triangular, rectangular). Most comparisons were made for $Pr \leq 10$, although one set of data was for $Pr = 50$. The models presented by Muzychka and Yovanovich (2004) and Gnielinski (1989, 1995) adopt a blending approach and contain theoretical results for both boundary layers and fully developed limits. The other referred equations (Garimella, *et al.,* 2001, Kim and Bullard, 2002) have a theoretical fully developed limit, but contain correlations for describing the boundary layers.

Kandlikar (2007) presented a roadmap for implementing minichannels in refrigeration and air-conditioning systems and outlined the advantages. Examples of such advantages are reduced heat exchanger size and reduced refrigerant charge in a minichannel heat exchanger, compared to heat exchangers with conventional round tubes ($d_b \approx 10$ mm).

1.4.3   Air-side Performance of Flat-tube Heat Exchangers

Jacobi and co-workers have made extensive studies of flat-tube heat exchangers with flat, wavy, strip and louvered fins under dry, wet and frosting conditions. The studies involve literature studies, calculations and experiments, and they present their results in two reports (Jacobi *et al.*, 2001, 2005). According to the authors, the research presented in those reports was probably the most comprehensive studies of flat-tube heat exchangers at that date. Jokar *et al.* (2005) studied the thermo-hydrodynamic performance of three minichannel louvered fin heat exchangers of an automotive air-conditioning system. They presented semi-empirical correlations for both the air and the liquid side obtained by using the modified Wilson-plot technique.

Kays and London (1984) presented experimental data in the form of graphs for different flat-tube heat exchanger geometries with continuous plain and ruffled fins and for inline and staggered tube arrangements. Data was presented down to $Re = 400 - 500$ and some, but not all, dimensional parameters were varied somewhat. Later, Rathod *el al.* (2007) translated those data into algebraic relations.

1.4.3.1 Plain Fins

Jacobi *et al.* (2005) performed experiments with a flat-tube heat exchanger with plain fins under dry, dehumidifying and frosting conditions. The heat exchanger had two tube rows in parallel, a tube height of 4.0 mm, a tube depth of 38 mm, a fin length of 20 mm and a fin pitch of 4.2 mm. The plain fins were continuous plate fins (no serpentine fins), and the total depth of the heat exchanger was 100 mm. The researchers found in their experiments with louvered fins that, if the tubes are in the vertical direction and the fins horizontal, the drainage of condensate water takes place through the fins (and not over the fin edge). Since this is not possible for non-interrupted surfaces, the plain fin heat exchanger was orientated in such a direction that the tubes were horizontal and the fins vertical. They found that for dry test conditions the heat transfer and friction factor performance could be predicted by uncomplicated duct-flow modelling. They compared the performance of this heat exchanger to a similar heat exchanger with wavy fins in a Reynolds number region of $300 < Re_{dh} < 2100$. They found the Colburn *j* factor to be higher or similar for the plain fins in the lower Reynolds number region ($Re \leq 1000$) compared to the wavy fins under both dry and wet conditions, while the opposite was true for higher Reynolds numbers. Almost the same relations were found for the friction factor, *f*. The Colburn *j* factor was not much affected by the condensation of water vapour for either the plain or the wavy fin geometry, while the friction factor was found to increase by a factor of 2.2 to 2.8.

During frosting conditions Jacobi *et al.* (2005) found plain and wavy fin geometries to operate for longer periods of time compared to the louver fin geometry. In addition, the plain and wavy fin geometry showed very little increase in thermal resistance as frost was deposited, in contrast to the louvered fins. The performance of the latter deteriorates quickly as frost accumulates, even though they have lower heat transfer resistance at dry conditions. Results from similar comparisons were later reported by some of the authors of the earlier mentioned report, Zhong *et al.* (2007). They also found the heat transfer resistance of plain fins to be relatively unaffected by frost, while it increased for the other fin geometries. The plain fins accumulated most frost,

but could also be operated for the longest time before the pressure drop penalty became too severe. However, since the experiments were performed at relatively high air velocities (around 2 m/s), the plain fins showed the highest heat transfer resistance compared to the other fin geometries throughout most of the tests.

1.4.3.2 Louvered Fins

A louvered fin geometry is often reported superior to plain fins (Jacobi *et al.*, 2001, 2005). Davenport (1983) compared test results from louvered samples with results from samples with plain fins. It was found that both *j* and *f* for the louvered samples were between 2 and 3.5 times greater than for the plain samples, depending on louver geometry. The results by Davenport (1983) also illustrated the irrelevance of hydraulic diameter for the performance of louvered surfaces, but showed that the hydraulic diameter was relevant for the samples with plain fins. Instead, for louvered surfaces, louver-pitch based *Re* was recommended. Colburn *j* factors were presented down to $Re_{Lp} = 100$ and not for lower *Re*. The reason was that the curves flattened at low velocities, which was thought to be caused by boundary layer thickening on the louver surface causing changes in the air flow pattern through the fins of the heat exchanger. Therefore, *j*-curves should not be extrapolated to lower *Re* values than those that have been verified, since this will almost certainly result in an overestimation. Achaichia and Cowell (1988) presented performance data for a range of plate and flat-tube and louver-fin geometries. Their resulting Stanton number (*St*) curve demonstrated characteristics that were consistent with the earlier findings by (for example) Davenport (1983); that at high *Re* the fluid flow is predominately parallel to the louvers, but as *Re* is reduced the flow direction becomes increasingly aligned with the plate fins. It was shown that this effect caused a flattening of the *St*-curves.

Jacobi *et al.* (2005) carried out experiments with a heat exchanger with louvered fins having a fin pitch of 5.08 mm and a louver pitch of 1.14 mm, and compared its performance for dry and wet conditions. The difference in performance was found to be very small, which proves that the flow is duct-orientated, as was expected for such large fin pitch. Therefore, no heat transfer enhancement by boundary-layer restarting was obtained for either of the test conditions.

1.4.4   Indirect (or Secondary-loop) Cooling Systems

1.4.4.1   General Experiences with Indirect / Secondary-loop Refrigeration Systems

In different papers, Ure (2003a, 2003b) aims to describe the experience gained from the European installations. This experience includes problems related to operation of these installations, from design to commissioning stages, and also lessons learnt from these applications. He points out that the selection of secondary refrigerant is of great importance, since their physical properties differ. It is essential to find the right balance between the viscosity, specific heat and thermal conductivity for optimum design efficiency. When it comes to the freezing point of the secondary refrigerant it is common practice to chose a fluid with a freezing point at least 5-10 °C below the system operating temperature, according to Ure (2003b). He also points out the importance of minimising air contamination for safe and reliable operation, and that the corrosion inhibitors are the most critical components of the secondary refrigerant.

Aittomäki and Kianta (2002) presented a project which had the aim of providing some specified tools and instructions for designing and building indirect cooling systems. The project developed a guide book for designers and contractors and a computer tool for dimensioning the pipe network. The guidebook covers the entire design of an indirect cooling system, including different types of cooling systems, secondary refrigerants, instructions for building the system, heat exchangers, control and balancing and defrosting.

Later, Melinder (2009) presented a handbook for indirect cooling and heat pump systems. This book gives guidelines to designers regarding, for example, selection of secondary refrigerants and different components and their placement in the system. In addition, the handbook contains information about environmental and safety aspects, corrosion and humidity control, maintenance and how to optimise the system from an energy-saving and economic point of view.

Granryd (2007) discusses optimum flow rates in indirect systems. He presents some examples and general relations for the pumping power resulting in minimal total energy demand and maximum net cooling capacity, since there are two different optima. In the examples given, the pumping power ratio (the ratio of the pumping power to the cooling capacity) is about 1-2 % when the object is to save energy, and about four times higher for maximising the net refrigerating system capacity. The author states that the impression is that, in

many practical cases, a higher pumping power is being used than would be optimal from an energy use point of view.

Other papers / articles dealing with general experiences with indirect systems are presented by Cooper (1997), Horton and Groll (2001), Hrnjak (1997), Nyvad and Lund (2000), Verwoerd *et al.* (1999) and Walker (2000).

1.4.4.2   Comparisons of Direct-expansion Systems with Indirect / Secondary-loop Refrigeration Systems

Indirect refrigeration systems can have some significant potential advantageous over direct refrigeration systems since, according to Ure (2003a, 2003b) for example, it is possible to design and manufacture factory-built compact refrigeration units with a small primary refrigerant charge. However, he also points out that a secondary refrigerant circuit means an extra cost for the pump and heat exchanger, and an added temperature difference.

A presentation given by Svensson, which was reported in the reference (Svensson, 2005), highlighted a number of benefits of a secondary loop refrigeration system. Except for that stated above, he claimed that experience from the field shows that the indirect refrigeration systems result in much lighter frost formation than is the case for a direct-expansion system. Less ice, which acts as insulator, leads to improved thermal conductivity. In addition, fewer defrosts are required, and if the defrost is done with warm secondary refrigerant from within the piping, instead of electric defrosting from outside the piping as in a direct-expansion system, the temperature of the displayed products remain more stable.

Lindborg (2004) claims that the investment cost for an indirect refrigeration system might be higher than that for a direct-expansion system, but that according to his experience many comparisons of real systems show that the indirect system is often more energy-efficient if it is energy use over the whole year that is compared, and not just the electric power requirement under design conditions. One of the reasons for this is that the evaporation temperature at part load can be kept less varying in an indirect system, resulting in a higher evaporation temperature and less frost formation compared to a direct refrigeration system. In addition, the defrost energy is less in an indirect system, partly due to less frost formation and partly due to the fact that the heat transfer surfaces needs less heating when defrosting is performed from within the tubes compared to from the outside, as in a direct-expansion system.

Horton and Groll (2003) compared the performances of a direct-expansion refrigeration system and a secondary loop refrigeration system of equivalent cooling capacities in a supermarket application. The comparison of the two systems was based on initial cost of purchasing and installing the two different systems and operating costs, including coefficient of performance, COP, and maintenance costs. The authors had developed and validated a numerical simulation model, which they used in predicting the refrigeration system performance. They found that an ammonia/hydrofluoroether secondary loop refrigeration system could deliver the same cooling capacity as a direct-expansion HCFC-22 refrigeration system, using 15 % less energy.

From the above, the conclusion can be drawn from the comparisons between indirect cooling systems and direct-expansion systems that, in many cases, the indirect cooling systems have been shown to be more efficient than the direct-expansion systems. However, the opposite is also reported in other papers, for example by Kruse (2005), who refers to measurements performed in a supermarket with an indirect cooling (refrigeration) system, where ammonia was used as the primary refrigerant and Tyfoxit as the secondary refrigerant. For this supermarket, the energy consumption was 15 % higher than that of a direct R404A or a R407C system. He also refers to other supermarkets, where the energy consumption was 18 % higher for an indirect system using Tyfoxit and 11 % higher for a system using High Cool (the author might have used the wrong spelling and meant "Hycool" – the same liquid as has been studied in this research work).

1.4.4.3 Environmental Benefits of Indirect / Secondary-loop Refrigeration Systems

Indirect refrigeration systems enable operation with small refrigerant charges. Environmental concerns over ozone depletion and global warming have led to the search for alternative refrigeration technologies. The aim is to minimise refrigerant usage and thereby leakages. Secondary refrigeration can be considered as one of the options available to designers to help overcome these global problems, according to Ure (2003a, 2003b).

1.4.4.4 Computer / Simulation Models

Arias (2005) has developed a computer model that predicts building heating and cooling loads, HVAC system performance and refrigeration system performance of a supermarket. The focus of the model is on energy use, environmental impact, i.e., Total Equivalent Warming Impact (TEWI) and life cycle cost (LCC). The program can simulate seven different system solutions for the refrigeration system in a supermarket (indirect system, direct-

expansion systems, cascade systems, systems with heat recovery etc). This model is an excellent tool for many types of comparison. However, it does not allow comparisons of using different types of cooling coils in the display cabinets, for example.

Horton and Groll (2000) developed a numerical model of secondary-loop refrigeration systems for medium-temperature supermarket applications to investigate the effect of various components and operating conditions on cycle efficiency. One of the first studies they conducted was to investigate the effect on cycle efficiency of leakage of heat into the supply and return lines due to inadequate insulation. It was concluded from the study that proper insulation of the secondary fluid distribution lines is extremely important to ensure good performance.

1.4.4.5   Liquid Secondary Refrigerants

In display cabinet applications, propylene glycol is widely used as the liquid secondary refrigerant, but there are many other secondary refrigerants available on the market. However, not all of them are suitable for supermarkets due to reliability and health aspects. Reliable thermophysical data are essential in order to predict the performance of a cooling system operated with any given certain secondary refrigerant.

Melinder (1997a, 1997b, 1997c) has made extensive investigations of thermophysical properties, such as density, specific heat, viscosity and thermal conductivity, of liquid secondary refrigerants. He presents data for several commonly used liquid secondary refrigerants in the form of charts and tables in the references Melinder (1997b) - English and French - and in Melinder (1997c) - Swedish and English. The secondary refrigerants investigated by Melinder (1997a, 1997b, 1997c) are principally aqueous solutions without additives. However, most of the secondary refrigerants available on the market do contain additives, e.g. inhibitors. In addition, there are secondary refrigerants consisting of a mixture of substances. In such situations, manufacturers' data of thermophysical properties are necessary. A later publication by Melinder includes some additional commercial secondary refrigerants in the comparisons (Melinder, 2005).

Other papers in which the properties of secondary coolants (refrigerants) are described and outlined are those by Briley (2004a, 2004b).

1.5 Motivation and Selection of Studied Parameter Range

1.5.1 Paper I

According to Melinder (2005) the correlation presented by Sieder and Tate (1936) can be used for laminar flow of liquid secondary refrigerants in a cooling coil, and the tube length used in the correlation might represent one straight tube length, but there is no reference to any experimental work. However, no papers known to the authors, except for the ones presented by Mao *et al.* (1998) and by Hong and Hrnjak (1999) to some extent (referred to above), deal with the questions: Which correlations should be used for a cooling coil application? Should the boundary layers be considered as developing or fully developed? Which is the most appropriate boundary condition – constant wall temperature or constant heat flux? For designers of cooling coils and indirect secondary loop refrigeration systems, this is important information. Consequently, there is a need for experimental results for full-scale cooling coils, and therefore such experiments have been performed and the results are presented in this paper.

1.5.2 Paper II

No experimental evaluation of the liquid-side heat transfer performance of multiport extruded-tube geometries similar to all those shown in Figure 2.2, and operated with different secondary refrigerant liquids, have been found in the literature by the authors of this paper. As stated above, studies of different rectangular-tube geometries have been found, but none for a geometry similar to the one of the MPE2 tube. In addition, no study was found that concerned Prandtl numbers as high as could be found in a heat exchanger operated with propylene glycol in a display cabinet application, which would be $Pr \approx 100$. Therefore, an experimental evaluation was performed for the three different tube geometries in the Prandtl number range $8.4 < Pr < 107$. One significant difference between the present study and the one performed by Garimella *et al.* (2001) is that, in their study, the tube was cooled, while in the present study it is heated (as would be the case in a display cabinet application). Then the bulk-to-wall property variation range, μ_b/μ_w, is greater than unity, and so the liquid viscosity at bulk temperature is higher than that at wall temperature.

In some other experimental studies of multiport tubes found in the literature - for example, the one performed by Agostini *et al.* (2006) - the tube has been heated using the Joule effect by passing an electric current from brazed electrodes through the tube wall, which means that the heat flux is constant

along the tube length. Other studies have used a coaxial heat exchanger, e.g. in the one performed by Garimella *et al.* (2001). However, in a liquid-to-air heat exchanger in a display cabinet application, neither the pure constant-temperature boundary condition nor the constant-heat flux boundary condition prevail. However, in experiments with full-scale cooling coils performed by Haglund Stignor *et al.* (2007) (Paper I) a better agreement was found with the Gnielinski (1989) model for the constant (uniform) wall temperature boundary condition than in the model presented by the same author for constant heat flux boundary condition (VDI, 1997, Gnielinski, 1995). Thus it was concluded that the constant-temperature boundary condition would generally describe the conditions at the wall better than the constant-heat flux boundary condition. Therefore, in the present study, a coaxial heat exchanger has been used in order to perform the experiments with wall conditions as close to the constant-temperature boundary condition as possible.

1.5.3 Paper III

No studies of how energy use and cost for a system are influenced by the selection of cooling coil / heat exchanger design were found in the literature survey. This was therefore the objective of this study, where different indirect cooling systems have been compared by studying a number of cases. Even though the cases are simplified versions of reality, they have been selected to be representative of a large number of supermarkets in Sweden. However, some of the cases are only hypothetical so far.

1.5.4 Paper IV

In a display cabinet application, due to frosting, the fin pitch is often equal to or greater than 5 mm in order to have long operating periods between the defrosts. If frosting could be minimised or avoided, the fin pitch could be decreased. However, due to the low air velocities and presence of dust and condensed water it is not desirable to have too small fin pitches in the heat exchangers. A fin pitch of around 4 mm has therefore been the focus of investigations for this study. A source database presented by Jacobi *et al.* (2005) shows that the louver pitch for most specimens ranges from 1 to 2.3 mm. Due to the low air velocities in a display cabinet application, the main air flow will almost certainly pass between the fins and not through the louver gaps, even if the fins are louvered. In such case, the louver will only result in an additional pressure drop over the heat exchanger. Under such circumstances, heat exchangers with flat tubes and plain (flat) fins will be preferable. Hence flat-tube heat exchangers with plain fins are an interesting

alternative for indirect cooling of the air in display cabinets and other applications where dehumidifying conditions are combined with low air velocities. In addition, for the display cabinet application, it was of interest to study the performance at even lower air velocities than has been done in earlier investigations. It was also of interest to find out if condensed water is drained as effectively for serpentine plain fins as for continuous plate fins. Therefore, two different flat-tube heat exchangers with plain fins of the different types and different tube depth have been investigated experimentally in this study.

1.5.5 Paper V

There are no other studies known to the authors of this paper investigating how much the energy efficiency of an indirectly cooled display cabinet would be improved if the traditional cooling coil was replaced by a flat-tube heat exchanger, FTHE, designed for the display cabinet application. This has therefore been the purpose of the present study.

2 Experiments

2.1 Description of Tested and Evaluated Objects

In this research work different types and designs of cooling coils with circular tubes and flat-tube heat exchangers have been studied both experimentally and theoretically in parameter studies. In most cases, the aim has been experimentally to verify promising designs resulting from the parameter studies. However, it is not always possible to find "real" designs or to construct prototypes that exactly match the desired designs. In the sections below, design parameters of the evaluated (experimentally or theoretically in models) cooling coils and heat exchangers are outlined in tables and figures. Further design parameters and, in some cases, descriptions of the manufacturing process can be found in the respective paper.

2.1.1 Conventional Cooling Coils

The dimensions of the cooling coils that were evaluated experimentally in Paper I and theoretically in Papers III and V are presented in Table 2.1 (see Figure 2.1 for description of nomenclature). As can be seen, the dimensions of cooling coils B5 and D are very similar.

Table 2.1.   Dimensions of evaluated conventional cooling coils.

	D	d	p_t	p_l	$n_{,t}$	$n_{,l}$	L_{tube}	N_{pc}	p_{fin}	δ_{fin}	Fin type	Paper No.(*)
	(mm)	(mm)	(mm)	(mm)			(mm)		(mm)	(mm)		(e / t)
B2	12.5	11.7	30.0	26.0	8	8	2250	4	4.0	0.25	wavy	I (e)
B5	10.0	9.3	25.0	21.7	10	10	500	10	4.0	0.20	wavy	I (e)
D	10.0	9.2	24.0	20.8	10	10	500	10	4.0	0.25	plain	III (t)
R	15.5	14.7	50.0	50.0	10	2	2250	2	6.0	0.25	plain	III (t) V (t)

*e = experimentally, t = theoretically
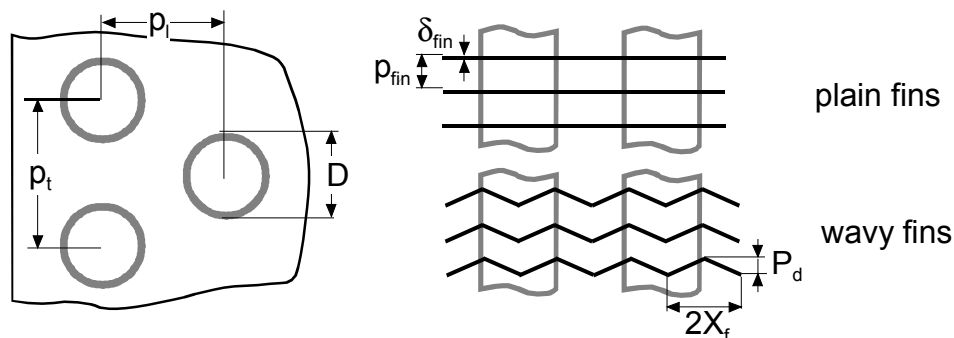
Figure 2.1.   Schematic pictures of nomenclature of cooling coils.

2.1.2 Multiport Extruded Tubes

Three different multiport extruded (MPE) tubes of aluminium with different cross-sections were evaluated in small-scale experiments in Paper II. The cross-sectional geometry of the tubes are shown in Figure 2.2 and in Table 2.2.
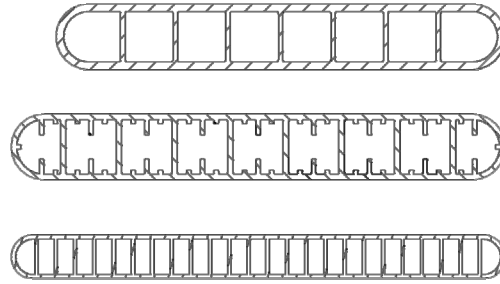
Figure 2.2.   Geometry of the cross-sections of the evaluated MPE tubes; MPE1 (top), MPE2 (middle) and MPE3 (bottom).

Table 2.2.   Dimensions of the evaluated MPE tubes

		MPE1	MPE2	MPE3
Outer dimensions	(mm^2)	41×6	45×6	45×4
Hydraulic diameter, d_h	(mm)	4.73	3.19	2.06
Hydraulic diameter (plain), $d_{h(plain)}$	(mm)		4.68	
Number of channels		8	9	25
Thickness of partitioning wall, δ_{fin}	(mm)	0.4	0.5 / 0.4	0.3
Square root of cross-sectional duct area, $\sqrt{A_{c,duct}}$	(mm)	4.68	4.44	2.15

2.1.3 Flat-tube Heat Exchangers

Two different heat exchanger types, having flat tubes and plain (flat) fins on the air side, were evaluated experimentally in Paper IV and theoretically in parameter studies in Papers III and V (only one in Paper III). The dimensions of the heat exchangers are presented in Table 2.3 (see Figure 2.3 - Figure 2.5 for description of nomenclature). Figure 2.5 describes the liquid circuitry of the heat exchangers. One of the heat exchanger is called "flat-fin-core" by its manufacturer, and is therefore denoted FFC in Paper IV. This heat exchanger type is denoted FTHE2 in Paper V. The other evaluated heat exchanger consists of multiport extruded tubes (MPE tubes) and folded serpentine flat (plain) fins on the air side. This heat exchanger is denoted MPET-HE in Paper IV, FTHE in Paper III, and FTHE1 in Paper V. As far as the air side of the heat exchanger is concerned, the main difference between FTHE1 (MPET-HE) and FTHE2 (FFC) type is that the latter heat exchanger type has continuous plain fins, while the FTHE1 heat exchanger has serpentine fins

22

folded between the flat tubes. In addition, the tube depth (or outer width), i.e. the length of the airside channels, is much greater for the FTHE1 heat exchanger than for the FTHE2 heat exchanger.

As can be seen in Table 2.3, even if the outer dimensions differ, the other design parameters of the FFC heat exchanger evaluated in Paper IV are almost identical to those of the various FTHE2 heat exchangers evaluated in Paper V. In the same way, the "inner" design parameters of the MPET-HE evaluated in Paper IV are very similar to the corresponding design parameters of the FTHE1 heat exchangers evaluated in paper III and V.

(a)

(b)

(c)
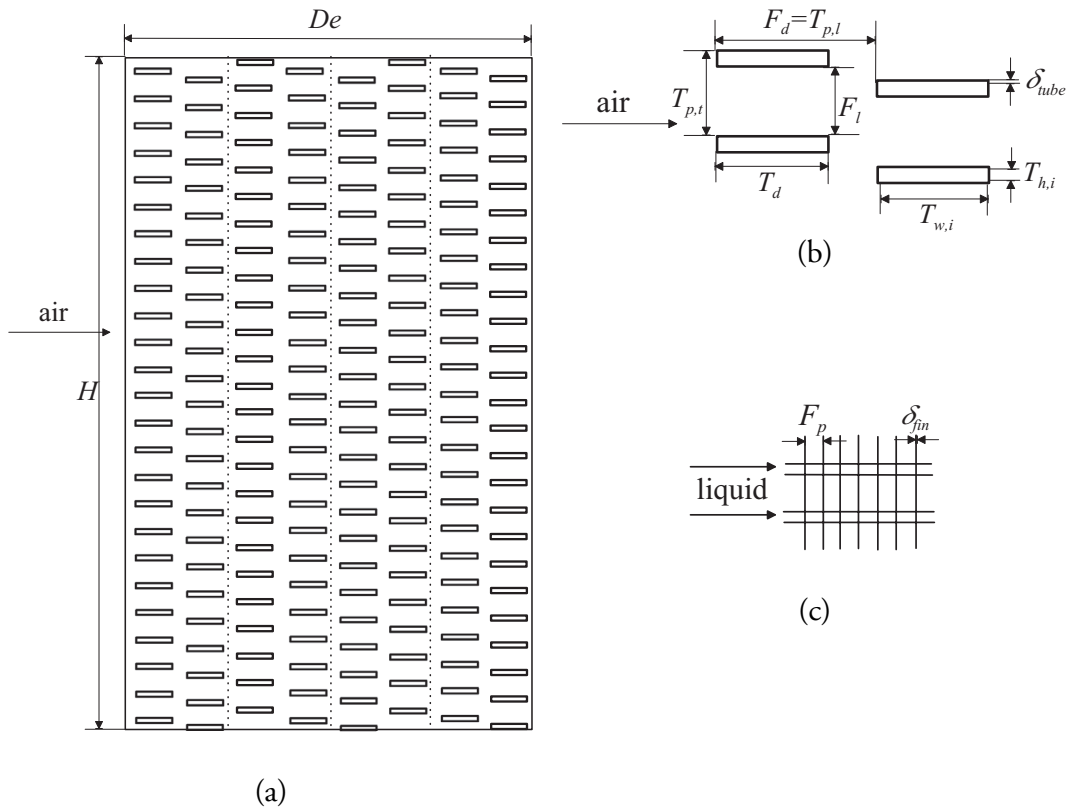
Figure 2.3.   Schematic drawing and nomenclature of the "flat-fin-core" heat exchanger denoted FFC (Paper IV); (a) side view of cross-section, (b) enlargement of cross-section of staggered tube layout, (c) plate fin geometry, (c)

Table 2.3.   Dimensions of the evaluated heat exchangers

			FTHE1									FTHE2						
Paper No.			*3, 5*	*5*	*5*	*5*	*5*	*5*	*5*	*5*	*4*	*5*	*5*	*5*	*5*	*5*	*5*	*4*
			4*10	4*10*2	6*7	6*7*2	8*5	8*5*2	10*4	10*4*2	MPET-HE	8*33	8*33*2	12*22	12*22*2	16*16*1	16*16*2	FFC
Dimension																		
Height	H	mm	250	250	167	167	125	125	100	100	250	330	330	220	220	160	160	250
Width (tube length)	W	mm	2250	1100	2250	1100	2250	1100	2250	1100	460	2250	1100	2250	1100	2250	1100	458
Depth	De	mm	200	200	300	300	400	400	500	500	118	152	152	228	228	304	304	152
Tube pitch, transversal	$T_{p,t}$	mm	25	25	23.8	23.8	25	25	25	25	23.1	10.0	10.0	10.0	10.0	10.0	10.0	10.0
Tube pitch, longitudinal	$T_{p,l}$	mm	50	50	50	50	50	50	50	50		19.0	19.0	19.0	19.0	19.0	19.0	19.0
Fin pitch	F_p	mm	4	4	4	4	4	4	4	4	3.95	4	4	4	4	4	4	3.61
Fin thickness	δ_{fin}	mm	0.2	0.2	0.2	0.2	0.2	0.2	0.2	0.2	0.20	0.11	0.11	0.11	0.11	0.11	0.11	0.11
Fin length	F_l	mm	19	19	17.8	17.8	19	19	19	19	19.1	7.7	7.7	7.7	7.7	7.7	7.7	7.7
Hydraulic diameter (air-side)	$d_{h,a}$	mm	6.3	6.3	6.3	6.3	6.3	6.3	6.3	6.3	6.3	5.2	5.2	5.2	5.2	5.2	5.2	4.8
Fin depth	F_d	mm	45.0	45.0	45.0	45.0	45.0	45.0	45.0	45.0	45.0	19.0	19.0	19.0	19.0	19.0	19.0	19.0
Tube depth	T_d	mm	45.0	45.0	45.0	45.0	45.0	45.0	45.0	45.0	45.0	13.6	13.6	13.6	13.6	13.6	13.6	13.6
Tube wall thickness	δ_{tube}	mm	0.4	0.4	0.4	0.4	0.4	0.4	0.4	0.4	0.4	0.2	0.2	0.2	0.2	0.2	0.2	0.2
Hydraulic diameter (liquid side)	$d_{h,b}$	mm	4.73	4.73	4.73	4.73	4.73	4.73	4.73	4.73	2.06	3.32	3.32	3.32	3.32	3.32	3.32	3.32
No. of tubes trans. to air flow	$N_{tube,t}$	(-)	10	10	7	7	5	5	4	4	10	33	33	22	22	16	16	25
No. of tubes, long. to air flow	$N_{tube,l}$	(-)	4	4	6	6	8	8	10	10	2	8	8	12	12	16	16	8
No. of passes (HEs), liquid side	n	(-)	4	4	6	6	4	4	5	5	2	4	4	4	4	4	4	4
No. of parallel tube-rows in each pass	$N_{tube,p}$	(-)	1	1	1	1	2	2	2	2	1	2	2	3	3	4	4	2
No. of parallel HEs, long. to air flow	$N_{HE,p}$	(-)	1	2	1	2	1	2	1	2	1	1	2	1	2	1	2	1
MPE tube	1'	1'	1'	1'	1'	1'	1'	1'	1'	1'	3	-	-	-	-	-	-	-

'MPE tube 1 but with 9 channels instead of 8
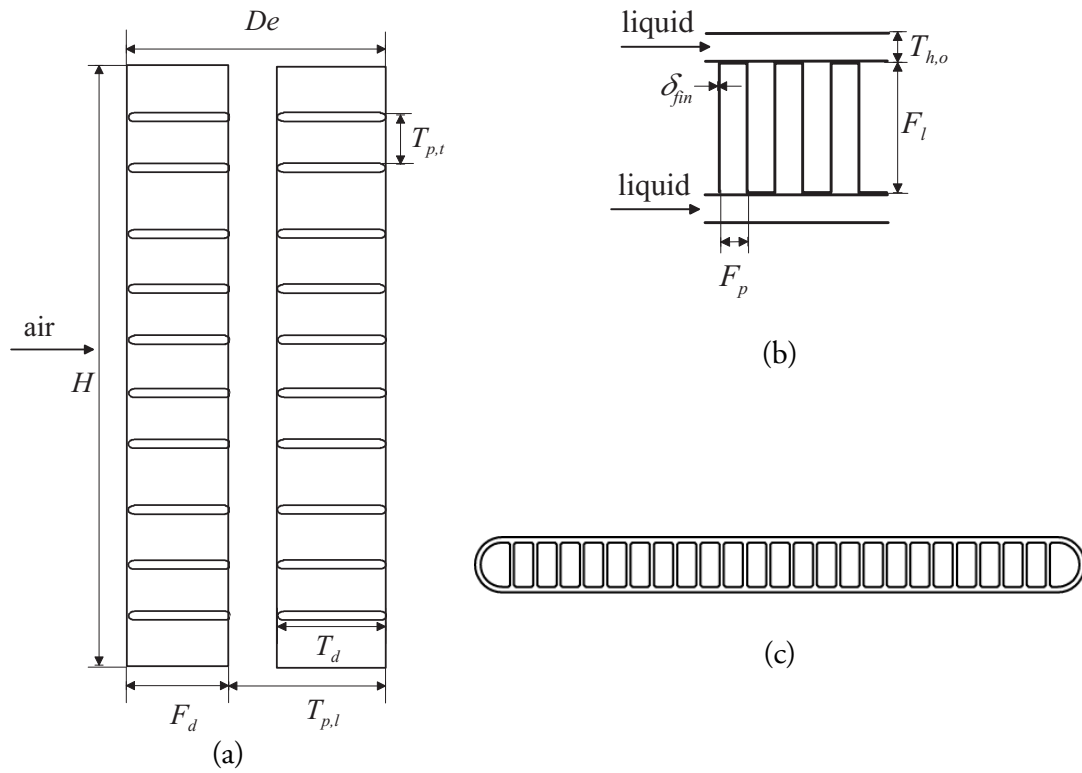
Figure 2.4. Schematic drawing and nomenclature of the multiport extruded tube heat exchanger denoted MPET-HE (Paper IV) (a) view of cross-section, (b) serpentine fin geometry, (c) cross-section of MPE tube.
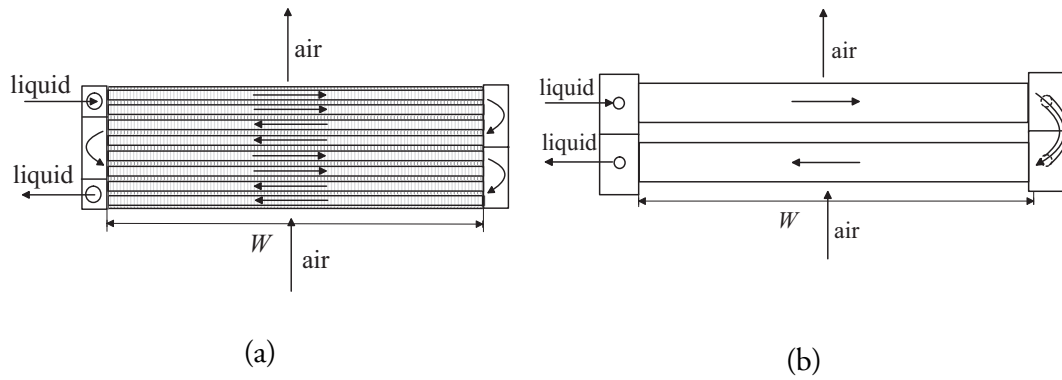
Figure 2.5. Liquid circuitry of the FFC and the MPET-HE heat exchangers (Paper 4).

2.2 Secondary Refrigerants used in the Experiments (Paper I, II and IV)

In this research project, three secondary refrigerants - propylene glycol (39 %$_w$), Temper –20 and Hycool 20 - have been used in the experiments. Thermophsyical data of these secondary refrigerants have also been used in the created calculation models. Temper –20 is the brand name of a mixture of aqueous solutions of potassium formate, potassium acetate and additives. Hycool 20 consists of an aqueous solution of potassium formate and additives. All three secondary refrigerants had the same freezing point, -20 °C. To be exact, Hycool 20 had a freezing point of –21.5 °C, but is recommend for applications requiring a freezing point at -20 °C. Thermophysical properties of the secondary refrigerants are shown in Figure 2.6.
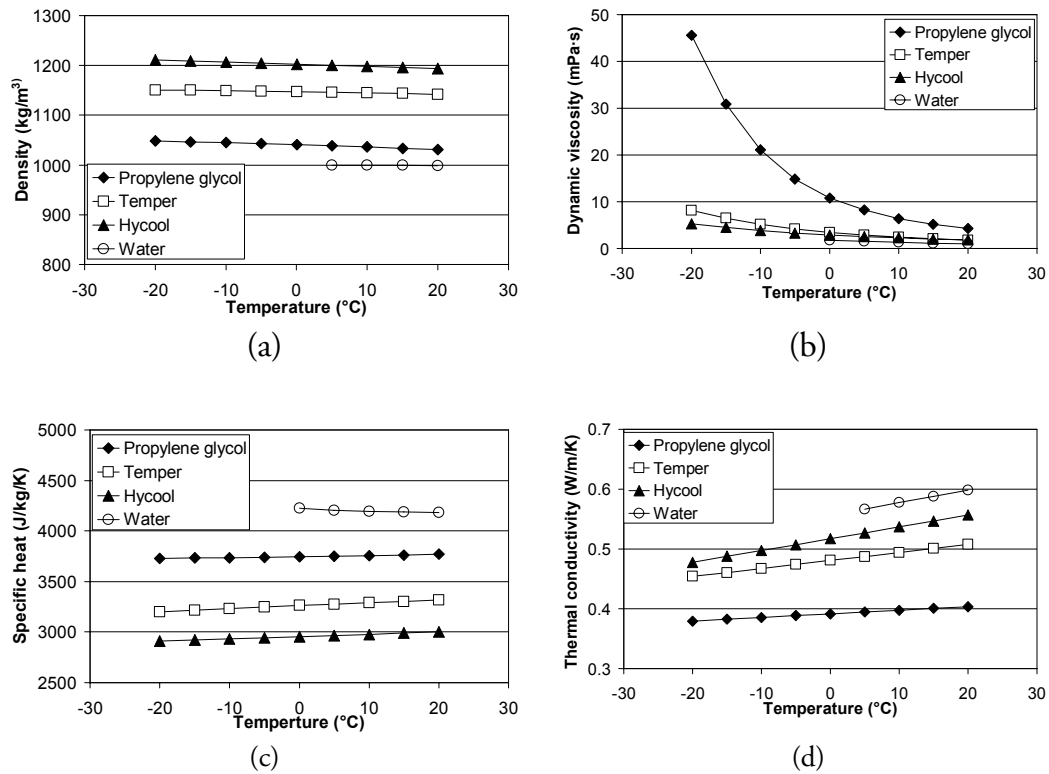
Figure 2.6.   Density, ρ (a), specific heat, c_p (b), dynamic viscosity, μ (c), and thermal conductivity, λ (d), of propylene glycol (39 %$_w$), Temper –20, Hycool 20 and water as a function of temperature.

Thermophysical data for propylene glycol were taken from Melinder (1997c) and Fahlén (1994), and manufacturers' data were used for Temper –20 and Hycool 20. In the small-scale experiments with a single tube, water was also used as a secondary refrigerant. Then data from Hellsten (1992) was used. The reason for choosing propylene glycol for the experimental evaluation was that it is a widely used secondary refrigerant in supermarket applications, even

though its performance in some situations is poor. Temper –20 and Hycool 20 and other secondary refrigerants with similar formulae have lately become more and more common. Their viscosity is lower than that of propylene glycol (see Figure 2.6b) and so they perform better than propylene glycol in many situations. However, one drawback of these aqueous solutions of organic salts is that they are corrosive when oxygen is present, which might lead to problems such as leakage. In order for systems operated with corrosive secondary refrigerants to deliver satisfactory performance, installation aspects such as material compatibility and deaeration of the system are very important.

2.3 Experimental Set-up and Methods

2.3.1 Experiments with Complete Heat Exchangers (Papers I and IV)

The experimental set-up used in the experiments with the complete heat exchangers, including the measuring points, is shown schematically in Figure 2.7. An air conditioning plant controlled temperature, humidity and flow. In order for the air flow to be homogeneous when reaching the heat exchanger, air duct sections were mounted upstream and downstream of the evaluated heat exchangers. A perforated plate was mounted at the inlet of the first duct section. In the study where the air side performance was the main focus of the investigations, the lengths of the duct sections were slightly more than seven hydraulic diameters of the duct cross-section (Paper IV). In the experiments presented in Paper I, the duct sections were somewhat shorter.

In Paper I, the air flow was measured by a vortex flow meter. For B2 this was used as a part flow meter in combination with a modified orifice plate. In the study presented in Paper IV, the air flow was measured by measuring the pressure difference over a Pitot tube by a micromanometer. The air temperature was measured before and after the heat exchangers in the air flow direction. The number of temperature sensors was dependent upon the cross-sectional area of the duct and the probability of temperature variations in the cross-section. In front of the heat exchanger, the air temperature was measured by one Pt-100 temperature sensor and five thermocouples distributed in the cross-section at a distance of 300 mm (B2 and B5), 225 mm (FFC) and 269 mm (MPET-HE) from the heat exchanger inlet. The thermocouples were used to determine the spatial and temporal temperature variations over the cross-section of the air-flow. Behind the heat exchanger, one (Paper IV and B5) or two (B2) Pt-100 sensors and nine (Paper IV and B5) or 15 (B2) thermocouples measured the air temperature at a distances of 300 mm (B2 and

B5), 365 mm (FFC) and 409 mm (MPET-HE) from the heat exchanger. All the Pt-100 sensors were shielded from radiation. The relative humidity of the air was measured by capacitive relative humidity meters (B2 and Paper IV) before and after the heat exchanger. For B5 a chilled mirror hygrometer was used instead to measure the humidity of the incoming air.

The air-side pressure drop was measured by a micromanometer. There were two cross-sections for pressure measurement; one prior to, and one after, the heat exchanger. Each such cross-section was preceded by a non-disturbed duct section, five hydraulic diameters (of the duct) long, and followed by a duct-section with a length of two hydraulic diameters (Paper IV). In each cross-section, there were four taps, one on each side of the duct. The atmospheric pressure was measured by a manometer.

The temperature and flow of the secondary refrigerant were controlled via a liquid loop. The liquid flow was measured by an inductive flow meter (Paper I) or by a Coriolis mass flow meter (Paper IV). The liquid temperatures in and out of the heat exchanger were measured by Pt-100 temperature sensors. In the experiments presented in Paper IV, each temperature sensor was preceded by a mixing device. The pressure drop on the liquid side of the heat exchanger was measured by a differential pressure transmitter.
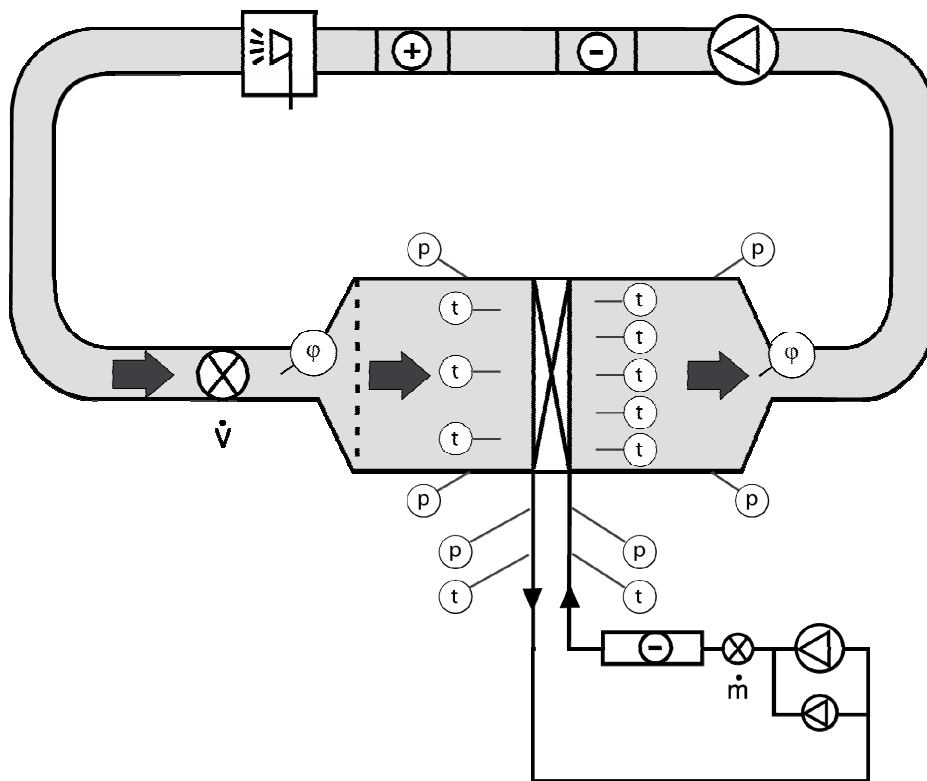
Figure 2.7.   Schematic drawing of the experimental set-up for complete heat exchangers, including measuring points (not to scale).

2.3.2   Small-scale Experiments on Single Tubes (Paper II)

A schematic picture of the experimental set-up is shown in Figure 2.8. The set-up consisted of three liquid loops. The heating loop (1) was filled with water; the test loop (2) contained the secondary refrigerant used in the evaluations, and ethylene glycol (50 %$_w$) circulated through the cooling loop (3). The MPE (Multi Port Extruded) tube that was evaluated was placed inside a tube with a circular cross-section of larger diameter (60 mm) than the outer dimensions of the MPE tube. The length of the test section was 2000 mm. The total length of the evaluated tube was 2400 mm and the test section was preceded by a 350 mm long non-heated tube section. In this way, the velocity profile of the liquid inside the tube is fully developed, but the temperature profile, starts to develop when the liquid enters the test section. Outside the outer tube there was a layer of 30 mm "Armaflex" insulation.

P	Pump
R	Controller
RV	Controlling valve
SV	Adjusting valve
AV	Closing valve
EP1	Electric heater
t	Temperature sensor
p	Pressure sensor
$\dot{m}$	Mass flow meter
$\dot{V}$	Volume flow meter
$\dot{W}_e$	Electric energy/power meter
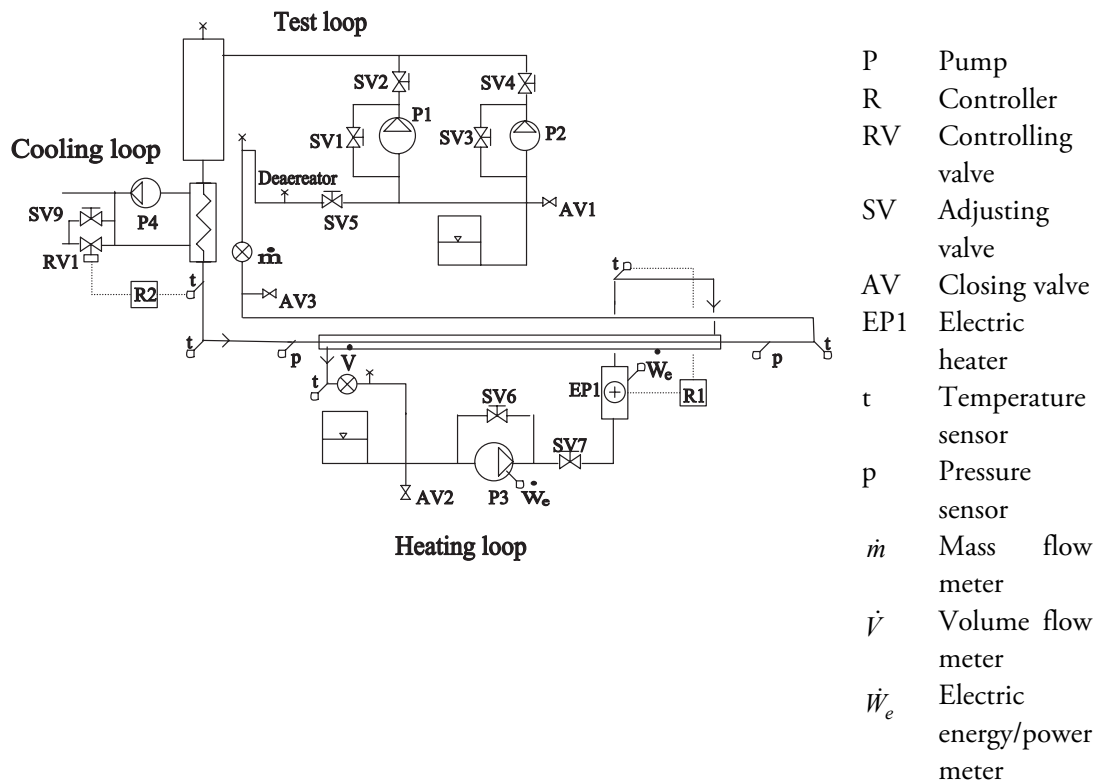
Figure 2.8.   Schematic drawing of the set-up for the small-scale experiments on single tubes, including measuring points (not to scale).

The temperature of the secondary refrigerant in the test loop was controlled by the cooling loop via a plate heat exchanger. A thyristor-controlled electric heater controlled the temperature of the water in the heating loop. The liquid flow in the test loop was measured by a Coriolis mass flow meter. The temperatures of the liquid entering and leaving the MPE test tube, and of the heating water entering and leaving the coaxial heat exchanger, were measured

29

by Pt-100 temperature sensors. An inductive volume flow meter measured the water flow. The outer surface temperature of the MPE tube was measured by 24 thermistor sensors, shown schematically in Figure 2.9. These were mounted in six different positions along the tube length; at 10, 400, 800, 1200, 1600 and 1990 mm from the inlet of the test section. In each position, there were four thermistor sensors; two on the upper side and two on the lower side. A heat conducting paste was used in order to ensure good thermal contact between the sensor and the tube wall. The sensors were mounted on the tube wall by tape. In addition, this tape insulated the sensors from the circulating water outside the test tube.

The inclined arrows in Figure 2.9 mark the measurement positions of the outer surface temperature of the MPE tube. The horizontal arrows mark the inlet and outlet of the liquid secondary refrigerant flow, and the vertical arrows mark the inlet and outlet of the heating water flow. In order to enable calculation of the energy balance of the system, the electric power input to the electric heater was measured by an electric energy meter, and the electric power input to the water pump was measured by an electric power meter.
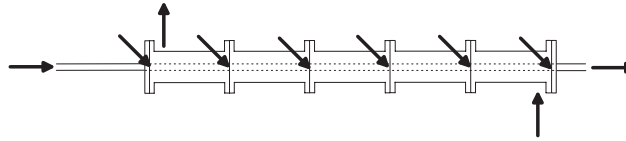
Figure 2.9.   Schematic illustration of the MPE tube placed inside a tube with a circular cross-section of larger diameter than the outer dimensions of the MPE tube. (Not to scale).

2.3.3   Data acquisition system

The data acquisition system was based on pulse counting for measurement of the liquid flows and for electric energy to the heater (Paper II). For the rest of the measurands, it was based on voltage measurements. When it comes to the temperature sensors, an energising current was generated by the data acquisition system and their resistance could be determined by measuring the voltage.

3 Data Reduction Methods

There are different methods for reducing the measurement data to heat transfer performance of a heat exchanger. However, even though the calculation procedures differ for the various methods, the output is the same. The methods that have been used in the different stages of this research work are described below. All the mentioned methods are thoroughly explained and described by Shah and Sekuliç (2003), and briefly summarised below (see section 3.1 - 3.3).

The (Log-) Mean Temperature Difference Method was used for the data reduction of the experiments with the conventional cooling coils, presented in Paper I, and the multiport tubes, presented in Paper II. This method was also applied in the model for predicting the heat transfer performance of conventional cooling coils, presented in Papers III and V.

Data reduction of the measurement results analysed in Paper IV, used the ε-NTU method in combination with the similar P-NTU method. These methods were also applied in the models for flat-tube heat exchangers used in the studies described in Papers III and V. The evaluated flat-tube heat exchangers consist of two to eight cross-flow heat exchangers, connected in series with an overall counter-flow arrangement. The reason for switching the data reduction method during the course of the research work was that it was not possible to find mathematical expressions of how to treat such a flow arrangement for the (Log-) Mean Temperature Difference Method, while such expressions could be found for the P-NTU method.

Under wet conditions, i.e. when condensation of water vapour occurs on the heat exchanger surface, the UA-$LMTD$ method was used for separation of the heat transfer resistance on the liquid and air sides in Paper IV, and for prediction of the total heat transfer resistance in Paper III and V.

3.1 ε-NTU Method

The ε-NTU method is very straightforward both when sizing (area unknown parameter) and rating (capacity or heat transfer rate unknown parameter) a heat exchanger. Generally, this method is used by automotive, aircraft air-

conditioning, refrigeration and other industries that design or manufacture compact heat exchangers.

In a heat exchanger, the heat transfer rate from the hot fluid to the cold fluid can be expressed as

$$\dot{Q} = \varepsilon \cdot C_{min} \cdot \left(t_{h,in} - t_{c,in}\right) = \varepsilon \cdot C_{min} \cdot \Delta t_{max} \tag{3.1}$$

where, ε, is the heat exchanger effectiveness, C_{min} is the minimum of C_h ($\dot{m} \cdot c_p$ on the hot side) and C_c ($\dot{m} \cdot c_p$ on the cold side) and $\Delta t_{max} = t_{h,in} - t_{c,in}$ is the fluid inlet temperature difference. The heat exchanger effectiveness, ε, is non-dimensional and is dependent on the number of transfer units, NTU, the heat capacity flow rate ratio, C_r, and the flow arrangement, where the functional relationship f is dependent on the flow arrangement.

$$\varepsilon = f(NTU, C_r, \text{flow arrangement}) \tag{3.2}$$

3.1.1 Heat Exchanger Effectiveness ε

Heat exchanger effectiveness ε is a measure of the thermal performance of a heat exchanger. It is defined as the ratio of the actual heat transfer rate from the hot fluid to the cold fluid to the maximum possible heat transfer rate $\dot{Q}_{max}$ thermodynamically permitted.

$$\varepsilon = \frac{\dot{Q}}{\dot{Q}_{max}} = \frac{C_h \cdot \left(t_{h,in} - t_{h,out}\right)}{C_{min} \cdot \left(t_{h,in} - t_{c,in}\right)} = \frac{C_c \cdot \left(t_{c,out} - t_{c,in}\right)}{C_{min} \cdot \left(t_{h,in} - t_{c,in}\right)} \tag{3.3}$$

As can be seen if $C_h = C_{min}$

$$\varepsilon = \frac{\left(t_{h,in} - t_{h,out}\right)}{\left(t_{h,in} - t_{c,in}\right)} \tag{3.4}$$

and if $C_c = C_{min}$

$$\varepsilon = \frac{\left(t_{c,out} - t_{c,in}\right)}{\left(t_{h,in} - t_{c,in}\right)} \tag{3.5}$$

3.1.2   Heat Capacity Flow Rate Ratio C_r

The heat capacity flow rate ratio C_r is a ratio of the smaller to larger heat capacity flow rate for the two fluid streams, so that $C_r \le 1$:

$$C_r = \frac{C_{\min}}{C_{\max}} = \frac{(\dot{m} \cdot c_p)_{\min}}{(\dot{m} \cdot c_p)_{\max}} \tag{3.6}$$

3.1.3   Number of Transfer Units *NTU*

The Number of Transfer Units *NTU* is defined as a ratio of the overall thermal conductance to the smaller heat capacity flow rate as shown below. If *U* is not a constant, the definition in the second equality should be applied.

$$NTU = \frac{U \cdot A}{C_{\min}} = \frac{1}{C_{\min}} \cdot \int U dA \tag{3.7}$$

3.1.4   Effectiveness-number of Transfer Unit Relationships

The heat exchanger effectiveness ε is a function of *NTU*, C_r and flow arrangement, such as (for example) counter-flow, parallel-flow or cross-flow. ε-*NTU* formulas (including C_r) for various heat exchanger flow arrangements, together with graphic solutions, can be found in handbooks and textbooks (e.g. Shah and Sekulic, 2003). Wherever possible, *NTU* as explicit functions of ε and C_r are also given for different flow arrangements. Examples of explicit ε-*NTU* functions for single-pass cross-flow heat exchangers with both fluids unmixed are given in Eq. 13 and Eq. 14 in Paper IV.

3.2   *P-NTU* Method

Historically, the *P-NTU* method was used to design shell-and-tube heat exchangers before the ε-*NTU* method became widely known in the 1940s, and the ε-*NTU* method is actually a variant of the *P-NTU*-method. The advantages of the *P-NTU* method are that it does not require definition of which of the fluids is the one with the minimum heat capacity flow rate, C_{min}, and it does not require determination of whether the heat exchangers are stream-symmetric or stream-asymmetric. However, the main reason for choosing the *P-NTU* method in this analysis is that, for the method, one may find an expression for several cross-flow heat exchangers connected in series in an overall counter-flow (see Eq. 9 and Eq. 10 in Paper IV), while it was not

possible to find such an expression for the ε-*NTU* method or the Log-Mean Temperature Difference Factor *F*.

In this method, the heat transfer rate from the hot to the cold fluid is expressed as

$$\dot{Q} = P_1 \cdot C_1 \cdot \Delta t_{max} = P_2 \cdot C_2 \cdot \Delta t_{max} \qquad (3.8)$$

where *P* is the temperature effectiveness for fluid 1 or 2 (depending on the subscript 1 or 2), *C* is the heat capacity flow rate for fluid 1 or 2 and the inlet temperature difference is $\Delta t_{max} = t_{h,in} - t_{c,in} = |t_{2,in} - t_{1,in}|$. The temperature effectiveness *P*, similar to ε, is non-dimensional and is dependent on the number of transfer units *NTU*, the heat capacity flow rate ratio, *R*, and the flow arrangement.

3.2.1   The Temperature Effectiveness *P*

The temperature effectiveness, *P*, is different for each fluid of a two-fluid heat exchanger. It is defined as the temperature drop (or rise) of a fluid to the inlet temperature difference.

$$P_1 = \frac{t_{1,out} - t_{1,in}}{t_{2,in} - t_{1,in}} \qquad (3.9)$$

$$P_2 = \frac{t_{2,out} - t_{2,in}}{t_{2,in} - t_{1,in}} \qquad (3.10)$$

From the definitions above, it is clear that for $C_1 = C_{min}$, $P_1 = \varepsilon$ and for $C_2 = C_{min}$, $P_2 = \varepsilon$.

3.2.2   Heat Capacity Flow Rate Ratio *R*

The heat capacity flow rate ratio is defined as

$$R_1 = \frac{C_1}{C_2} = \frac{t_{2,in} - t_{2,out}}{t_{1,out} - t_{1,in}} \qquad (3.11)$$

$$R_2 = \frac{C_2}{C_1} = \frac{t_{1,out} - t_{1,in}}{t_{2,in} - t_{2,out}} \qquad (3.12)$$

From the definitions above, it is clear that for $C_1 = C_{min}$, $R_1 = C_r$ and for $C_2 = C_{min}$, $R_2 = C_r$.

3.2.3 *P-NTU* Functional Relationships

Similar to the heat exchanger effectiveness ε, the temperature effectiveness P_1 is a function of NTU_1, R_1 and flow arrangement and P_2 is a function of NTU_2, R_2 and flow arrangement. The textbook written by Shah and Sekulić (2003), includes formulae for P_1-NTU_1 (including R_1) for various heat exchanger flow arrangements, together with graphic solutions. Formulae for many different series and parallel coupling (single and multipass) flow arrangements are also presented. Eq. 9 in Paper IV is one example.

3.3 Mean Temperature Difference Method

The mean temperature difference method is straightforward when the overall heat transfer conductance for a heat exchanger with known area is to be determined (as in Papers I and II), and when the size (area) of a heat exchanger with known heat transfer performance and heat flow rates is to be found. However, an iterative procedure is necessary when rating a heat exchanger (capacity or heat transfer rate being the unknown parameter). This method is generally used by process, power and petrochemical industries that design or manufacture shell-and-tube and other non-compact heat exchangers.

3.3.1 Log-Mean Temperature Difference

The log-mean temperature difference (*LMTD* or Δt_{lm}) is defined as

$$\Delta t_{lm} = \frac{\Delta t_I - \Delta t_{II}}{\ln(\Delta t_I / \Delta t_{II})} \tag{3.13}$$

In this case, Δt_I and Δt_{II} are temperature differences between two fluids at each end of a heat exchanger. For a counter-flow heat exchanger

$$\Delta t_I = t_{h,in} - t_{c,out} \tag{3.14}$$

and

$$\Delta t_{II} = t_{h,out} - t_{c,in} \tag{3.15}$$

For a parallel-flow heat exchanger

$$\Delta t_I = t_{h,in} - t_{c,in} \qquad\qquad (3.16)$$

and

$$\Delta t_{II} = t_{h,out} - t_{c,out} \qquad\qquad (3.17)$$

For all other flow arrangements, such as (for example) crossflow, the heat exchanger is hypothetically considered as a counter-flow unit and the logarithmic mean temperature difference is evaluated according to Eq. 3.13 - Eq. 3.15. The logarithmic mean temperature difference represents the maximum temperature potential for heat transfer that can be obtained only in a counterflow heat exchanger.

3.3.2   Log-Mean Temperature Difference Correction Factor *F*

The heat transfer rate in a heat exchanger can be represented by

$$\dot{Q} = U \cdot A \cdot \Delta t_m \qquad\qquad (3.18)$$

Here, Δt_m is the true (or effective) mean temperature difference. The value of Δt_m is different for different exchanger flow arrangements, even if the inlet and outlet temperatures are the same. However, Δt_{lm} is the same for all flow arrangements (except for the parallel-flow arrangement).

The log-mean temperature difference correction factor is defined as the ratio of the true mean temperature difference to the log-mean temperature difference.

$$F = \frac{\Delta t_m}{\Delta t_{lm}} \qquad\qquad (3.19)$$

Thus,

$$\dot{Q} = U \cdot A \cdot F \cdot \Delta t_{lm} \qquad\qquad (3.20)$$

F is dimensionless and depends on the temperature effectiveness *P*, the heat capacity flow rate ratio *R* and the flow arrangement. *F* is unity for a true counterflow (and parallel-flow) heat exchanger. For other flow arrangements, explicit functions and / or graphic solutions of *F* can be found in handbooks and textbooks, for example in (Shah and Sekulic, 2003). *F* does not represent the effectiveness of a heat exchanger, but is a gauge of the actual heat exchanger performance in comparison with the counterflow heat exchanger performance. The heat exchanger (or multiport tube) evaluated in Paper II was a true counterflow heat exchanger and the heat exchangers evaluated in Paper I were considered as counterflow heat exchangers since they had at least eight passes on the liquid side, i.e., *F* was set to unity.

3.4 Separation of Heat Transfer Resistance under Dry and Wet Conditions

Under dry conditions the total heat transfer resistance, 1/(U·A), can be separated according the following expression (Shah and Sekuliç, 2003):

$$\frac{1}{U \cdot A} = \frac{1}{\eta_{0,b} \cdot \alpha_b \cdot A_b} + R_{b,f} + R_w + R_{a,f} + \frac{1}{\eta_{0,a} \cdot \alpha_a \cdot A_a} \qquad (3.21)$$

If $R_{b,f}$, R_w and $R_{a,f}$ are assumed to be negligibly small, the expression above is reduced to

$$\frac{1}{U \cdot A} = \frac{1}{\eta_{0,b} \cdot \alpha_b \cdot A_b} + \frac{1}{\eta_{0,a} \cdot \alpha_a \cdot A_a} \qquad (3.22)$$

Under wet conditions, i.e. when condensation of water vapour takes place on the heat exchanger surface, the Logarithmic-Mean Temperature Difference Method (the *UA-LMTD* method) or the Logarithmic-Mean Enthalpy Difference Method (the *HA-LMED* method) can be used for data interpretation. Jacobi *et al.* (2005) and Jacobi and Xia (2005) compared the two methods, and found the former to provide more accurate results, especially for partially wet surface conditions. Therefore, this method has been applied in the studies presented in Papers III, IV and V. According to Jacobi *et al.* (2005) and Jacobi and Xia (2005), the total heat transfer resistance, based on the sensible cooling capacity, can be expressed as shown below.

$$\frac{1}{(U \cdot A)_s} = \frac{1}{\eta_{0,b} \cdot \alpha_b \cdot A_b \cdot \left(\dot{Q}_{a,s} / \dot{Q}_a \right)} + \frac{1}{\eta_{0,a} \cdot \alpha_a \cdot A_a} \qquad (3.23)$$

If total heat transfer resistance is instead based on the total cooling capacity, $\dot{Q}_a$, and $\dot{Q}_a = \dot{Q}_b$ the expression above becomes

$$\frac{1}{(U \cdot A)_{tot}} = \frac{1}{\eta_{0,b} \cdot \alpha_b \cdot A_b} + \frac{1}{\eta_{0,a} \cdot \alpha_a \cdot A_a \cdot \left(\dot{Q}_b / \dot{Q}_{a,s}\right)} \qquad (3.24)$$

The expression described by Eq. 3.24 has been used in the studies presented in Papers III, IV and V. The reason for replacing $\dot{Q}_a$ with $\dot{Q}_b$ was to obtain better measurement uncertainty in Paper IV. (Paper III and Paper V present theoretical studies, and there $\dot{Q}_a = \dot{Q}_b$ by definition).

4   Summary of Publications

4.1   Paper I

The candidate performed the experiments, with some assistance from laboratory staff, and was the main author of the paper.

Haglund Stignor, C., Sundén, B., and Fahlén, P., 2007, Liquid Side Heat Transfer and Pressure Drop in Finned-Tube Cooling-Coils Operated with Secondary Refrigerants, *International Journal of Refrigeration*, Vol. 30, pp. 1278-1289.

In this study, full-scale experiments were performed with two different conventional cooling coils (see Table 2.1) intended for display cabinets. Heat transfer and pressure drop on the liquid side for three different single-phase secondary refrigerants were studied and compared to predictions by existing correlations. Predominantly, the laminar flow regime was studied. The studied range for the other parameters concerning the cooling coils and the liquids are $9.3 < d < 11.7$ mm, $0.5 < L_{tube} < 2.25$ m ($54 < L_{tube}/d < 192$) and $12 < \mathrm{Pr} < 96$. The results show that when predicting the heat transfer performance on the liquid side of a cooling coil, the Gnielinski (1989) model for thermally developing laminar flow and uniform wall temperature boundary conditions (T) gives good agreement for $0.0014 < x^* < 0.017$ if $50 < Re < 1700$, assuming a new entrance length is formed after each U-bend. Eighty-nine % (17 of 19) of the test points for which $Re < 2000$ and $x^* < 0.02$ are predicted within ± 10 %. In addition, these entrance lengths must be accounted for, when predicting the pressure drop on the liquid side of the cooling coil. Good agreement was found when accounting for a new entrance length following each U-bend according to Langhaar (1942). This means including an extra head loss (except for the U-bend itself) in the pressure drop correlation. Uncertainty of measurement can be a problem in this type of investigation, and this has been taken into consideration when analysing the results.

4.2   Paper II

The candidate performed the experiments, with some assistance from laboratory staff, and was the main author of the paper.

Haglund Stignor, C., Sundén, B., and Fahlén, P., 2009. An Experimental Study of Liquid Phase Heat Transfer in Multiport Minichannel Tubes, *Accepted for publication in Heat Transfer Engineering*, Vol. 30, No. 12 or 13.

This study has experimentally evaluated heat transfer on the tube side of three different minichannel tubes, known as MPE (MultiPort Extruded) tubes, with different cross-section geometries (see Figure 2.2 and Table 2.2). The geometry of the tube channels or ducts was rectangular, with different aspect ratios, and one of the tubes incorporated surface enlargements inside the channels. Evaluations were performed with four different secondary refrigerant liquids; water, propylene glycol, Hycool 20 and Temper -20. The laminar flow regime was the main focus of the investigations. The sum of the heat transfer resistance on the outer (water) side of the tube and through the tube wall was determined by using the "Wilson-plot" method, which is described by (for example) Kumar (2001) and Shah and Sekuliç (2003). Surface temperature measurements were performed by thermistors to verify that the separation of the thermal resistances by the "Wilson plot" method resulted in reasonable values.

The objective was to find out how best to predict the heat transfer performance of complete heat exchangers consisting of such tubes, and the experimentally determined data were therefore compared with a number of correlations, models and relations. Despite the shape of the minichannels, the best overall agreement was found with a model presented by Gnielinski (1989) for laminar flow, developing temperature profile and fully developed velocity profile in circular tubes with the constant wall temperature boundary condition. Nevertheless, good agreement was also found, sometimes in limited regions, with the other correlations and models with which comparisons were made.

For the tube with surface enlargements in the form of longitudinal fins, the results show that a different characteristic length than the classical hydraulic diameter should be used. This could either be the hydraulic diameter obtained when ignoring the surface enlargements, or the square root of the cross-sectional area of the duct. None of the correlations succeeded in predicting the experimentally determined mean Nusselt numbers for the tube with many (25) and narrow channels for the higher x^* values ($x^* > 0.20$). In this x^* region, the measured values tend to be lower than the predicted ones. The same trend for the Nusselt number in the lower laminar regime (i.e., high x^* values) was found by Agostini *et al.*, (2002, 2004, 2006) and Fernando *et al.* (2008). Possible explanations are longitudinal conduction or gross-flow maldistribution.

4.3   Paper III

The candidate performed the calculations and was the main author of the paper.

Haglund Stignor, C., Sunden, B., Fahlén, P, 2007. Design of different types of secondary loop cooling systems in supermarkets - comparison of energy use and costs. In: *Proceedings of International Congress of Refrigeration*, Beijing, China, ICR07-B01-387.

This paper presents a theoretical case study comparing five different cases of indirect cooling systems in supermarkets. The studied case supermarket had 25 display cabinets for merchandise that should be kept with the temperature range $0 - 8°C$ (dairy, eggs, meat etc.) and five display cabinets for $0 - 4°C$ (fresh meat etc.) The influence of the selection of cooling coil / heat exchanger design and type of secondary refrigerant was investigated. Two of the cases have display cabinets with traditional conventional cooling coils, and in one of the cases the display cabinets are equipped with more efficient conventional cooling coils. Finally, for two of the cases, there are flat-tube heat exchangers in the display cabinets. The secondary liquid refrigerants, Propylene glycol, 39 %$_w$, or Temper -20, are assumed to be used. The first case is representative of a large number of supermarkets in Sweden, but the others are rare or so far only hypothetical. The results show that significant savings of both energy and costs can be achieved for an indirect cooling system by replacing a traditional conventional cooling coil by a more efficient unit; either a more efficient conventional cooling coil, or a properly designed flat-tube heat exchanger. It is also shown that replacing propylene glycol, 39 %$_w$, by Temper -20 in a system with traditional conventional cooling coils, results in lower energy use, but a system with more efficient heat exchangers, e.g. flat-tube heat exchangers, adapted to the laminar flow regime, is less sensitive to the choice of secondary refrigerant. In addition, it is found that too high values of the liquid flow rate in an indirect cooling system result in a high investment cost, since larger dimensions of the components are required. An iterative procedure is suggested for finding the optimal operating point, and this procedure is presented and evaluated with good results in this study.

4.4 Paper IV

The candidate performed the experiments together with the fourth co-author and with some assistance from laboratory staff. She was the main author of the paper.

This paper describes experimental evaluation of two different heat exchangers having flat tubes and plain fins on the air side (see Table 2.3). One of the heat exchangers had continuous plate fins (FFC or FTHE2), while the other had serpentine fins between the tube rows (MPET-HE or FTHE1). The latter heat exchanger had considerably larger tube depth than the former; 45 mm as against 13.6 mm. The applied test conditions were appropriate for a display cabinet application, and other applications involving a low air velocity (0.23 – 1.2 m/s) in combination with condensation of water vapour in the air. Heat transfer and pressure drop during dry and wet test conditions were compared and related to theoretical predictions for different assumptions. The influence of air velocity, air humidity and inclination angle was investigated.

The results show that the heat exchanger with continuous plate fins (FFC or FTHE2) might suffer from wake regions or bad contact between the tubes and the fins. This degrades the heat transfer performance somewhat, at least for the lowest air flow rates. However, at these air flow rates, the heat transfer performance is not significantly affected by the occurrence of condensate water on the fin surfaces, while this is the case for the higher air flow rates that were evaluated. The results also reveal that, for the plain serpentine-fin heat exchanger (MPET-HE or FTHE1), the heat transfer can be predicted relatively well by modelling the flow as simultaneously developing duct flow at dry test conditions. For dehumidifying test conditions, the heat transfer performance is reduced by a maximum of 18 % at the evaluated air flow rates. For both heat exchangers, wet heat transfer surfaces lead to an increased pressure drop, which can be partly compensated by a forward inclination, which helps drain the condensate water out of the heat exchangers to some extent. However, the inclination does not affect the heat transfer performance much.

4.5   Paper V

The candidate performed the calculations and was the main author of the paper.

In this last paper, different designs of flat-tube heat exchangers with plain fins have been evaluated theoretically in a parameter study in order to evaluate their potential in indirectly cooled display cabinets. Two different types of flat-tube heat exchangers were considered; one with serpentine fins (FTHE1), and one with continuous plate fins (FTHE2). Both the flat-tube heat exchanger types were adapted to the laminar flow regime on the liquid side as well as on the air side. The performance of the two heat exchanger types had previously been verified experimentally under dehumidifying conditions (Paper IV). The applied optimising criteria assumed a floating condensing temperature of the chiller and, apart from the pressure drop of the heat exchanger itself, also included the pressure drops of the other components of the indirect cooling (secondary loop) system, such as piping, valves and liquid cooler. The results show that considerable savings in the required electric drive power to compressors, pumps and fans can be obtained, in comparison to the traditional cooling coil. The savings amounted to up to 15 %. All the evaluated flat-tube heat exchangers were almost equally efficient, although those with plate fins showed somewhat better values. In addition, the flat-tube heat exchangers could operate with a minimal temperature difference of around 1 K between the outgoing air and the incoming liquid of the heat exchanger. This makes frost-free operation possible for many display cabinet applications. Hence the savings will be even greater than the above-mentioned 15 %, since frost-free operation is much less likely to be true for the traditional cooling coil.

5 Additional Results - Verification of Frost-free Operation

Basically, frosting occurs on the fins of a heat exchanger if the dew-point temperature of the air is higher than the surface temperature and the surface temperature is below the freezing point of water, 0 °C, but not if the surface has a higher temperature. However, before frosting occurs, there is normally a period when liquid, supercooled water persists, even down to temperatures as low as -30 °C. The degree and duration of supercooling depends mainly on the degree of supersaturation of the water vapour and the character of the heat exchanger surface, i.e. presence of irregularities and whether it is hydrophilic or hydrophobic (Fahlén, 1996). In order to arrive at a first estimate of the temperature to which the surface of the evaluated heat exchangers could be supercooled, without frosting taking place on the fin surfaces, some tests were performed.

5.1 Procedure

The tests were performed in the same set-up as was used in the study presented in Paper IV (see section 2.3.1). Experiments were carried out both with the MPET heat exchanger and the FFC heat exchanger (see 2.1.3). The inlet air temperature was set (depending on the depth of the heat exchangers) to obtain a temperature difference of about 1 K between the liquid inlet temperature and the outlet air temperature. The humidity was set as high as was possible in the air-conditioning plant. To start with, the liquid temperature was set just above freezing, at approximately 1 °C. When stable conditions had been reached, the liquid inlet temperature was lowered to, for example, -2 °C and flow rates, temperatures and the air humidity were measured to verify that stable conditions were sustained. In addition, the pressure drop on the air side was measured as an indicator of whether frosting occurred on the fins or not. The fin surface was also visually examined regularly by using fibre optics.

5.2   Results

Figur 5.1 and Figur 5.2 show the results from the tests with the two flat-tube heat exchangers. For the MPET heat exchanger - the one with serpentine plain fins - frost-free operation could be obtained at a liquid inlet temperature of -2.6 °C, while frosting occurred at a 0.6 K lower inlet temperature. This is indicated by the air side pressure drop being constant for the former case, but increasing dramatically for the latter test. Frost-free operation was also verified by visual examination using fibre optics. For the FFC heat exchanger - the one with continuous plain fins and thinner tubes - frosting took place on the fins at an inlet temperature of -2.5°C, but not at -1.4°C. For this heat exchanger, it took much longer time to reach stable conditions. A slight increase is seen in the pressure drop, even in the frost-free case. However, this slight increase is only an effect of condensate build-up, which was verified by using the fibre optics to view the fins surfaces. For this latter heat exchanger, tests were also performed at an inlet temperature of -2.1°C, but here the results were ambiguous. In one test, frost started to build up on the surface, and in another it did not.

The results from these experiments confirm that frost-free operation is possible for these types of flat-tube heat exchangers at the required liquid inlet temperatures described in Paper V. However, in both cases, the conditions seemed to be rather unstable. When frosting had started in one part of the heat exchanger (closest to the liquid inlet), often the whole surface was covered by frost, even if the liquid outlet temperature was higher than where frost-free operation had been obtained in other tests. If both the temperature of the liquid entering the heat exchanger and the air coming out of the heat exchanger is below 0 °C, frosting will probably occur sooner or later. However, in reality, the cooling demand of the display cabinet will probably not be as high as at the design condition for more than half a day (for example). When the cooling demand drops, the control valve will close, the surface temperature rises and hence a new period with supercooling will start the next time the control valve opens. Further investigation is therefore needed in order to clarify more certainly when frosting does or does not occur. Such a test might also be performed with the heat exchangers installed in a display cabinet, in order to obtain conditions as close to reality as possible.
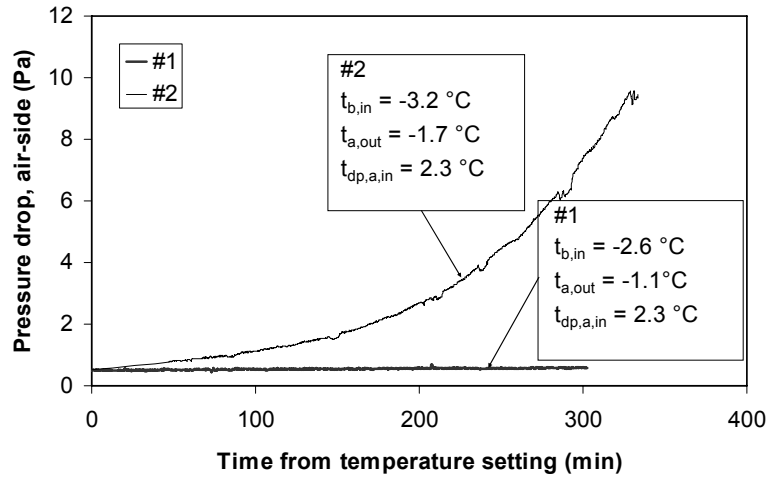
Figur 5.1.   Pressure drop during tests for verification of frost-free operation with the MPET heat exchanger (FTHE1 type).
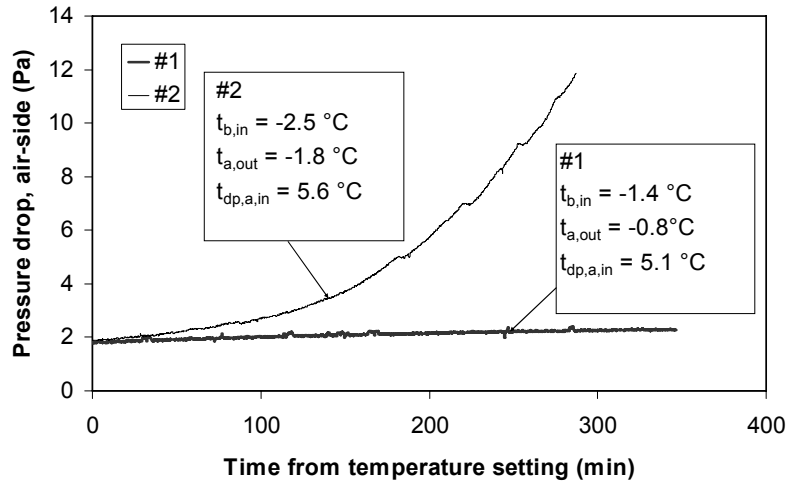
Figur 5.2.   Pressure drop during tests for verification of frost-free operation with the FFC heat exchanger (FTHE2 type).

47

6   Discussion

The sections below present and discuss the choices of test points in the experimental studies and the selection of optimisation conditions. The economic aspects of switching from one heat exchanger type to another in a specific application are also considered to some extent. Some other possible applications for the evaluated heat exchangers are discussed, and finally ways for obtaining further improvement of the performance are presented.

6.1   Selection of Test Points and Measurement Uncertainty

When designing a test plan for evaluation of the heat transfer performance, compromises must almost always be considered due to opposing wishes and practical limitations. According to Shah and Sekuliç (2003), when evaluating a heat exchanger, the operating conditions should be set to obtain an *NTU* value between 0.5 and 3.0 in order to obtain good measurement uncertainty. On the other hand, in the studies presented in Papers I and II, the heat transfer performance on the outside was determined at one set of test points (e.g. in Paper II by the Wilson-plot method). Then the outside conditions were kept constant, as the heat transfer performance on the heat exchanger inside (or liquid side) was evaluated for different flow rates. Therefore, at the two ends of the test series (highest or lowest flow rate), the *NTU* might have been outside the range of 0.5 - 3.0. Of course, this could have been avoided by doubling and tripling the number of test points, but then it becomes a question of practical limitations.

When it comes to the study presented in Paper IV, in order to get the most accurate values of the air-side *Nu* or *j* value, the test might have been performed on a single-pass cross-flow heat exchanger. However, in the actual study it was of interest to evaluate the effect of the condensed water on the heat transfer and pressure drop performance. There was therefore a desire to evaluate multipass heat exchangers as similar as possible to what they would have been like in a real display cabinet application. In some tests, the *NTU* value was above 3.

However, the measurement uncertainty has been estimated for each test point separately and has been taken into account when analysing the results. Those test points associated with too large uncertainty have been excluded. In order to minimise the measurement uncertainty, the overall temperature differences have been much larger than would have been the case in a real display cabinet application. However, since the analysis is based on dimensionless numbers, this should not affect the results.

When it comes to boundary conditions, neither a completely constant temperature nor a completely constant heat flux boundary condition has been obtained in any of the tests. The same is true in most cases for the real application, where the airflow in a display cabinet is cooled by a liquid-to-air heat exchanger. An exception is if $\Delta t_a = \Delta t_b$, when the constant heat flux boundary condition applies, and another exception is when $\Delta t_b \approx 0$ (very high liquid flow rate), when the constant-temperature boundary condition applies. However, the purpose of these studies was to find which assumptions and correlations that were most appropriate to use, when predicting the heat transfer performance in a real application. In all tests, the constant-temperature boundary condition was found to result in the best agreement.

The application of the different data reduction methods always introduces uncertainties to some extent, since different assumptions are invoked. Examples of such is the assumption of uniform overall heat transfer conductance U over the entire heat transfer surface, and the assumption of perfect mixing between the passes in a heat exchanger. The influence of the former has been evaluated for the study presented in Paper II (see Appendix B). On the other hand, the influence of the latter (perfect mixing) has not been evaluated in detail. Nevertheless, the same procedures have been applied, both when reducing measurement data and when predicting the performance of a real application, which ought to cancel out the uncertainties to some extent.

6.2   Selection of Optimising Criteria

As stated by Axell (2002), the performance of display cabinets can vary to a relatively large extent. Axell (2002) presents the results from a technology procurement project carried out in Sweden for open vertical display cabinets in 1997. In the first step, the present state of the art was assessed by testing six display cabinets in accordance with prEN441 (1993). These cabinets (2,5 m long and with a total display area of approximately 5 m²) had a heat extraction rate which ranged from 3 kW to 4 kW. The heat extraction rate of the winner

was 1.6 kW. These figures show that there is a significant energy-saving potential for display cabinets. Even though these figures are now more than ten years old, and there is a significant saving potential, there is no indication that open vertical display cabinets as found in supermarkets today are much more efficient than they were in 1997 (Monier *et al.* 2007).

The performance of the display cabinet for which the heat exchanger should be optimised was selected by consulting the studies presented by Axell (2002). The selected data presented in Table 6.1 are selected to be representative for a typical display cabinet working in a Nordic climate but are not an absolute average. A display cabinet with a cooling demand of 3.0 kW could of course have a higher air flow rate and a smaller temperature range (optimisation for such a display cabinet was performed in the study presented in Paper III), or the opposite. Similarly, the humidity of the inlet air could be lower and the air flow rate higher and vice versa, and the cooling demand would still be 3.0 kW. However, the assumed humidity of the inlet air represents a dew point temperature of 6.1 °C, which could well be representative for the indoor air of a supermarket in a Nordic climate during a large part of the year. However, the air flow rate and inlet and outlet conditions of the air were selected to give the display cabinet reasonable conditions to maintain the temperature of the merchandise between 0 and 8 °C.

Table 6.1.   Optimising Criteria for Heat Exchangers/Cooling coils

Cooling demand of display cabinet	
Cooling capacity on the liquid side, $\dot{Q}_b$:	3.0 kW
Sensible cooling capacity on the air side, $\dot{Q}_{a,s}$:	1.8 kW
Air flow into the heat exchanger, $\dot{V}_{a,in}$:	648 m³/h
Air temperature into the heat exchanger, $t_{a,in}$:	8.0 °C
Relative humidity of air into the heat exchanger, $\varphi_{a,in}$[a]	88 %
Air temperature out of the heat exchanger, $t_{a,out}$	0.0 °C
Relative humidity of air out of heat exchanger, $\varphi_{a,in}$[a]	100 %
Dimensions of heat exchanger/cooling coil	
Total width (*W*):	2.25 m
Height(*H*)×depth(*De*):	0.05 m²
Minimal fin pitch, F_p:	4.0 mm
Total width (*W*):	2.25 m

[a] Values corresponding to the given cooling demand on the liquid side

6.3   Cost Estimate of FTHE1 and FTHE2

Traditional cooling coils consist of aluminium fins on expanded copper tubes, while the FTHE1 type heat exchangers consist only of aluminium, which is much less expensive than copper. The FTHE2 type heat exchanger has brass tubes and copper fins. The production cost of the flat-tube heat exchangers is most certainly higher than for a conventional cooling coil. However, this is very dependent upon the production volumes. The FTHE1 type heat exchangers in particular involve high investment cost for machinery and furnaces, which make high production volumes necessary for a competitive price. However, the investment cost for the other heat exchangers types are by no means negligible, and the flexibility of the different production techniques differ. Since the production cost of (in particular) the FTHE1 type heat exchangers are so strongly related to the production volume, and the suggested heat exchanger design exists only as a prototype, a fair cost comparison seemed impossible to make. Therefore, the cost of the raw material for the heat exchanger cores (excluding U-bends and headings) has been compared instead. This will at least give a perception of the lowest possible hypothetical cost for a heat exchanger with infinitely large production volumes. In addition, this comparison can give a hint of whether there are any savings to be made on the raw material cost that could be applied in production, by changing from traditional cooling coils to flat-tube heat exchangers.

The results are shown in the Table 6.2 below. They show that even if the FTHE1 heat exchanger consists only of aluminium, it has almost the same raw material cost as the traditional cooling coil, CC R, since it is denser. However, compared to the CC D cooling coil, (see Table 2.1) the energy efficiency of which is not far from that of the FTHE1 type heat exchanger (see Paper III), the raw material cost of the FTHE1 heat exchanger is less than half. When it comes to the FTHE2 type heat exchanger, its raw material cost exceeds the costs of the others considerably. The reason for this is partly that it is a very dense heat exchanger, but also that it consists to a large extent of copper, which is an expensive metal. Only the cost for one FTHE1 type and one FTHE2 type heat exchanger is displayed in the table: the reason for this is that all the evaluated heat exchanger designs have the same outer volume, which makes their material costs almost identical.

Table 6.2. Comparison of the raw material cost for different heat exchangers types (for explanation of heat exchanger designs, see Table 2.1 and Table 2.3).

		FTHE1-4*10	CC R	CC D	FTHE2- 8*33
Fins					
Material		Al	Al	Al	Cu
$Mass_{fin}$	(kg)	12.5	12.7	16.8	27.7
Cost	(SEK/kg)*	18.2	18.2	18.2	48.6
$Cost_{fin}$	(SEK/HE)*	227	231	307	1348
Tubes					
Material		Al	Cu	Cu	$Brass_{(70Cu30Zn)}$
$Mass_{tube}$	(kg)	18.8	7.6	21.5	32.8
Cost	(SEK/kg)*	18.2	48.6	48.6	37.5
$Cost_{tube}$	(SEK/HE)*	342	371	1048	1230
Total					
$Cost_{tot}$	(SEK/HE)*	569	601	1354	2577

*1 € = 9.61 SEK (July 2008)

6.4 Performance of FTHE1 and FTHE2 in Air-Conditioning Applications

In order for FTHE to be cost efficient, relatively large production volumes are required. It is therefore of interest to investigate how the geometries (fin types, fin pitch, tube pitches etc.) suggested for display cabinet applications would compete in other similar, but not identical, applications, such as air conditioning. The heat exchangers evaluated in Paper IV were therefore tested at climatic conditions in accordance with SS-EN 1216 (1998) (Heat exchangers – Forced circulation air-cooling and air-heating coils – Test procedure for establishing the performance). The results from the measurements are presented in Table 6.2. Calculation results from a program (AIACalc, program version 0803.01) developed by AIA, (a Swedish coil manufacturer) are given for a conventional cooling coil with circular tubes below each result for the flat-tube heat exchangers. (The reason for not using the model for conventional cooling coils applied in Papers III and V was that this model was not verified for sufficiently high air velocities). Calculations have been performed for cooling coils having the same fin pitch and approximately the same total volume as the flat-tube heat exchangers. The coil height was as close as possible to the selected tube configuration.

For air-conditioning applications, water is the most common secondary coolant liquid. Water was therefore given as the liquid in the AIACalc

calculations. For the flat-tube heat exchangers, measurement results are given for propylene glycol (39 %$_w$) in the table below. An exception is the pressure drop on the liquid side, which has been recalculated (or predicted) for the thermophysical properties of water, which reduces the pressure drop. The reason was to make the data comparable with the data for the conventional cooling coils. Of course, a change of liquid from propylene glycol (39 %$_w$) to water would affect the heat transfer performance as well, although to only a very small extent, since the flat-tube heat exchangers are adapted to the laminar flow regime.

The results show that the flat-tube heat exchangers could deliver the same heat transfer performance at considerably lower pressure drop, both on the air and on the liquid side. The air-side pressure drop affects the required fan power, and a low pressure drop is very desirable in a ducted air-conditioning system, since the air normally passes through the coil even at periods when there is no cooling demand. It can be seen in the table below that it is somewhat harder for the FTHE1 heat exchanger to compete with the conventional cooling coils. In air-conditioning applications, the air velocities are much higher than in display cabinet applications - around 2.5 m/s compared to below 1 m/s for a display cabinet application. Therefore, in this case, application of a louvered fin geometry would probably improve the heat transfer performance considerably. Nevertheless, a louvered fin geometry would result in a higher air-side pressure drop, which could be reduced by decreasing the total heat exchanger volume and thereby the heat transfer area.

Table 6.3.   Performance of various heat exchangers in air-conditioning applications.

Heat Exchanger	$t_{a,in}$	$\varphi_{a,in}$	$t_{a,out}$	$t_{b,in}$	$t_{b,out}$	$Q_{a,s}$	Δp_a	$\Delta p_b(H2O)$[a]
	°C	%	°C	°C	°C	W	Pa	kPa
FFC (FTHE2)	27,1	46,8	16,4	6,9	18,7	3589	51,7	0,6
CC_{30*26_8*6-1}[b]	27,1	46,8	16,0	6,9	18,7	3830	85,0	35
CC_{30*26_8*6-2}	27,1	46,8	17,3	6,9	18,7	3370	81,0	6,0
FFC (FTHE2)	27,1	77,0	17,7	7,1	18,8	3193	71,5	1,0
CC_{30*26_8*6-1}	27,1	77,0	17,3	7,1	18,8	3340	122	123
CC_{30*26_8*6-2}	27,1	77,0	18,4	7,1	18,8	2990	120	17
MPET-HE (FTHE1)	27,0	48,0	19,7	7,1	12,1	2428	21,0	1,2
$CC_{35*30.3\_8*3-2}$	27,0	48,0	18,4	7,1	12,1	2840	25,0	14
$CC_{35*30.3\_8*3-4}$	27,0	48,0	20,6	7,1	12,1	2130	23,0	8,0
MPET-HE (FTHE1)	27,1	74,7	21,0	7,2	13,4	2037	22,3	1,4
$CC_{35*30.3\_8*3-2}$	27,1	74,7	20,0	7,2	13,4	2360	34,0	15
$CC_{35*30.3\_8*3-4}$	27,1	74,7	21,8	7,2	13,4	1750	32,0	6,0

[a] Predicted (not measured) values also for the FTHEs

[b] $CC_{Tp,t*Tp,l\_nt*nl-Np,c}$

6.5   Other Applications

As mentioned in the introduction, during the course of this research work the legislation regarding direct cooling (or direct-expansion, DX) systems has been changed. In addition, direct cooling systems operating with carbon dioxide as the refrigerant have been introduced in supermarkets. However, the indirect systems are still very popular but their future is not totally clear. Nevertheless, all the findings in this research work regarding the air side are valid for heat exchangers where condensation occurs on the air side. Although operation with carbon dioxide as refrigerant involves very high working pressures, a flat-tube heat exchanger consisting of minichannel tubes (such as MPE tubes) would be very suitable, since, according to Kandlikar (2007), this type of tube can handle high pressures while maintaining a compact design. However, Kandlikar (2007) also reports that the implementation of minichannels in evaporators has lagged behind implementation in condensers. The reason for this is mainly instability concerns due to the occurrence of reverse flow in

some of the channels. The reversed flows are caused by the rapid growth of vapour bubbles near the inlet regions of the channels. Further research is therefore needed in this area.

For mobile air conditioning, the European Community requires the use of refrigerants with global warming potentials (GWP) less than 150 in all new-type vehicles starting in 2011, and in all new vehicles by 2017. The only commercially available refrigerants that have a GWP below this threshold are carbon dioxide (R-744) and HFC-152a (R-152-a). The former requires completely new components, and the latter has the disadvantage of being somewhat flammable. However, this can be successfully mitigated by applying a secondary loop (or indirect cooling) system. The refrigerant would therefore be contained completely within the engine compartment, and the liquid secondary refrigerant would be pumped to the passenger compartment. Ghodbane *et al.* (2007) designed such an energy-efficient secondary loop system and found the cooling performance to be equal to, or better than, a baseline HFC-134s system. They also found the warming impact of direct refrigerant emissions to be reduced by at least 94 %. The findings from the research work presented in this thesis can be valuable input in the further development of energy-efficient secondary loop mobile air-conditioning systems.

6.6   Further Improvement of Heat Exchanger Performance

As motivated earlier, a plain fin geometry was chosen for the flat-tube heat exchangers due to the relatively low air velocities in combination with condensation of water vapour in a display cabinet application. The heat transfer performance (*Nu*) for a simultaneously developing flow is positively dependent on *Re* and *Pr*. One way to increase *Re,* and thus *Nu,* is to increase the air velocity, which is considered in the study presented in Paper V. Another way would be to increase the hydraulic diameter by increasing the fin pitch, F_p, but this would lead to decreased heat transfer area (if the total heat exchanger volume is to be maintained) which would reduce the overall heat transfer performance.

For a louver fin geometry, the heat transfer performance (*Nu*) is also positively dependent on *Re* and *Pr*. However, in the definition of *Re,* the louver pitch, L_p, is used as the characteristic length (instead of d_h). Therefore, for a louver fin geometry, it is possible to increase *Re* by increasing L_p, thus increasing the heat transfer performance of a louvered geometry without affecting the heat transfer

area (when the total heat exchanger volume is maintained unaltered). In addition, if the dimensions of the louver pitch and louver angle were made sufficiently large, the risk of condensate clogging the louver gaps would be reduced considerably. However, a louver-fin geometry would result in an increased air-side pressure drop.

For the reasons mentioned above, in order further to improve the performance of flat-tube heat exchangers for display cabinets, a louver-fin geometry with $L_p \approx F_p = 4$ mm should be evaluated. The evaluated heat exchanger designs with the lowest heights have the highest air velocities, and these are therefore most suitable for a louvered-fin geometry. As an example, FTHE1-8*5 obtains $Re_{dh} \approx 400$ and would obtain $Re_{Lp} \approx 250$. It was found in Paper V that the flat-tube heat exchangers with plain fins could operate with a minimum temperature difference of approximately 1 K. Since this temperature difference is already very small, the improved heat transfer performance would not lead to much of an increase in liquid inlet temperature (and thus raised evaporation temperature and compressor performance). Nevertheless, an improved air-side heat transfer performance would result in an improved overall conductance U. This would allow the overall heat transfer area, and thereby heat exchanger volume, to be reduced with unaltered UA-value. The introduction of a suitable louvered-fin design would therefore first and foremost result in raw material cost reduction.

The addition of vortex generators to the plain fins could be an alternative to enhance the air side heat transfer. This has been investigated for flat-tube geometries in dry conditions down to $Re \approx 400 - 600$ by several researchers (e.g. Fiebig *et al.* (1994), Wang *et al.* (2002a, 2002b), Gao *et al.* (2003) and Smotrys *et al.* (2003). The introduction of vortex generators has led to increased heat transfer but also to increased pressure drop. Sommers and Jacobi (2004, 2005) investigated air-side heat transfer augmentation during frosting conditions with a plain fin and tube heat exchanger with round tubes and a fin pitch of 8.5 mm down to $Re = 500$, and found a considerable reduction in the heat transfer resistance. Again, the heat exchanger designs with the highest air flow rates (i.e. FTHE1-8*5 and FTHE1-10*4) are probably the most suitable for vortex generators.

In dehumidifying heat exchangers, fin surfaces with small contact angles reduce the air-side pressure drop. This can be achieved by applying hydrophilic coatings on the fin surfaces. This was, for example, studied by Hong and Webb (2000). They also found the uncoated aluminium surface to show improved wettability (smaller contact angles) with increased number of test cycles. This was believed to occur due to surface oxidation and

contamination. McLaughlin and Webb (2000) compared the air-side performance of a coated and an uncoated evaporator with louvered fins. They found that the hydrophilic coating significantly improved the heat transfer performance during wet conditions. This finding indicated that the coating decreased the amount of louver bridging by decreasing the amount of condensate retained on the evaporator core.

The performance of the suggested heat exchanger designs presented in this thesis could therefore possibly be improved further by application of a suitable coating. However, for the one with aluminium fins, the difference might be slight, since the surface already has a small contact angle and since the fin spacing is relatively large. However, for the louvered fin design suggested above, a surface with as small a contact angle as possible should be used to avoid louver bridging.

7   Conclusions

This research work has sandwiched experimental studies with calculations and parameter studies, with the overall objective of finding an energy-efficient heat exchanger design for indirectly cooled display cabinets. The purpose of the experimental work was initially to find which correlations and relations that should be used in the models applied in the parameter studies, and also to verify the resulting models. The purpose of the parameter studies was first and foremost to find suitable heat exchanger geometries, and also to find which parameter ranges that should be studied in the experimental work.

The most important conclusion from this research work is that considerable energy savings can be obtained by using more energy-efficient heat exchangers in indirectly cooled display cabinets. Designs for such heat exchangers, consisting of flat tubes and plain fins, are suggested. These heat exchanger designs have been adapted to the laminar flow regime on the liquid side and on the air side. The methodology of this research work makes the performance of the suggested heat exchanger designs well verified experimentally.

The results from the experimental investigations on two different flat-tube heat exchangers types, one with plain serpentine fins and one with continuous plate fins, show that the heat transfer performance of the former can be predicted relatively well by modelling the flow as simultaneously developing duct flow under dry test conditions. However, the case is not the same for the latter heat exchangers type at the air flow rates encountered in a display cabinet application, since it might suffer from wake regions (most probable) or bad contact between the tubes and the fin, which reduces the performance somewhat. The performance is adversely affected to some extent in most test points by the occurrence of condensate water on the fin surface for both heat exchanger types. However, the influence of air velocity and water content on this deterioration differs somewhat for the two heat exchangers types. For conditions similar to those of display cabinets, the heat transfer and pressure drop performance is only affected to little or no extent by the occurrence of condensate water.

Taking the results from the experimental investigation into consideration, models for the two different heat exchanger types were created. A number of different flat-tube heat exchanger geometries were evaluated in a parameter

study, and all of them were almost equally efficient. This implies that a number of heat exchanger designs, having different outer geometries (height, depth, length) but the same total volume, are suggested. This means that display cabinet designers can select the one which best suits a specific display cabinet. The results showed that the flat-tube heat exchanger could operate with a minimal temperature difference of around 1 K, which leads to good likelihood of frost-free operation in a display cabinet application. Frost-free operation at the required temperatures has also been verified experimentally.

The results from the experimental investigations on the heat transfer performance on the liquid side of heat exchangers (cooling coils) and different tubes show that best agreement for the laminar flow regime was found with the Gnielinski (1989) model for thermally developing flow and uniform wall temperature boundary conditions. For the cooling coil, a new entrance length should be assumed to be formed after each U-bend. Although this model is first and foremost valid for ducts with circular cross-section, it nevertheless predicted the heat transfer performance of the multiport tubes quite well, even though the shape of the ducts differed from the circular. However, for the tube with surface enlargements in form of longitudinal fins, another characteristic length than the classical hydraulic diameter should be used. This could either be the hydraulic diameter obtained when ignoring the surface enlargements, or the square root of the cross-sectional area of the duct.

The results from the parameter study show that, for an indirectly cooled display cabinet, considerable savings (up to 15 %) in the required electric drive power can be obtained by replacing the traditional cooling coils by suitably designed flat-tube heat exchangers. In addition, the required temperature difference for the flat-tube heat exchangers is so small that frost-free operation is possible, which would result in even larger savings. Many comparisons show that indirect (or secondary loop) cooling systems already are as energy-efficient or even more efficient than a system where the refrigerant evaporates in the cooling coil tubes (direct-expansion system). However, some studies show the opposite: namely, that an indirect system uses up 18 % more energy due the extra heat exchange stage and the pumping of liquid. However, even in the worst case here, by replacing the heat exchangers in the display cabinets, the indirect system can compete with the direct-expansion system when it comes to energy utilisation, at the same time as operating with much lower refrigerant charges (and thus less leakage and less environmental impact) and a more constant merchandise temperature.

References

Achaichia, A., and Cowell, T. A., 1988, Heat Transfer and Pressure Drop Characteristics of Flat Tube and Louvered Plate Fin Surfaces, *Experimental Thermal and Fluid Science*, vol. 1, no. 2, pp. 147-157.

Agostini, B., Bontemps, A., and Thonon, B., 2006, Effects of Geometrical and Thermophysical Parameters on Heat Transfer Measurements in Small-Diameter Channels, *Heat Transfer Engineering*, vol. 27, no. 1, pp. 14-24.

Agostini, B., Watel, B., Bontemps, A., and Thonon, B., 2002, Friction Factor and Heat Transfer Coefficient of R134a Liquid Flow in Mini-Channels, *Applied Thermal Engineering*, vol. 22, no. 16, pp. 1821-1834.

Agostini, B., Watel, B., Bontemps, A., and Thonon, B., 2004, Liquid Flow Friction Factor and Heat Transfer Coefficient in Small Channels: An Experimental Investigation, *Experimental Thermal and Fluid Science*, vol. 28, no. 2-3, pp. 97-103.

Aittomäki, A., and J., K., 2002, Designing of Indirect Cooling Systems. *Proc. Urbana-Champaign int. Conf., IIR*, Urbana-Champaign, IL, USA, pp. 132-140.

Arias, J., 2005, Energy Usages in Supermarkets - Modelling and Field Measurements, PhD Thesis, Royal Institue of Technology, Stockholm, Sweden.

Axell, M., 2002, Vertical Display Cabinets in Supermarkets - Energy Efficiency and the Influence of Air Flows, PhD Thesis, Chalmers University of Technology.

Axell, M., and Fahlén, P., 1998, Promotion of Energy Efficient Display Cabinets. *Proc. Proceedings of the International Conference "Refrigerated transport, storage and retail display" of IIR D1, D2/3*, Cambridge, United Kingdom, pp. 244-251.

Brackbill, T. P., and Kandlikar, S. G., 2007, Effect of Sawtooth Roughness on Pressure Drop and Turbulent Transition in Microchannels, *Heat Transfer Engineering*, vol. 28, no. 8-9, pp. 662-669.

Briley, G. C., 2004a, Secondary Coolants, *ASHRAE Journal*, no. June, pp. 36.

Briley, G. C., 2004b, Secondary Coolants, Part II, *ASHRAE Journal*, no. November, pp. 42.

Caney, N., Marty, P., and Bigot, J., 2007, Friction Losses and Heat Transfer of Single-Phase Flow in a Minichannel, *Applied Thermal Engineering*, vol. 27, pp. 1715-1721.

Cavallini, A., Del Col, D., Doretti, L., Matkovic, M., Rossetto, L., and Zilio, C., 2005, Condensation Heat Transfer and Pressure Gradient inside Multiport Minichannels, *Heat Transfer Engineering*, vol. 26, no. 3, pp. 45-55.

Clarke, R., and Finn, D. P., 2008, Numerical Investigation of the Influence of Heat Exchanger U-Bends on the Temperature Profile and Heat Transfer of Secondary Working Fluids. *Proc. Eurotherm 2008*, Eindhoven, Netherlands.

Cooper, P. J., 1997, Experience with Secondary Loop Refrigeration Systems in European Supermarkets. *Proc. Int. Conf. Ozone Prot. Technol.*, Baltimore, USA, pp. 506-515.

Davenport, C. J., 1983, Correlations for Heat Transfer and Flow Friction Characteristics of Louvered Fin. *Proc. 21st National Heat Transfer Conf.*, Seattle, vol. 225 (issue), pp. 19-27.

EAL-R2, *Expression of the Uncertainty of Measurement*, 1 ed., EAL European Cooperation for Accreditation of Laboratories, 1997.

Fahlén, P., 1994, Performance Tests of Air Source Heat Pumps under Frosting Conditions - Quality of Results, SP report 1994:01, SP Swedish National Testing and Research Institute.

Fahlén, P., 1996, Frosting and Defrosting of Air-Coils, PhD Thesis, Chalmers University of Technology.

Fahlén, P., 2000, Butikskyla (in Swedish), SP report 2000:03, SP Swedish National Testing and Research Institute.

Fernando, P., Palm, B., Ameel, T., Lundqvist, P., and Granryd, E., 2008, A Minichannel Aluminium Tube Heat Exchanger - Part I: Evaluation of Single-Phase Heat Transfer Coefficients by the Wilson Plot Method, *International Journal of Refrigeration*, vol. 31, pp. 669-680.

Fiebig, M., Valencia, A., and Mitra, N. K., 1994, Local Heat Transfer and Flow Losses in Fin-and-Tube Heat Exchangers with Vortex Generators: A Comparison of Round and Flat Tubes, *Experimental Thermal and Fluid Science*, vol. 8, no. 1, pp. 35-45.

Gao, S. D., Wang, L. B., Zhang, Y. H., and Ke, F., 2003, The Optimum Height of Winglet Vortex Generators Mounted on Three-Row Flat Tube Bank Fin, *Journal of Heat Transfer*, vol. 125, no. 6, pp. 1007-1016.

Garimella, S., Dowling, W. J., Van Der Veen, M., and Killion, J. D., 2001, The Effect of Simultaneously Developing Flow on Heat Transfer in Rectangular Tubes, *Heat Transfer Engineering*, vol. 22, no. 6, pp. 12-25.

Ghodbane, M., Craig, T. D., and Baker, J. A., 2007, Demonstration of an Energy-Effcient Secondary Loop HFC-152a Mobile Air Conditioning System, Delphi Thermal System Division, Delphi Corporation for U.S. Evironmental Protection Agency, December.

Gnielinski, V., 1989, Zur Wärmeübertragung bei laminarer Rohrströmung und konstanter Wandtemperatur (in German), *Chemieingenieurtechnik*, vol. 61, no. 2, pp. 160-161.

Gnielinski, V., 1995, Ein neues Berechnungsverfahren für die Wärmeübertragung im Übergangsbereich zwischen laminarer und turbulenter Rohrströmung (in German), *Forschung im ingenieurwesen – Engineering Research,* vol. 61, no. 9, pp. 240-248.

Granryd, E., 2007, Optimal Flow Rates in Indirect Systems. *Proc. 22st International Congress of Refrigeration*, Beijing, pp. ICR07-B1-1376.

Grohmann, S., 2005, Measurement and Modeling of Single-Phase and Flow-Boiling Heat Transfer in Microtubes, *International Journal of Heat and Mass Transfer*, vol. 48, no. 19-20, pp. 4073-4089.

GUM, *Guide to the Expression of Uncertainty in Measurement*, 2nd ed., Geneva, Switzerland, International Organization for Standardization, 1995.

Haglund, C., and Fahlén, P., 2001, Jämförelse av metoder för att förbättra värmöverföring och tryckfall i köldbärarkylda kylbatterier med laminära vätskeflöden (in Swedish), *Proc. Nordic conference "16. Nordiske kølemøde, 9. Nordiske varmepumpedage"*, Copenhagen, Denmark, pp. 263-272.

Haglund Stignor, C., 2002, Liquid Side Heat Transfer and Pressure Drop in Finned-Tube Cooling-Coils, Thesis for the Degree of Licentiate of Engineering, Lund Institute of Technology.

Haglund Stignor, C., Fahlén, P., Sundén, B., and Eriksson, D., 2003, Optimal Operation for Cooling-Coils for Display Cabinets in Secondary Loop Refrigeration Systems. *Proc. 21st International Congress of Refrigeration*, Washington D.C., pp. ICR0275.

Haglund Stignor, C., Sundén, B., and Fahlén, P., 2007, Liquid Side Heat Transfer and Pressure Drop in Finned-Tube Cooling-Coils Operated with Secondary Refrigerants, *International Journal of Refrigeration*, vol. 30, no. 7, pp. 1278-1289.

Hausen, H., 1943, Darstellung, Des Wärmeüberganges in Rohren Durch Verallgemeinerte Potenzbeziehungen (in German), *Z. VDI Beihefte Verfahrenstechniik*, no. 4, pp. 91-98.

Hellsten, G., 1992, *Tabeller Och Diagram, Energi- och Kemiteknik (in Swedish)*, 1st ed., Almqvist & Wiksell Förlag AB, Falköping, Sweden.

Hong, K., and Webb, R. L., 2000, Wetting Coatings for Dehumidifying Heat Exchangers, *HVAC and Research*, vol. 6, no. 3, pp. 229-242.

Hong, S. H., and Hrnjak, P. S., 1999, Heat Transfer in Thermally Developing Flow of Fluids with High Prandtl Numbers Preceding and Following U-Bend, Air Conditioning and Refrigerating Center, University of Illinois Urbana-Champaign, October.

Horton, W. T., and Groll, E. A., 2000, Modelling of Secondary Loop Refrigeration Systems for Medium Temperature Supermarket Applications. *Proc. 4th IIR-Gustav Lorentzen Conf. Nat. Working Fluids,* West Lafayette, USA.

Horton, W. T., and Groll, E. A., 2001, Analysis of a Medium-Temperature Secondary Loop Refrigerating System, *ASHRAE Trans.*, vol. 107, no. 2, pp. 459-465.

Horton, W. T., and Groll, E. A., 2003, Secondary Loop Refrigeration in Supermarket Applications: A Case Study. *Proc. 21st int. Congr. Refrig.,* Washington, DC, pp. ICR0345.

Hrnjak, P. S., 1997, The Benefits and Penalties Associated with the Use of Secondary Loops. *Proc. ASHRAE-NIST Conf.*, Gaithersburg, pp. 85-95.

Hrnjak, P. S., 2000, Heat Transfer Issues in Laminar Flow of Single-Phase Secondary Refrigerants through the Pipes. *Proc. Workshop for IEA HPP Annex 26 Advanced Supermarket Refrigeration / Heat Recovery Systems*, Stockholm, Sweden,

Jacobi, A. M., Park, Y., Tafti, D., and Zang, X., 2001, An Assessment of the State of the Art, and Potential Design Improvements, for Flat-Tube Heat Exchangers in Air Conditioning and Refrigeration Applications - Phase 1, Air-Conditioning and Refrigeration Technology Institute (ARTI), September.

Jacobi, A. M., Park, Y., Zhong, Y., Michna, G., and Xia, Y., 2005, High Performance Heat Exchangers for Air-Conditioning and Refrigeration Applications (Non-Circular Tubes), Air-Conditioning and Refrigeration Technology Institute (ARTI), July.

Jacobi, A. M., and Xia, Y., 2005, Air-Side Data Interpretation and Performance Analysis for Heat Exchangers with Simultaneous Heat and Mass Transfer: Wet and Frosted Surfaces, *International Journal of Heat and Mass Transfer*, vol. 48, no. 25-26, pp. 5089-5102.

Jokar, A., Hosni, M. H., and Eckels, S. J., 2005, Correlations for Heat Transfer and Pressure Drop of Glycol-Water and Air Flows in Minichannel Heat Exchangers. *Proc. American Society of Heating, Refrigerating and Air-Conditioning Engineers, ASHRAE 2005 Annual Meeting, Jun 25-29 2005*, Denver, CO, United States, vol. 111 PART 2, pp. 213-224.

Kandlikar, S., 2007, A Roadmap for Implementing Minichannels in Refrigeration and Air-Conditioning Systems - Current Status and Future Directions, *Heat Transfer Engineering*, vol. 28, no. 12, pp. 973-985.

Kandlikar, S., Garimella, S., Li, D., Colin, S., and King, M., 2006, *Heat Transfer and Fluid Flow in Minichannels and Microchannels*, 1st ed., pp. 87-136, Elsevier Ltd., Oxford.

Kays, W. M., and London, A. L., 1984, *Compact Heat Exchangers*, 3rd ed., pp. 104-114, McGraw-Hill Book Company,

Kazachki, G. S., and Hinde, D. K., 2006, Secondary Coolant Systems for Supermarkets, *ASHRAE Journal*, no. September, pp. 35-46.

Kim, M.-H., and Bullard, C. W., 2002, Air-Side Thermal Hydraulic Performance of Multi-Louvered Fin Aluminum Heat Exchangers, *International Journal of Refrigeration*, vol. 25, no. 3, pp. 390-400.

Kruse, H., 2005, Commerical Refrigeration - on the Way to Sustainability. *Proc. IIR International Commercial Refrigeration Conference*, Vicenza, Italy, pp. 1.

Kumar, R., Varma, H. K., Agrawal, K. N., and Mohanty, B., 2001, A Comprehensiv Study of Modified Wilson Plot Technique to Determine the Heat Transfer Coefficient During Condensation of Steam and R-134a over Single Horizontal Plain and Finned Tubes, *Heat Transfer Engineering*, vol. 22, pp. 3-12.

Kuznetsov, V. V., and Shamirzaev, A. S., 2007, Boiling Heat Transfer for Freon R21 in Rectangular Minichannel, *Heat Transfer Engineering*, vol. 28, no. 8, pp. 738 - 745.

Langhaar, H. L., 1942, Steady Flow in the Transition Length in a Straight Tube, *Journal of Applied Mechanics*, vol. 9, pp. A55-A58.

Lei, N., Skandakumaran, P., and Ortega, A., 2006, Experiments and Modeling of Multilayer Copper Minichannel Heat Sinks in Single-Phase Flow. *Proc. 10th Intersociety Conference on Thermal and Thermomechanical Phenomena and Emerging Technologies in Electronic Systems, ITherm*, San Diego, pp. 9-18.

Lelea, D., Nishio, S., and Takano, K., 2004, The Experimental Research on Microtube Heat Transfer and Fluid Flow of Distilled Water, *International Journal of Heat and Mass Transfer*, vol. 47, no. 12-13, pp. 2817-2830.

Lindborg, A., 2004, Energiförhållanden för Indirekta System (in Swedish), *Kulde*, no. 3, pp. 26-30.

Madrid, F., Caney, N., and Marty, P., 2007, Study of a Vertical Boiling Flow in Rectangular Mini-Channels, *Heat Transfer Engineering*, vol. 28, no. 8, pp. 753 - 760.

Mao, Y., Terrell, W., and Hrnjak, P., 1998, Performance of a Display Case at Low Temperatures Refrigerated with R404a and Secondary Coolants. *Proc. IIF-IIR - Commission D1, D2/3*, Cambridge, UK, pp. 181-189.

Maråk, K. A., 2007, Liquid Phase Heat Transfer in Circular Microchannels at Low Temperatures. *Proc. 22nd International Congress of Refrigeration*, Beijing, pp. ICR07-A02-1072.

McLaughlin, W., J., and Webb, R., L., 2000, Wet Air Side Performance of Louver Fin Automotive Evaporators, *SAE Technical Paper Series*, no. 2000-01-0574, pp. 1-10.

Melinder, Å., 1997a, Heat Transfer and Other Characteristics of Low Temperature Liquid Secondary Refrigerants. *Proc. IIR (IIF) Conference "Heat transfer issues in natural refrigerants", Commission B1, with E1 & E2*, College Park, USA, pp. 150-159.

Melinder, Å., 1997b, *Thermophysical Properties of Liquid Secondary Refrigerants - Tables and Diagrams for the Refrigeration Industry*, International Insitute of Refrigeration, Paris, France.

Melinder, Å., 1997c, *Thermophysical Properties of Liquid Secondary Refrigerants - Charts and Tables, Handbook No 12 of the Swedish Society of Refrigeration*, 2nd ed., Swedish Society of Refrigeration, Stockholm.

Melinder, Å., 2005, Properties of Various Secondary Fluids for Supermarket Applications. *Proc. IIR International Conference Thermophysical Properties and Transfer Processes of Refrigerants*, Vicenza, Italy.

Melinder, Å., 2009, *Handbok om indirekta kyl- och värmepumpssystem (In Swedish),* To be published by the Swedish Society of Refrigeration in 2009, Kullavik.

Minea, V., 2007, Energy Efficiency of a Supermarket Refrigeration/Heat Recovery System with Secondary Fluids. *Proc. The 22nd International Congress of Refrigeration*, Beijing, China, pp. ICR07-B01-191.

Morini, G. L., 2004, Single-Phase Convective Heat Transfer in Microchannels: A Review of Experimental Results, *International Journal of Thermal Sciences*, vol. 43, no. 7, pp. 631-651.

Morini, G. L., 2006, Scaling Effects for Liquid Flows in Microchannels, *Heat Transfer Engineering*, vol. 27, no. 4, pp. 64 - 73.

Morini, G. L., and Spiga, M., 2007, The Role of the Viscous Dissipation in Heated Microchannels, *ASME Journal of Heat Transfer*, vol. 129, no. 3, pp. 308-318.

Moshfeghian, M., 1978, Fluid Flow and Heat Transfer in U-Bends, PhD Thesis, Oklahoma State University.

Muzychka, Y. S., and Yovanovich, M. M., 2004, Laminar Forced Convection Heat Transfer in the Combined Entry Region of Non-Circular Ducts, ASME *Journal of Heat Transfer*, vol. 126, no. February, pp. 54-61.

Nyvad, J., and Lund, S., 2000, Indirect Cooling with Ammonia in Supermarkets, *Celsius*, vol. 28, no. 5, pp. 20-21.

Rathod, M. K., Niyati, K. S., and Prabhakaran, P., 2007, Performance Evaluation of Flat Finned Tube Fin Heat Exchanger with Different Fin Surfaces, *Applied Thermal Engineering*, vol. 27, no. 11-12, pp. 2131-2137.

Shah, R. K., and London, A. L., 1978, *Laminar Flow Forced Convection in Ducts - Supplement 1*, pp. 477, Academic Press, New York.

Shah, R. K., and Sekulić, D. P., 2003, *Fundamentals of Heat Exchanger Design*, 1st ed., pp. 232-299, John Wiley & Sons, Inc., Hoboken, N.J. USA.

Shin, J. S., and Kim, M. H., 2005, An Experimental Study of Flow Condensation Heat Transfer inside Circular and Rectangular Mini-Channels, *Heat Transfer Engineering*, vol. 26, no. 3, pp. 36-44.

Sieder, E. N., and Tate, C. E., 1936, Heat Transfer and Pressure Drop of Liquids in Tubes, *Industrial and Engineering Chemistry*, vol. 28, pp. 1429.

Smotrys, M. L., Ge, H., Jacobi, A. M., and Dutton, J. C., 2003, Flow and Heat Transfer Behavior for a Vortex-Enhanced Interrupted Fin, *ASME Journal of Heat Transfer*, vol. 125, no. 5, pp. 788-794.

Sommers, A. D., and Jacobi, A. M., 2004, Air-Side Heat Transfer Augmentation of a Refrigerator Evaporator Using Vortex Generation. *Proc. International Refrigeration and Air Conditioning Conference at Purdue*, Purdue University, West Lafayette, USA, pp. R034, 8 p.

Sommers, A. D., and Jacobi, A. M., 2005, Air-Side Heat Transfer Augmentation of a Refrigerator Evaporator Using Vortex Generation, International Journal of Refrigeration, vol. 28, pp. 1006-1017.

Svensson, K., 2005, Secondary Refrigeration Systems Offer Important Environmental Benefits, *ScanRef*, no. 4, pp. 28-29.

Ure, Z., 2003a, Secondary Refrigeration Developments and Experiences in Europe. *Proc. International Congress of Refrigeration 2003*, Washington DC, USA, pp. ICR0007.

Ure, Z., 2003b, Secondary Refrigeration - European Experiences, *ScanRef*, no. 3, pp. 37-40.

Verwoerd, M., Liem, N., and Gerwen, R. J. M. v., 1999, Performance of a Frozen Food Display Cabinet with Potassium Formate as Secondary Refrigerant. *Proc. 20th Int. Congr. Refrig.*, Sydney, Australia, paper no. 552.

Walker, D. H., 2000, Low-Charge Refrigeration for Supermarkets, *IEA HPC Newsl*, vol. 18, no. 1, pp. 13-16.

Wang, C.-C., 2000a, Recent Progress on the Air-Side Performance of Fin-and-Tube Heat Exchangers, *International Journal of Heat Exchangers*, vol. 1, no. 1, pp. 49-76.

Wang, L. B., Zhang, Y. H., Su, Y. X., and Gao, S. D., 2002a, Local and Average Heat/Mass Transfer over Flat Tube Bank Fin Mounted in-Line Vortex Generators with Small Longitudinal Spacing, *Journal of Enhanced Heat Transfer*, vol. 9, no. 2, pp. 77-87.

Wang, L. B., Ke, F., Gao, S. D., and Mei, Y. G., 2002b, Local and Average Characteristics of Heat/Mass Transfer over Flat Tube Bank Fin with Four Vortex Generators Per Tube, *ASME Journal of Heat Transfer*, vol. 124, no. 3, pp. 546-552.

Webb, R. L., 1994, *Principles of Enhanced Heat Transfer*, 1st ed., John Willey & Sons Inc., New York.

Wilbulswas, P., 1966, Laminar Flow Heat Transfer in Noncircular Ducts, Ph.D. Thesis, London University.

Zhong, Y., Xia, Y., and Jacobi, A. M., 2007, An Experimental Study of Louver-, Wavy- and Plain-Fin Flat-Tube Heat Exchanger Performance under Frosting Conditions. *Proc. The 22nd International Congress of Refrigeration*, Beijing, China, pp. ICR07-B02-586.

EC Regulation No 852/2004 of the European Parliament and of the Council of 29 April 2004 on the hygiene of foodstuffs, 2004.

EC Regulation No 842/2006 of the European Parliament and of the Council of 17 May 2006 on certain fluorinated greenhouse gases, 2006.

Kylbranschens Samarbetsstiftelse, KYS, 1994, *Svensk kylnorm, Faktablad 6 (in Swedish)*

Livsmedelsverket, 1996, *SLV FS 1996:5 Statens livsmedelsverks kungörelse med föreskrifter och allmänna råd om hantering av livsmedel (in Swedish)*

Naturvårdsverket, 1988, *Statens naturvårdsverks kungörelse med föreskrifter om kyl- och värmepumpanläggningar innehållande CFC, övriga CFC, haloner, HCFC och HFC, "Köldmediekungörelsen"; SNFS 1988:3 MS10, (in Swedish).*

Naturvårdsverket, 1997, *Kylanläggningar och värmepumpar – med ozonnedbrytande köldmedier eller HFC-köldmedier, Köldmediekungörelsen med kommentarer, Allmänna råd 97:2, (in Swedish).*

SFS 2007:846, Förordning om fluorerade växthusgaser och ämnen som bryter ned ozonskiktet, (in Swedish), 2007.

prEN441 Refrigerated Display Cabinets, (1993), CEN.

SS-EN1216, Heat Exchangers - Forced Circulation Air-Cooling and Air-Heating Coils - Test Procedure for Establishing the Performance, (1998), CEN.

VDI-Wärmeatlas - Berechnunsblätter für den Wärmeubergang, Springer-Verlag, (1997), Berlin, Germany.

Appendix A
Uncertainty of Measurements (Paper I, II and IV)

The uncertainty of measurements has been evaluated according to Guide to the Expression of Uncertainty in Measurement, GUM (1995) and EAL-R2 (1997). The former method establishes general rules for establishing and expressing uncertainty of measurements that can be followed in most fields of physical measurements. The latter method is in accordance with the former one, but concentrates on the method most suitable for measurements in a calibration laboratory.

According to these methods, the measurand or (output quantity), Y, is the particular quantity subject to measurement. The output quantity depends on a number of input quantities, X_i ($i = 1,2,3 ..,N$) according to the functional relationship. The model function f describes how values of the output quantity Y can be determined from the input quantities X_i.

$$Y = f(X_1, X_2, ..,X_N) \qquad (A.1)$$

An estimate of the measurand Y, the output estimate y, is obtained from Eq. (A.2) using input estimates x_i for the values of the input quantities X_i

$$y = f(x_1, x_2,.., x_N) \qquad (A.2)$$

Evaluation of Uncertainty of Measurement of Input Estimates

The uncertainty of measurement associated with the input estimates is evaluated according to either a "Type A" or a "Type B" method of evaluation. The Type A evaluation of standard uncertainty is the method of evaluating the uncertainty by the statistical analysis of a series of observations. In this case, the standard uncertainty $u(x_i)$ is the experimental standard deviation of the mean that follows from an averaging procedure or an appropriate regression analysis. The Type B evaluation of standard uncertainty $u(x_i)$ is the method of evaluating the uncertainty by means other than statistical analysis of a series of observations. In this case, the evaluation of the standard uncertainty is based on some other scientific knowledge.

Calculation of the Standard Uncertainty of the Output Estimates

For the uncorrelated input quantities, the square of the standard uncertainty associated with the output estimate y is given by

$$u^2(y) = \sum_{i=1}^{N} u_i^2(y) \qquad\qquad (A.3)$$

The quantity $u_i(y)$ $(i = 1,2,..,N)$ is the contribution to the standard uncertainty associated with the output estimate y resulting from the standard uncertainty associated with the input estimate x_i

$$u_i(y) = c_i \cdot u_i(x_i) \qquad\qquad (A.4)$$

where c_i is the sensitivity coefficient associated with the input estimate x_i, i.e. the partial derivative of the model function f with respect to X_i, evaluated at the input estimate x_i,

$$c_i = \frac{\partial f}{\partial x_i} = \frac{\partial f}{\partial X_i} \qquad (X_1 = x_1 ... X_N = x_N) \qquad\qquad (A.5)$$

If the model function f is a sum or a difference of the input quantities X_i

$$f(X_1, X_2,.., X_N) = \sum_{i=1}^{N} (p_i \cdot X_i) \qquad\qquad (A.6)$$

the output estimate y is given by the corresponding sum or difference of the input estimates

$$y(x_i) = \sum_{i=1}^{N} (p_i \cdot x_i) \qquad\qquad (A.7)$$

whereas the sensitivity coefficients equal p_i and the square of the standard uncertainty associated with the output estimate can be calculated according to

$$u^2(y) = \sum_{i=1}^{N} \left(p_i^2 \cdot u^2(x_i) \right) \qquad\qquad (A.8)$$

If the model function f is a product or quotient of the input quantities X_i

$$f(X_1, X_2,.., X_N) = c \cdot \prod_{i=1}^{N} X_i^{p_i} \qquad\qquad (A.9)$$

the output estimate again is the corresponding product or quotient of the input estimates

$$y = c \cdot \prod_{i=1}^{N} x_i^{p_i} \tag{A.10}$$

The sensitivity coefficient is equal to $p_i \cdot y/x_i$ in this case and an expression analogous to Eq. (A.8) is obtained from Eq. (A.3), if the relative standard uncertainties $w(y) = u(y)/|y|$ and $w_i = u(x_i)/|x_i|$ are used.

$$w^2(y) = \sum_{i=1}^{N} \left(p_i^2 \cdot w^2(x_i) \right) \tag{A.11}$$

Expanded Uncertainty of Measurement

The expanded uncertainty of measurement U, is obtained by multiplying the standard uncertainty $u(y)$ of the output estimate by a coverage factor k,

$$U = k \cdot u(y) \tag{A.12}$$

In cases where a normal (Gaussian) distribution can be attributed to the measurand, and the standard uncertainty associated with the output estimate has sufficient reliability, the standard coverage factor $k = 2$ must be used. The assigned expanded uncertainty corresponds to a coverage probability of approximately 95 %.

The uncertainty of the calculated quantities has been calculated in a manner analogously to Eq. (A.8) and Eq. (A.11). As an example, the uncertainty of the cooling capacity on the liquid side, $\dot{Q}_b$, has been calculated according to the expression below. The expanded uncertainty of the results of the experiments is presented in the graphs were the results are displayed.

$$\dot{Q}_b = \dot{V}_b \cdot \rho_b \cdot c_{pb} \cdot (t_{bout} - t_{bin}) \tag{A.13}$$

$$\left[U(\dot{Q}_b) \right]^2 = \left[\frac{\partial \dot{Q}_b}{\partial(\dot{V}_b)} \cdot U(\dot{V}_b) \right]^2 + \left[\frac{\partial \dot{Q}_b}{\partial(\rho_b)} \cdot U(\rho_b) \right]^2 + \left[\frac{\partial \dot{Q}_b}{\partial(c_{pb})} \cdot U(c_{pb}) \right]^2 +$$
$$\left[\frac{\partial \dot{Q}_b}{\partial(t_{bout} - t_{bin})} \cdot U(t_{bout} - t_{bin}) \right]^2 \tag{A.14}$$

Estimated Expanded Uncertainty for Measurands, Dimensions and Tabulated Values

Table A.1 below presents the estimated expanded uncertainties for each measurand used in the experiments outlined in Paper II. (The corresponding tables for the experiments presented in Papers I and IV can be found in these papers.) These values are based on long-time experience of the different measurement devices and installations. Fahlén, (1994) presented detailed uncertainty budgets for capacity measurements on brine-cooled air coils, and his report was consulted when estimating the uncertainties displayed below. In addition, the tables show the estimated uncertainty for some calculated dimensions and for the calculated energy balances. The estimated uncertainty for the measurement results are shown in the graphs where these results are presented.

Table A.1. Estimated expanded uncertainties in Paper II

Measurands	Unit	MPE1	MPE2	MPE3
Liquid measurands				
Liquid mass flow rate, $\dot{m}_b$	%	± 0.5	± 0.5	± 0.5
Liquid temperature, t_b	K	± 0.1	± 0.1	± 0.1
Liquid temperature difference, Δt_b	K	± 0.1	± 0.1	± 0.1
Concentration by weight[b]	%	± 1	± 1	± 1
Liquid density, ρ_b	%	± 0.2	± 0.2	± 0.2
Liquid density[a], ρ_b	%	± 0.2	± 0.2	± 0.2
Specific heat capacity[a], $c_{p,b}$	%	± 3 (± 1[c])	± 3 (± 1[c])	± 3 (± 1[c])
Dynamic viscosity[a], μ_b	%	± 3[d] (± 5[e])	± 3[d] (± 5[e])	± 3[d] (± 5[e])
Thermal conductivity[a], λ_b	%	± 3	± 3	± 3
Electric measurands				
Electric power (pump), $\dot{W}_{e,p}$	%	± 0.5	± 0.5	± 0.5
Electric power (heater), $\dot{W}_{e,heater}$	%	± 2	± 2	± 2
Calculated values				
Heat flux rate, $\dot{Q}_b$	%	± 1 - 4	± 1 - 4	± 1 - 4
$U(Nu_{b,m})_{measurands}$	%	± 5 - 7	± 6 - 14	± 8 - 18
Dimensions				
Shortest duct side, l_1	%	± 3.4	± 3.4	± 10.6
Longest duct side, l_2	%	± 3.0	± 3.0	+7.2 / -13.4
$U(Nu_{b,m})_{dimensions}$ (if independent)	%	± 0.1	± 0.1	± 1.3
$U(Nu_{b,m})_{dimensions}$ (if dependent)		± 0.3	± 0.3	+6.6 / -5.0
Data reduction[f]				
$U(Nu_{b,m})_{data\ reduction}$	%	± 4	± 4	± 4

[a]Uncertainty for tabulated values taking the uncertainty regarding the temperature (and concentration) into account.

74

[b]Valid for propylene glycol. (Liquids premixed by the manufacturer were used in the experiments with the other secondary refrigerants and the density of the liquids was checked.)

[c]Valid for water

[d]Valid for Temper -20 and Hycool 20

[e]Valid for propylene glycol, 39 %$_w$

[f]See Appendix B

Appendix B
Additional Information for Paper II

Estimation of Measurement Uncertainty due to the Applied Data Reduction Methodology

The data reduction procedure applied by using Eq. (1) – Eq. (10) in Paper II implies that the heat transfer resistance is equal along the entire test section. However, in these experiments, the flow regime is laminar and the heat transfer coefficient is higher at the beginning of the tube compared to further down the tube length. In order to estimate the extent of the error caused by using this data reduction procedure for these tests in the laminar flow regime, stepwise calculations have been performed along the test section. In these stepwise calculations the tube was divided into 200 segments, each 10 mm long. The local tube-side heat transfer coefficient was calculated by using the model for mean Nusselt number according to Eq. B.28 (see page 82) in Eq. B.1 below. The applied correlation (Eq. B.28) was selected since relatively good agreement between measured and predicted data had been found for this correlation (see Paper II) for the MPE1 tube. When evaluating experimental data, thermophysical properties at the arithmetic mean temperature of the liquid were used when applying the data reduction procedure according to Eq. (1) – Eq. (10) in Paper II. However, in the stepwise calculations, thermophysical properties at the predicted temperature of the actual segment were used when calculating the local Nusselt number.

$$Nu_{b,x*} = \frac{d}{dx*}\left(Nu_{b,m} \cdot x*\right)$$

(B.1)

The main relations used in the stepwise calculations are displayed below. However, not all the iteration loops are presented.

$$t_{b,1} = t_{b,in}$$
(B.2)

$$t_{W,1} = t_{W,out}$$
(B.3)

$$\dot{Q}_{b,tot,1} = 0$$
(B.4)

$$\mu_{b,i} = f(secondary\ refrigerant,\ t_{b,i})$$
(B.5)

$$\mu_{b,wall,i} = f(secondary\ refrigerant,\ t_{b,w,i})$$
(B.6)

77

$$\lambda_{b,i} = f(\textit{secondary refrigerant, } t_{b,i}) \tag{B.7}$$

$$c_{p,b,i} = f(\textit{secondary refrigerant, } t_{b,i}) \tag{B.8}$$

$$\mathrm{Re}_{b,i} = \frac{d_h \cdot \dot{m}_b}{A_c \cdot \mu_{b,i}} \tag{B.9}$$

$$\mathrm{Pr}_{b,i} = \frac{c_{p,b,i} \cdot \mu_{b,i}}{\lambda_{b,i}} \tag{B.10}$$

$$x_i = x_{i-1} + 0.01 \tag{B.11}$$

$$x^*_{\,i} = \frac{x_i}{d_h \cdot \mathrm{Re}_{b,i} \cdot \mathrm{Pr}_{b,i}} \tag{B.12}$$

$$Nu_{b,i} = \left(3.66^3 + 0.7^3 + \left(1.077 \cdot (x^*_{\,i})^{-1/3} - 0.7 \right)^3 \right)^{1/3} \cdot \left(\frac{\mu_{b,i}}{\mu_{b,i}} \right)^{0.14} \tag{B.13}$$

$$(U \cdot A)_i = \frac{1}{R_{W\&w} \cdot (l_{tube}/l_x) + \dfrac{d_h}{Nu_{b,i} \cdot \lambda_{b,i} \cdot A_b \cdot (l_x/l_{tube})}} \tag{B.14}$$

$$\dot{Q}_{b,i} = \frac{UA_i \cdot (t_{W,i-1} - t_{b,i-1})}{\left(1 - UA_i \cdot \left(1 / \left(\dot{V}_W \cdot \rho_{W,i} \cdot c_{p,W,i} \right) - 1 / \left(\dot{m}_b \cdot c_{p,b,i} \right) \right) \right)} \tag{B.15}$$

$$t_{b,i} = t_{b,i-1} + \frac{\dot{Q}_{b,i}}{\dot{m}_b \cdot c_{p,b,i}} \tag{B.16}$$

$$t_{W,i} = t_{W,i-1} + \frac{\dot{Q}_{b,i}}{\dot{V}_W \cdot \rho_{W,i} \cdot c_{p,W,i}} \tag{B.17}$$

$$t_{w,i} = t_{b,i} + \dot{Q}_{b,i} \cdot \frac{d_h}{Nu_{b,i} \cdot \lambda_{b,i} \cdot A_b \cdot (l_x/l_{tube})} \tag{B.18}$$

$$t_{b,out,Gnielinski} = t_{b,i=201} \tag{B.19}$$

$$t_{W,in,Gnielinski} = t_{W,i=201} \tag{B.20}$$

$$\dot{Q}_{b,Gnielinski} = \sum_{i=1}^{201} \dot{Q}_{b,i} \qquad (B.21)$$

If the tube-side heat transfer could have been described completely by the Gnielinski model, Eq. B.28, then the outlet temperature of the secondary refrigerant would have been in accordance with $t_{b,out,Gnielinski}$ (Eq. B.19) and the inlet temperature of the water in accordance with $t_{W,in,Gnielinski}$ (Eq. B.20). These values, in combination with the measured inlet temperature of the secondary refrigerant, $t_{b,in}$, and the measured outlet temperature of the water, $t_{w,out}$, which were used as start values in the stepwise calculations, could be used for calculating a "new" logarithmic mean temperature difference, $\Delta t_{lm,Gnielniski}$ according to Eq. B.22 below.

$$\Delta t_{lm,Gnielinski} = \frac{\left(t_{W,in,Gnielinski} - t_{b,out,Gnielinski}\right) - \left(t_{W,out} - t_{b,in}\right)}{\ln\left(\left(t_{W,in,Gnielinski} - t_{b,out,Gnielinski}\right) / \left(t_{W,out} - t_{b,in}\right)\right)} \qquad (B.22)$$

By using the cooling capacity (heat flow rate) resulting from the stepwise calculations, $\dot{Q}_{b,Gnielinski}$ (Eq. B.21) and the logarithmic mean temperature difference calculated according to Eq. B.22, a hypothetical "experimentally determined" mean Nusselt number could be calculated according to Eq. B.23 - Eq. B.25 below.

$$\left(U \cdot A\right)_{Gnielinski} = \frac{\dot{Q}_{b,Gnielinski}}{\Delta t_{lm,Gnielinski}} \qquad (B.23)$$

$$\alpha_{b,Gnielinski} = \frac{1}{A_b \cdot \left(1/\left(U \cdot A\right)_{Gnielinski} - R_{W\&w}\right)} \qquad (B.24)$$

$$Nu_{b,Gnielinski,measured} = \frac{\alpha_{b,Gnielinski} \cdot d_h}{\lambda_b} \qquad (B.25)$$

This Nusselt number can then be compared with the correlated mean Nusselt number by the same correlation, Eq. B.28 (see page 82), $Nu_{b,Gnielinski\ modelled}$. Thermophysical data for the arithmetic mean temperature of the liquid was used when applying this model in the evaluation of the results presented in the main text body of Paper II. This was also the case for Eq. B.25. The arithmetic mean temperature of the liquid was calculated according to Eq. B.26 below.

$$t_{b,am,Gnielinski} = \frac{t_{b,in} + t_{b,out,Gnielinski}}{2} \qquad (B.26)$$

By comparing these two Nusselt numbers, an estimate of the extent of the error caused by using the data reduction procedure according Eq. (1) – Eq. (10) in Paper II could be obtained. A ratio could be calculated as follows.

$$X_{Gnielinski} = \frac{Nu_{b,Gnielinski,\text{mod}elled}}{Nu_{b,Gnielinski,measured}}$$

(B.27)

An equal heat transfer along the entire tube length is assumed when applying the data reduction procedure according Eq. (1) – Eq. (10) in Paper II. This will overestimate the temperature difference, which in turn will underestimate the Nusselt number (X > 1). On the other hand, the fact that thermophysical properties at the arithmetic mean temperature of the liquid are used when calculating the correlated mean Nusselt number, but the predicted temperature of the actual segment is used in the stepwise calculations, counteracts this effect to some extent. Therefore $X_{Gnielinski}$, can also be lower than unity.

The evaluation procedure described above, Eq. B.2 - Eq. B.27, was performed for the test points of the MPE1 tube. The resulting $X_{Gnielinski}$ values are plotted against x^* in Figure B.1 As can be seen, the difference between the "measured" and modelled mean Nusselt number is less than 4 % in all test points of the MPE1 tube. However, this difference is not negligible, but it is relatively small in comparison with the measurement uncertainty of the experimentally determined mean Nusselt number. Therefore, the possible error in the evaluation of the experimentally determined mean Nusselt number, due to the assumption that the heat transfer resistance is equal along the tube length and the application of thermophysical properties at the arithmetic mean temperature difference, has been treated as a contribution to the total expanded uncertainty for the mean Nusselt number. The expanded contribution to the total uncertainty for the experimentally determined mean Nusselt number, due to the applied data reduction methodology, $U(Nu)_{data\ reduction}$, has been set to 4 % for $k = 2$ for all test points performed with the three MPE tubes.
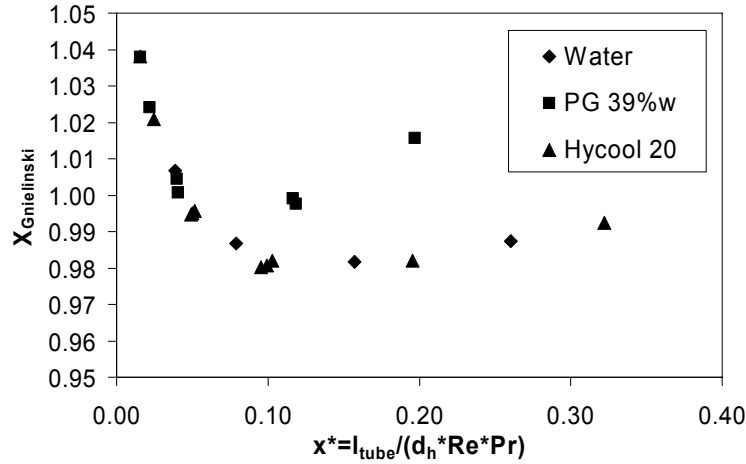
Figure B.1   The relation between the correlated and the fictive "measured" mean Nusselt number, $X_{Gnielinski}$ for the MPE1 tube.

Verification of the "Wilson plot" method

In this study the "Wilson plot" method, described by (for example) Kumar *et al.* (2001) and Shah and Sekuliç (2003), was used for determination of the sum of heat transfer resistance on the outside of the tube and the resistance through the tube wall, $R_{W\&w}$. In order to verify that the separation of the thermal resistances by the "Wilson plot" method resulted in reasonable values, surface temperature measurements were performed by thermistor temperature sensors mounted on the outer surface of the tube. Stepwise calculations were then carried out along the entire length of the test section using the inlet temperature of the secondary refrigerant and the outlet temperature of the water as starting values (described in the preceding section). In the calculations the test section was divided into 200 segments, and the tube-side heat transfer coefficient was calculated by using the Gnielinski (1989) model for local Nusselt numbers (see Eq. B.1) derived from the one for mean Nusselt number, given by Eq. B.28 and Eq. B.29.

Figure B.2 below show the results from such a stepwise calculation for a test point at $x^* = 0.040$ ($Re = 102$) in Figure 4 of paper II, where good agreement had been found with this Gnielinski model. The symbols represent measured values and the lines values predicted in the stepwise calculations. It can be seen that the measurements performed by the thermistor temperature sensors agree well with the wall temperature predicted by using the Gnielinski (1989) model in the stepwise calculations. However, one exception is for the thermistors placed closest to the inlet of the water to the test section (closest to the outlet of the secondary refrigerant) and might be explained by higher turbulence

intensity on the outside of the MPE tube, since they are placed very close to the water inlet. Another explanation can simply be poorer thermal contact for those thermistors. It is unlikely that the heat transfer coefficient on the inside of the tube is very much lower at this end of the tube than it is over the rest of the tube. The figure also shows that the predicted outlet temperature of the secondary refrigerant and the predicted inlet temperature of the water agree well with the measured values.
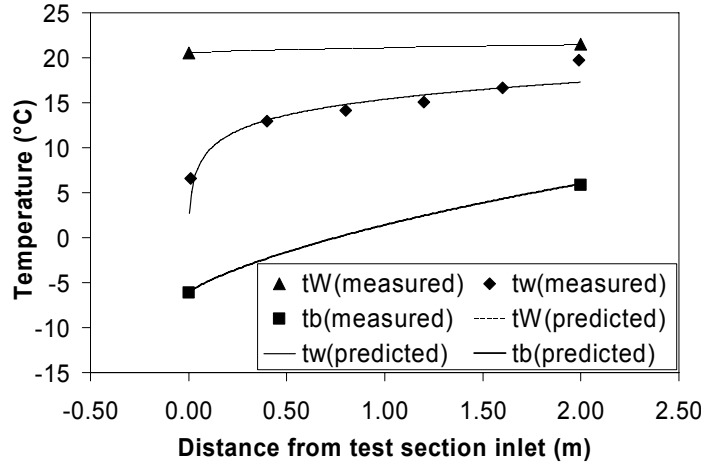
Figure B.2   Temperature profile of the secondary refrigerant (propylene glycol, 39 %w), of the water outside the tube and of the tube wall for a test point were the $Re = 102$ and $x^* = 0.040$.

Models and Correlations used in the Comparison of Experimentally Determined Data

"Gnie [20]" in Paper II, Gnielinski (1989) quoted in VDI (1997)

$$Nu_{b,m} = \left(3.66^3 + 0.7^3 + \left(1.615 \cdot (x*)^{-1/3} - 0.7 \right)^3 \right)^{1/3}$$
(B.28)

$$x* = \frac{l_{tube}}{d_h \cdot Re_b \cdot Pr_b}$$
(B.29)

Valid range: *Laminar flow, developing temperature profile, fully developed velocity profile, constant (uniform) wall temperature boundary condition.*

"K. and B. mod. [24]" in Paper II, Kim and Bullard (2002) refer to private communication with N.-H. Kim

$$Nu_{b,m} = Nu_{ref} + 0.0499 \cdot \text{Re}_b \cdot \text{Pr}_b \frac{d_h}{l_{tube}} \qquad \text{(B.30)}$$

Nu_{ref} = fully developed limit for a rectangular duct with the actual aspect ratio according to Shah and London (1978), Table 43 $\qquad$ (B.31)

Valid range: *$150 \leq Re_b \leq 500$*

"G. et al. [8]" i Paper II, Garimella *et al.* (2001)

$$Nu_{b,m} = \left(Nu_{lam}^{10} + \left\{ \frac{\exp[(360 - \text{Re})/925]}{Nu_{lam}^{2}} + \frac{1}{Nu_{turb}^{2}} \right\}^{-5} \right)^{0.1} \qquad \text{(B.32)}$$

$$Nu_{lam} = \left(Nu_{fd}^{3} + \left\{ \frac{0.468 \cdot (d_h/l_{tube}) \cdot \text{Re}_b \cdot \text{Pr}_b}{1 + 0.165 \cdot [(d_h/l_{tube}) \cdot \text{Re}_b \cdot \text{Pr}_b]^{2/3}} \right\}^{3} \right)^{1/3} \cdot \left(\frac{\mu_b}{\mu_w} \right)^{0.25} \qquad \text{(B.33)}$$

$$Nu_{fd} = 8.235 \cdot \left(\begin{array}{l} 1 - 2.0421 \cdot \gamma + 3.0853 \cdot \gamma^2 - 2.4765 \cdot \gamma^3 \\ + 1.0578 \cdot \gamma^4 - 0.1861 \cdot \gamma^5 \end{array} \right) \qquad \text{(B.34)}$$

$$Nu_{turb} = 0.012 \cdot \text{Re}_b^{0.85} \cdot \text{Pr}_b^{0.4} \cdot \left[1 + \left(\frac{d_h}{l_{tube}} \right)^{2/3} \right] \cdot \left(\frac{\mu_b}{\mu_w} \right)^{0.25} \qquad \text{(B.35)}$$

Valid range: *$0.029 < \gamma < 0.108$, $1.737 < d_h \text{ (mm)} < 3.018$, $0.140 < l_{tube} \text{ (m)} < 0.689$, $118 < Re_b < 10\ 671$, $6.48 < Pr_b < 16.20$, $0.243 < \mu_b/\mu_w < 0.630$, simultaneously developing flow.*

"M. and Y. [25]" in Paper II, Muzychka and Yovanovich (2004)

$$Nu_{\sqrt{A_{c,duct}}}(z^*) = \left[\left(\frac{C_4 \cdot f(\mathrm{Pr})}{\sqrt{z^*}} \right)^m + \left(\left\{ C_2 \cdot C_3 \left(\frac{f \cdot \mathrm{Re}_{\sqrt{A_{c,duct}}}}{z^*} \right)^{1/3} \right\}^5 + \left\{ C_1 \cdot \left(\frac{f \cdot \mathrm{Re}_{\sqrt{A_{c,duct}}}}{8 \cdot \sqrt{\pi} \cdot \gamma^{\zeta}} \right) \right\}^5 \right)^{m/5} \right]^{1/m} \tag{B.36}$$

$$f(\mathrm{Pr}) = \frac{0.564}{\left[1 + \left(1.664 \cdot \mathrm{Pr}^{1/6} \right)^{9/2} \right]^{2/9}} \tag{B.37}$$

$C_1 = 3.24$

$C_3 = 0.409$

for the UWT (uniform wall temperature) boundary condition.

$C_2 = 3/2$

$C_4 = 2$

for average Nusselt number

$\zeta = 1/10$

for ducts with rounded corners or right-angled corners (> 90 °).

$$z^* = \frac{l_{tube}}{\sqrt{A_{c,duct}} \cdot \mathrm{Re}_{\sqrt{A_{c,duct}}} \cdot \mathrm{Pr}_b} \tag{B.38}$$

$$m = 2.27 + 1.65 \cdot \mathrm{Pr}^{1/3} \tag{B.39}$$

$$f \cdot \mathrm{Re}_{\sqrt{A_{c,duct}}} = \frac{12}{\sqrt{\gamma} \cdot (1 + \gamma) \cdot \left[1 - \frac{192 \cdot \gamma}{\pi^5} \cdot \tanh \left(\frac{\pi}{2 \cdot \gamma} \right) \right]} \tag{B.40}$$

for fully hydrodynamically developed flow

Valid range: *0.1 < Pr_b < ∞, 0 < z* < ∞, as reproduced here – for the uniform wall temperature boundary condition, for ducts with rounded corners or right angled corners (> 90 °) and for hydrodynamically fully developed flow.*

<u>Hausen's correlation, Hausen (1943)</u>

$$Nu_m = 3.65 + \frac{0.0668 \cdot \mathrm{Re}_b \cdot \mathrm{Pr}_b \cdot d_h / l_{tube}}{1 + 0.045 \cdot \left(\mathrm{Re}_b \cdot \mathrm{Pr}_b \cdot d_h / l_{tube}\right)^{2/3}} \tag{B.41}$$

Valid range: *Laminar flow, developing temperature profile, fully developed velocity profile.*

Summary of Measurement Results

The tables below list the most important measured values for the various test points.

Table B1. Measured values for the various test points for the MPE1 tube

Variable	$t_{b,in}$	$t_{b,out}$	$\dot{m}_b$	$t_{W,in}$	$t_{W,out}$	$\dot{V}_W$	$\dot{W}_{e,tot}$
Unit	(°C)	(°C)	(kg/h)	(°C)	(°C)	(m³/h)	W
Water	8.3	11.7	563.8	21.7	20.5	1.73	2249
Water	8.0	11.6	531.9	21.7	20.5	1.73	2275
Water	8.1	11.8	499.8	21.5	20.3	1.72	2176
Water	8.0	12.0	451.0	21.5	20.4	1.73	2104
Water	8.2	11.5	566.7	21.5	20.4	1.71	2181
Water	8.2	11.6	532.1	21.5	20.4	1.71	2132
Water	8.2	11.7	499.0	21.3	20.2	1.71	2035
Water	8.1	11.9	450.4	21.4	20.3	1.73	1987
Water	8.1	11.8	448.2	21.4	20.3	1.65	1938
Water	8.4	11.6	564.8	21.6	20.4	1.65	2110
Water	7.4	12.5	200.4	21.5	20.9	1.73	1182
Water	5.6	14.5	98.5	21.2	20.7	1.73	1033
Water	4.2	18.0	49.7	21.3	20.8	1.73	810
Water	4.3	20.0	30.1	21.3	20.9	1.73	569
PG 39%$_w$	-2.6	2.9	373.9	21.6	20.5	1.72	2077
PG 39%$_w$	-3.8	3.4	266.9	21.5	20.4	1.72	1945
PG 39%$_w$	-6.1	5.8	147.5	21.5	20.5	1.72	1796
PG 39%$_w$	-13.5	13.6	50.6	21.4	20.6	1.72	1401
PG 39%$_w$	-12.3	13.8	49.8	21.4	20.6	1.72	1381
PG 39%$_w$	-14.2	18.4	30.0	21.3	20.8	1.72	994
PG 39%$_w$	6.9	13.0	146.5	21.3	20.8	1.71	921
Hycool 20	-2.3	2.3	631.9	21.6	20.2	1.73	2460
Hycool 20	-3.3	3.3	397.9	21.6	20.4	1.73	2202
Hycool 20	-6.3	6.3	200.9	21.4	20.3	1.73	2114
Hycool 20	-11.2	11.4	103.2	21.3	20.3	1.73	1936
Hycool 20	-14.7	17.8	50.7	21.3	20.6	1.73	1369
Hycool 20	-13.7	20.3	30.9	21.3	20.8	1.73	873
Hycool 20	2.8	11.1	201.1	21.4	20.7	1.72	1399
Hycool 20	-0.5	14.5	101.5	21.3	20.6	1.72	1273
Hycool 20	12.1	16.0	199.8	21.2	20.9	1.72	668
Hycool 20	10.4	17.7	100.1	21.2	20.9	1.71	611

Table B2. Measured values for the various test points for the MPE2 tube

Variable	$t_{b,in}$	$t_{b,out}$	$\dot{m}_b$	$t_{W,in}$	$t_{W,out}$	$\dot{V}_W$	$\dot{W}_{e,tot}$
Unit	(°C)	(°C)	(kg/h)	(°C)	(°C)	(m³/h)	W
Water	7.7	12.1	452.0	21.6	20.3	1.72	2334
Water	7.7	12.3	401.1	21.6	20.4	1.72	2144
Water	6.8	13.3	200.6	21.5	20.6	1.73	1524
Water	4.3	15.7	100.4	21.4	20.6	1.73	1331
Water	4.3	19.2	49.9	21.2	20.7	1.73	869
Water	4.2	20.8	31.9	21.4	21.1	1.71	614
PG 39%$_w$	-3.8	3.9	350.3	21.7	20.2	1.71	2767
PG 39%$_w$	-4.2	4.5	299.4	21.7	20.3	1.71	2690
PG 39%$_w$	-6.9	5.8	197.6	21.7	20.3	1.71	2574
PG 39%$_w$	-10.4	9.9	103.5	21.5	20.3	1.71	2189
PG 39%$_w$	-13.3	16.1	51.5	21.5	20.6	1.71	1601
PG 39%$_w$	-13.6	19.9	30.3	21.5	20.9	1.71	1044
PG 39%$_w$	2.9	11.1	195.8	21.4	20.5	1.72	1646
PG 39%$_w$	0.2	13.8	102.0	21.4	20.6	1.72	1442
PG 39%$_w$	-3.4	17.7	50.0	21.4	20.8	1.71	1102
PG 39%$_w$	11.9	15.9	199.1	21.3	20.8	1.71	839
PG 39%$_w$	10.4	17.5	99.0	21.4	21.0	1.72	742
PG 39%$_w$	8.8	19.2	50.4	21.3	20.9	1.71	556
Hycool 20	-3.0	3.1	605.4	21.6	20.0	1.72	3094
Hycool 20	-4.5	4.3	398.6	21.6	20.1	1.72	2937
Hycool 20	-5.6	5.7	300.5	21.8	20.3	1.71	2835
Hycool 20	-8.2	7.8	201.8	21.8	20.4	1.71	2711
Hycool 20	-13.7	13.5	101.2	21.6	20.4	1.72	2295
Hycool 20	-14.5	19.3	50.8	21.5	20.7	1.71	1419
Hycool 20	-14.3	20.7	30.9	21.1	20.6	1.71	894
Hycool 20	1.7	12.3	200.4	21.6	20.6	1.71	1779
Hycool 20	-1.9	16.0	102.7	21.6	20.7	1.71	1538
Temper -20	-3.0	3.2	539.7	21.8	20.2	1.70	3062
Temper -20	-3.9	4.1	402.1	21.8	20.2	1.71	2918
Temper -20	-5.0	5.2	303.3	21.8	20.3	1.72	2804
Temper -20	-7.1	7.2	202.9	21.8	20.4	1.72	2644
Temper -20	-12.3	12.7	99.5	21.6	20.4	1.72	2228
Temper -20	-14.0	18.7	49.7	21.5	20.7	1.72	1462
Temper -20	-14.0	20.7	31.6	21.5	20.9	1.72	990
Temper -20	-1.2	15.6	98.8	21.7	20.9	1.71	1511
Temper -20	2.0	11.7	200.5	21.6	20.6	1.71	1784

Table B3. Measured values for the various test points for the MPE3 tube

Variable		$t_{b,in}$	$t_{b,out}$	$\dot{m}_b$	$t_{W,in}$	$t_{W,out}$	$\dot{V}_W$	$\dot{W}_{e,tot}$
Unit		(°C)	(°C)	(kg/h)	(°C)	(°C)	(m³/h)	W
	Water	7.9	12.0	468.3	21.5	20.3	1.73	2278
	Water	7.7	12.4	399.6	21.5	20.4	1.73	2221
	Water	7.2	13.0	305.3	21.5	20.3	1.73	2068
	Water	6.0	14.2	201.1	21.5	20.4	1.73	1940
	Water	4.5	17.6	100.7	21.5	20.6	1.73	1534
	Water	4.6	20.4	49.3	21.4	20.8	1.73	909
	Water	4.6	21.0	31.1	21.3	20.9	1.73	593
	PG 39%$_w$	-8.6	8.5	174.7	20.9	19.3	1.72	3043
	PG 39%$_w$	-11.7	13.9	100.7	21.7	20.3	1.72	2636
	PG 39%$_w$	-13.3	18.9	52.0	21.5	20.6	1.72	1731
	PG 39%$_w$	-13.1	20.7	32.2	21.3	20.7	1.72	1110
	PG 39%$_w$	11.4	17.1	175.6	21.4	20.8	1.73	1052
	PG 39%$_w$	-1.6	15.9	100.7	21.5	20.5	1.73	1830
	PG 39%$_w$	9.6	18.3	105.9	21.4	20.8	1.73	9710
	Temper -20	-0.5	7.8	395.7	21.6	20.0	1.73	3010
	Temper -20	-3.3	7.9	299.9	21.1	19.5	1.73	3034
	Temper -20	-6.9	9.8	202.5	21.4	19.8	1.73	3058
	Temper -20	-14.7	15.1	101.8	21.7	20.3	1.73	2707
	Temper -20	-14.6	20.0	50.8	21.4	20.6	1.73	1571
	Temper -20	-14.2	21.2	31.8	21.5	20.9	1.73	995
	Temper -20	-3.0	17.2	100.4	21.6	20.6	1.73	1832
	Temper -20	1.0	13.2	200.3	21.6	20.4	1.73	2215

Appendix C
Additional Information for Paper IV

Definition of Theoretical Nusselt Numbers

In Paper IV, experimentally determined Nusselt numbers and pressure drops on the air side were compared with "theoretical" ones. In order to be able to establish or calculate the various theoretical values, different assumptions were made concerning the boundary conditions and the temperature and velocity profile of the "duct flow" (developing or developed). This appendix lists the expressions defining how the theoretical Nusselt numbers, pressure drops and friction factors have been calculated.

<u>Nusselt number for fully developed flow</u>

$$Nu_{a,0,fd} = 3.673 \text{ (FFC)} \tag{C.1}$$

Interpolated data from Table 42 in Shah and London (1978)

$$Nu_{a,0,fd} = 4.439 \text{ (MPET-HE)} \tag{C.2}$$

Interpolated data from Table 42 in Shah and London (1978)

$$d_{h,a,1} = \frac{4 \cdot F_l \cdot \left(F_p - \delta_{fin}\right)}{2 \cdot \left[F_l + \left(F_p - \delta_{fin}\right)\right]} \text{ (FFC)} \tag{C.3}$$

$$d_{h,a,1} = \frac{4 \cdot \left(F_l - \delta_{fin}\right) \cdot \left(F_p - \delta_{fin}\right)}{2 \cdot \left[\left(F_l - \delta_{fin}\right) + \left(F_p - \delta_{fin}\right)\right]} \text{ (MPET-HE)} \tag{C.4}$$

$$\alpha_{a,0,fd} = \frac{Nu_{a,0,fd} \cdot \lambda_a}{d_{h,a,1}} \tag{C.5}$$

$$\alpha_{a,fd} = \eta_0 \cdot \alpha_{a,0,fd} \tag{C.47}$$

$$Nu_{a,fd} = \frac{\alpha_{a,fd} \cdot d_{h,a,1}}{\lambda_a} \tag{C.7}$$

<u>Nusselt number for simultaneously developing flow</u>

$$A_{c,a,1} = W \cdot \left(1 - \frac{\delta_{fin}}{F_p}\right) \cdot H \cdot \left(1 - \frac{\left(T_{h,i} + 2 \cdot \delta_{tube}\right)}{T_{p,t}}\right) \text{ (FFC)} \tag{C.8}$$

89

$$A_{c,a,1} = W \cdot \left(1 - \frac{\delta_{fin}}{F_p}\right) \cdot \left(H - N_{tube,t} \cdot \left(T_{h,o} + \delta_{fin}\right)\right) \text{(MPET-HE)} \tag{C.9}$$

$$u_{a,\max,1} = \frac{\dot{V}_a \rho_{a,\dot{V}_a}}{\rho_a} \cdot \frac{1}{A_{c,a,1}} \tag{C.10}$$

$$\mathrm{Re}_{a,d_h,1} = \frac{u_{a,\max,1} \cdot \rho_a \cdot d_{h,a,1}}{\mu_a} \tag{C.11}$$

$$x_{a,1}{}^* = \frac{T_d}{d_{h,a,1} \cdot \mathrm{Re}_{a,d_h,1} \cdot \mathrm{Pr}_a} \tag{C.12}$$

$$Nu_{a,0,sd,1} = 4.1345 + 0.0395 \cdot \left(\frac{1}{x_{a,1}{}^*}\right) - 0.00006 \cdot \left(\frac{1}{x_{a,1}{}^*}\right)^2 \text{ (FFC)} \tag{C.13}$$

Curve fit of interpolated data from Table 52 in Shah and London (1978)

$$d_{h,a,2} = 2 \cdot \left(F_p - \delta_{fin}\right) \text{ (FFC)} \tag{C.14}$$

$$A_{c,a,2} = W \cdot \left(1 - \frac{\delta_{fin}}{F_p}\right) \cdot H \text{ (FFC)} \tag{C.15}$$

$$v_{a,\max,2} = \frac{\rho_{a,V_a}}{\rho_a} \cdot \frac{1}{A_{c,a,2}} \text{ (FFC)} \tag{C.16}$$

$$\mathrm{Re}_{a,d_h,2} = \frac{u_{a,\max,2} \cdot \rho_a \cdot d_{h,a,2}}{\mu_a} \text{ (FFC)} \tag{C.17}$$

$$x_{a,2}{}^* = \frac{F_d - T_d}{d_{h,a,2} \cdot \mathrm{Re}_{a,d_h,2} \cdot \mathrm{Pr}_a} \text{ (FFC)} \tag{C.18}$$

$$Nu_{a,0,sd,2} = 5.4935 + 0.03267 \cdot \left(\frac{1}{x_{a,2}{}^*}\right) - 0.000038 \cdot \left(\frac{1}{x_{a,2}{}^*}\right)^2 \text{ (FFC)} \tag{C.19}$$

Curve fit of interpolated data from Table 52 in Shah and London (1978)

$$A_{a,fin} = n \cdot 2 \cdot \left(\frac{W}{F_p} \cdot \left(\begin{array}{c} H \cdot 2 \cdot F_d - \\ \frac{H}{T_p} \cdot 2 \cdot \left(\left(T_{h,i} + 2 \cdot \delta_{tube}\right) \cdot \left(T_{w,i} + 3 \cdot \delta_{tube}\right)\right) \end{array}\right)\right) \text{(FFC)} \tag{C.20}$$

$$A_{a,fin} = n \cdot 2 \cdot \frac{W}{F_p} \cdot N_{fin,t} \cdot (F_l - \delta_{fin}) \cdot F_d \quad \text{(MPET-HE)} \tag{C.21}$$

$$A_{a,tube} = 2 \cdot \left((T_{h,i} + 2 \cdot \delta_{tube}) + (T_{w,i} + 3 \cdot \delta_{tube})\right) \cdot \left(1 - \frac{\delta_{fin}}{F_p}\right) \cdot$$
$$W \cdot \frac{H}{T_p} \cdot n \cdot 2 \quad \text{(FFC)} \tag{C.22}$$

$$A_{a,tube} = n \cdot N_{tube,t} \cdot P_{tube,o} \cdot W \cdot \left(1 - \frac{\delta_{fin}}{F_p}\right) \quad \text{(MPET-HE)} \tag{C.23}$$

$$A_{a,tot} = A_{a,fin} + A_{a,tube} \tag{C.24}$$

$$A_{a,fin,2} = 2 \cdot (F_d - T_d) \cdot n \cdot 2 \cdot H \cdot \frac{W}{F_p} \quad \text{(FFC)} \tag{C.25}$$

$$Nu_{a,0,sd} = Nu_{a,0,sd,1} \cdot \left(\frac{A_{a,tot} - A_{a,fin,2}}{A_{a,tot}}\right) + Nu_{a,0,sd,2} \cdot \left(\frac{A_{a,fin,2}}{A_{a,tot}}\right) \tag{C.26}$$
(FFC)

$$Nu_{a,0,sd} = 5.1652 + 0.03759 \cdot \left(\frac{1}{x_{a,1}*}\right) - 0.000067 \cdot \left(\frac{1}{x_{a,1}*}\right)^2 \tag{C.27}$$
(MPET-HE)
Curve fit of interpolated data from Table 52 in Shah and London (1978)

$$\alpha_{a,0sd} = \frac{Nu_{a,0,sd} \cdot \lambda_a}{d_{h,a,1}} \tag{C.28}$$

$$\alpha_{a,sd} = \eta_0 \cdot \alpha_{a,0,sd} \tag{C.29}$$

$$Nu_{a,sd} = \frac{\alpha_{a,sd} \cdot d_{h,a,1}}{\lambda_a} \tag{C.30}$$

The fin efficiency for the FFC was calculated using the expressions presented by Shah and Sekulić (2003), modified for conditions where condensation of water vapour takes place according to Jacobi *et al.* (2005) (or Jacobi and Xia (2005)): see the expressions below. However, the expressions after the second equality sign in Eq. C.33 are the candidates own development, valid for a heat exchanger with continuous plain fins and flat tubes. For the MPET heat

exchanger, the two outer fin layers have the same fin length as the other fins, but are not surrounded by tubes on both sides. Therefore, the fin efficiency is somewhat lower for the outer fin layers. For this reason, a weighted fin efficiency was calculated in Eq. C.38 from Eq. C.31, Eq. C.32, Eq. C.34 and Eq. C.36 - Eq. C.37.

$$l = \frac{F_l - 2 \cdot \delta_{fin}}{2} \tag{C.31}$$

$$l_2 = F_l - \delta_{fin} \ \text{(MPET-HE)} \tag{C.32}$$

$$m = \left(\frac{\alpha_{a,0} \cdot \frac{\dot{Q}_b}{\dot{Q}_{a,sens}} \cdot P}{\lambda_{fin} \cdot A_k} \right)^{1/2} = \left(\frac{\alpha_{a,0} \cdot \frac{\dot{Q}_b}{\dot{Q}_{a,sens}} \cdot \left(2 \cdot F_d + 2 \cdot \delta_{fin} \right)}{\lambda_{fin} \cdot \left(T_d \cdot \delta_{fin} \right)} \right)^{1/2} \tag{C.33}$$

$$\approx \left(\frac{2 \cdot \alpha_{a,0} \cdot \frac{\dot{Q}_b}{\dot{Q}_{a,sens}} \cdot F_d}{\lambda_{fin} \cdot \left(T_d \cdot \delta_{fin} \right)} \right)^{1/2}$$

(FFC)

$$m = \left(\frac{\alpha_{a,0} \cdot \frac{\dot{Q}_b}{\dot{Q}_{a,sens}} \cdot P}{\lambda_{fin} \cdot A_k} \right)^{1/2} = \left(\frac{2 \cdot \alpha_{a,0} \cdot \frac{\dot{Q}_b}{\dot{Q}_{a,sens}}}{\lambda_{fin} \cdot \delta_{fin}} \cdot \left(1 + \frac{\delta_{fin}}{F_l} \right) \right)^{1/2} \tag{C.34}$$

(MPET-HE)

$$\eta_{fin} = \frac{\tanh(m \cdot l)}{m \cdot l} \text{(FFC)} \tag{C.35}$$

$$\eta_{fin,1} = \frac{\tanh(m \cdot l)}{m \cdot l} \ \text{(MPET-HE)} \tag{C.36}$$

$$\eta_{fin,2} = \frac{\tanh(m \cdot l_2)}{m \cdot l_2} \ \text{(MPET-HE)} \tag{C.37}$$

$$\eta_{fin} = \frac{\eta_{fin,1} \cdot A_{a,fin,1} + \eta_{fin,2} \cdot A_{a,fin,2}}{A_{a,fin}} \ \text{(MPET-HE)} \tag{C.38}$$

$$\eta_0 = 1 - \frac{A_{fin}}{A_{tot}} \cdot \left(1 - \eta_{fin}\right) \tag{C.39}$$

$$\alpha_{a,fd} = \eta_0 \cdot \alpha_{a,0,fd} \tag{C.40}$$

$$\alpha_{a,sd} = \eta_0 \cdot \alpha_{a,0,sd} \tag{C.41}$$

$$Nu_{a,fd} = \eta_0 \cdot Nu_{a,0,fd} \tag{C.42}$$

$$Nu_{a,sd} = \eta_0 \cdot Nu_{a,0,sd} \tag{C.43}$$

<u>Pressure drop for fully developed and developing flow</u>

$$\sigma_{a,1} = \frac{A_{c,a,1}}{W \cdot H} \tag{C.44}$$

$$\sigma_{a,2} = \frac{A_{c,a,1}}{A_{c,a,2}} \text{ (FFC)} \tag{C.45}$$

K_c and K_e values are taken from Chapter 5 in Kays and London (1984)

$$K_{c,a,1} = 0.95 \text{ (FFC)}$$

$$K_{c,a,2} = 0.94 \text{ (FFC)}$$

$$K_{c,a} = 0.93 \text{ (MPET-HE)}$$

$$K_{e,a,1} = -0.53 \text{ (FFC)}$$

$$K_{e,a,2} = -0.55 \text{ (FFC)}$$

$$K_{e,a} = -0.57 \text{ (MPET-HE)}$$

$$f_{a,fd} = \frac{15.904}{\mathrm{Re}_{a,d_h,1}} \text{ (FFC)} \tag{C.46}$$

Interpolated data from Table 42 in Shah and London (1978)

$$f_{a,fd} = \frac{19.0705}{\mathrm{Re}_{a,d_h,1}} \text{ (MPET-HE)} \tag{C.47}$$

Interpolated data from Table 42 in Shah and London (1978)

$$G_{c,a} = v_{a,\max} \cdot \rho_a \tag{C.48}$$

$$\Delta p_{a,calc,fd} = \frac{G_{c,a}^2}{\left(2 \cdot \rho_{a,in}\right)} \cdot \left[\begin{array}{l} f_{a,fd} \cdot \dfrac{A_{a,tot}}{A_{c,a}} \cdot \dfrac{\rho_{a,in}}{\rho_a} + \left(K_{c,a,1} + 1 - \sigma_{a,1}^2 \right) \\[2mm] + 2 \cdot \left(\dfrac{\rho_{a,in}}{\rho_{a,out}} - 1 \right) - \\[2mm] \left(1 - \sigma_{a,1}^2 - K_{e,a,1} \right) \cdot \dfrac{\rho_{a,in}}{\rho_{a,out}} \end{array} \right] \tag{C.49}$$

$$x_{a,1}^+ = \frac{T_d}{d_{h,a,1} \cdot \mathrm{Re}_{a,d_h,1}} \tag{C.50}$$

$$x_{a,2}^+ = \frac{F_d - T_d}{d_{h,a,2} \cdot \mathrm{Re}_{a,d_h,2}} \textbf{ (FFC)} \tag{C.51}$$

$$f_{a,app,sd,1} = \left[\begin{array}{l} 17.6847 + 0.22461 \cdot \left(\dfrac{1}{x_{a,1}^+} \right) \\[3mm] - 0.00025 \cdot \left(\dfrac{1}{x_{a,1}^+} \right)^2 \end{array} \right] \cdot \frac{1}{\mathrm{Re}_{a,d_h,1}} \textbf{ (FFC)} \tag{C.52}$$

Curve fit of interpolated data from Table 47 in Shah and London (1978)

$$f_{a,app,sd,2} = \left[\begin{array}{l} 17.6847 + 0.22461 \cdot \left(\dfrac{1}{x_{a,2}^+} \right) \\[3mm] - 0.00025 \cdot \left(\dfrac{1}{x_{a,2}^+} \right)^2 \end{array} \right] \cdot \frac{1}{\mathrm{Re}_{a,d_h,2}} \textbf{ (FFC)} \tag{C.53}$$

Curve fit of interpolated data from Table 47 in Shah and London (1978)

$$f_{a,app,sd} = \left[\begin{array}{l} 18.9597 + 0.24876 \cdot \left(\dfrac{1}{x_{a,1}^+} \right) \\[3mm] - 0.000491 \cdot \left(\dfrac{1}{x_{a,1}^+} \right)^2 \end{array} \right] \cdot \frac{1}{\mathrm{Re}_{a,d_h,1}} \textbf{ (MPET-HE)} \tag{C.54}$$

Curve fit of interpolated data from Table 47 in Shah and London (1978)

$$\Delta p_{a,calc,sd} = \frac{G_{c,a}^2}{\left(2 \cdot \rho_{a,in}\right)} \cdot \begin{bmatrix} f_{a,app,sd,1} \cdot \dfrac{N_{tube,l} \cdot T_d}{r_{h,a,1}} \cdot \dfrac{\rho_{a,in}}{\rho_a} \\[2ex] + f_{a,app,sd,2} \cdot \dfrac{N_{tube,l} \cdot \left(F_d - T_d\right)}{r_{h,a,2}} \cdot \left(\dfrac{A_{c,a,1}}{A_{c,a,2}}\right)^2 \cdot \dfrac{\rho_{a,in}}{\rho_a} \\[2ex] + \left(K_{c,a,1} + 1 - \sigma_{a,1}^2\right) \\[1ex] + \left(N_{tube,l} - 1\right) \cdot \left(K_{c,a,2} + 1 - \sigma_{a,2}^2\right) \\[1ex] + 2 \cdot \left(\dfrac{\rho_{a,in}}{\rho_{a,out}} - 1\right) - \left(1 - \sigma_{a,1}^2 - K_{e,a,1}\right) \cdot \dfrac{\rho_{a,in}}{\rho_{a,out}} \\[2ex] - \left(N_{tube,l} - 1\right) \cdot \left(1 - \sigma_{a,2}^2 - K_{e,a,2}\right) \cdot \dfrac{\rho_{a,in}}{\rho_{a,out}} \end{bmatrix} \qquad \text{(C.55)}$$

$$\text{(FFC)}$$

$$\Delta p_{a,cal,sd} = \frac{G_{c,a}^2 \cdot N_p}{\left(2 \cdot \rho_{a,in}\right)} \cdot \begin{bmatrix} f_{a,app,sd} \cdot \dfrac{T_d}{r_{h,a,1}} \cdot \dfrac{\rho_{a,in}}{\rho_a} + \left(K_{c,a} + 1 - \sigma_{a,1}^2\right) \\[2ex] + 2 \cdot \left(\dfrac{\rho_{a,in}}{\rho_{a,out}} - 1\right) \\[2ex] - \left(1 - \sigma_{a,1}^2 - K_{e,a,1}\right) \cdot \dfrac{\rho_{a,in}}{\rho_{a,out}} \end{bmatrix} \qquad \text{(C.56)}$$

$$\text{(MPET-HE)}$$

Summary of Measurement Results

The tables below list the most important measured values for the various test points.

Table C1. Measured values for the various test points for the FFC heat exchanger

Variable	γ	$t_{b,in}$	$t_{b,out}$	$\dot{m}_b$	$t_{a,in}$	$t_{a,out}$	$t_{dp,a,in}$	$\dot{V}_a$	ΔP_a
Unit	°	(°C)	(°C)	(kg/h)	(°C)	(°C)	(°C)	(l/s)	Pa
FFC HT, dry									
	1	7.5	12.1	182	30.6	8.2	3.9	32	1.1
	1	4.3	8.6	198	28.3	5.1	-1.1	32	1.7
	1	4.4	8.7	205	28.3	5.1	-2.7	33	1.4
	1	4.5	7.2	326	28.4	5.0	-3.7	33	1.7
	1	4.3	13.7	210	29.2	7.7	-4.1	80	5.4
	1	4.6	18.0	204	29.5	11.5	-3.5	135	12.4
	1	10.7	21.4	208	31.4	16.4	9.0	138	13.5
	1	4.6	14.6	300	29.7	10.0	-2.4	136	13.2
	1	10.6	19.0	300	31.5	15.1	7.8	138	13.1
	1	10.5	17.1	402	31.5	14.4	7.9	138	12.9
	10	4.7	9.0	198	28.0	5.3	-7.9	32	
HT,wet									
	1	0.4	6.0	202	29.3	1.2	8.9	27	1.7
	1	0.8	7.3	201	29.7	1.9	8.1	33	2.2
	1	0.9	5.3	301	29.7	1.6	8.0	33	2.6
	1	0.9	9.1	200	29.9	2.3	15.5	33	2.3
	1	0.8	9.2	201	29.9	2.4	15.5	33	2.3
	1	0.8	6.5	300	29.8	1.7	15.6	33	2.3
	1	0.7	13.5	206	31.5	6.4	9.7	80	6.8
	1	1.0	15.9	205	31.1	8.2	15.4	80	8.3
	1	0.6	12.3	297	31.0	6.0	15.2	80	8.4
	1	1.1	19.1	201	31.0	10.1	21.3	79	10.0
	1	0.4	14.7	297	31.0	6.8	21.2	79	8.8
	1	0.8	17.4	212	32.0	10.2	9.4	135	15.5
	1	1.4	19.6	203	31.5	12.9	15.5	137	17.1
	1	0.8	15.8	302	31.4	10.1	15.2	137	19.4
	1	1.2	23.5	204	31.5	16.6	23.4	137	21.2
	1	0.1	20.3	297	31.5	13.2	23.4	136	23.9
	10	0.8	7.4	200	30.2	2.1	8.7	32	
	10	0.9	9.7	197	30.2	2.7	16.3	34	1.9
	10	0.9	13.2	207	31.5	6.4	9.1	78	6.2
	10	0.9	15.9	210	31.4	8.2	16.6	79	
	10	1.2	18.2	207	31.9	10.9	9.2	136	14.4

Cont. Table C1

PD, air, iso

γ				$t_{a,mean}$			$\dot{V}_a$	
1				20.6			285	45.6
1				22.0			190	23.7
1				20.8			145	15.9
1				20.9			98	8.9
1				21.9			47	3.1
1				20.8			29	1.5

PD, liquid

γ	$t_{b,in}$	$t_{b,out}$	$\dot{m}_b$	$t_{a,in}$	$t_{a,out}$	$t_{dp,a,in}$	$\dot{V}_a$	ΔP_b
1	0.4	6.00	202	29.3	1.2	8.9	27	2.87E+03
1	1.1	19.06	201	31.0	10.1	21.3	79	1.86E+03
1	0.4	14.73	297	31.0	6.8	21.2	79	3.22E+03
1	1.2	23.49	204	31.5	16.6	23.4	137	1.53E+03
1	0.1	20.28	297	31.5	13.2	23.4	136	2.60E+03

PD, liquid, iso

γ	$t_{b,mean}$	$\dot{m}_b$	ΔP_b
1	20.7	98	6.63E+02
1	20.8	200	1.33E+03
1	21.1	299	1.93E+03
1	20.9	381	2.47E+03

Table C2. Measured values for the various test points for the MPET heat exchanger

Variable	γ	$t_{b,in}$	$t_{b,out}$	$\dot{m}_b$	$t_{a,in}$	$t_{a,out}$	$t_{dp,a,in}$	$\dot{V}_a$	ΔP_a
Unit	°	(°C)	(°C)	(kg/h)	(°C)	(°C)	(°C)	(l/s)	Pa

MPET-HE
HT, dry

γ	$t_{b,in}$	$t_{b,out}$	$\dot{m}_b$	$t_{a,in}$	$t_{a,out}$	$t_{dp,a,in}$	$\dot{V}_a$	ΔP_a
1	4.6	8.7	198	29.7	7.4	2.2	33	0.5
1	4.6	7.4	299	29.8	7.0	2.2	33	0.5
1	7.3	11.1	200	30.1	9.9	5.3	34	0.5
1	7.4	9.9	303	29.9	9.6	5.6	34	0.5
1	4.6	12.4	199	31.0	13.7	-1.8	82	1.9
1	4.5	9.8	307	30.8	12.8	1.6	83	1.9
1	4.5	9.9	300	30.9	12.9	-2.1	82	1.9
1	4.7	14.8	200	31.4	18.3	-2.0	142	3.8
1	4.5	11.9	296	31.5	17.3	-2.0	142	3.9
10	7.2	10.9	201	29.4	9.6	-0.5	33	0.4
10	7.2	10.9	201	29.4	9.6	-0.5	33	0.4

HT,wet

1	0.6	6.3	197	29.9	5.0	8.2	33	0.7
1	0.6	4.5	300	29.9	4.4	8.0	33	0.7
1	0.9	7.9	201	30.0	5.9	16.3	34	0.8
1	0.6	5.7	298	29.9	5.1	16.3	33	0.8
1	0.2	9.8	200	30.9	12.3	9.0	79	2.7
1	0.8	12.3	200	31.1	14.2	16.1	82	3.2
1	0.4	9.1	299	31.0	12.9	16.1	82	3.2
1	0.6	11.0	301	30.7	14.2	21.8	81	3.3
1	1.0	14.8	201	30.6	15.8	21.9	81	3.2
1	0.5	11.0	300	30.8	17.2	15.8	138	7.1
1	1.0	14.3	202	30.9	18.5	15.8	137	7.0
1	1.0	16.7	207	30.9	19.8	21.1	137	7.3
10	0.4	6.2	200	29.3	4.6	8.9	33	0.5
10	0.3	7.7	200	29.2	5.1	16.5	32	0.6
10	0.2	12.0	202	30.7	13.3	16.4	78	2.6
10	0.4	15.1	199	30.8	15.1	22.7	78	2.4
10	0.2	17.4	204	31.4	20.1	22.0	138	6.0
10	0.3	14.6	200	31.2	18.5	16.2	139	5.8

PD, air, iso

				$t_{a,mean}$				
1				19.5			37	0.7
1				20.1			50	1.1
1				20.3			100	2.8
1				20.2			151	5.2
1				20.2			205	7.8
1				20.2			244	10.1
1				20.1			287	12.9

PD, liquid, iso

	$t_{b,mean}$							ΔP_b
1	21.3		315.2					5.82E+04
1	21.1		195.4					3.60E+04
1	20.6		105.3					1.96E+04
1	20.3		48.6					9.16E+03
1	21.3		32.8					5.96E+03
1	20.9		14.2					2.62E+03